# JOURNAL OF CAVE AND KARST STUDIES

August 2002
Volume 64 Number 2
ISSN 1090-6924
A Publication of the National Speleological Society

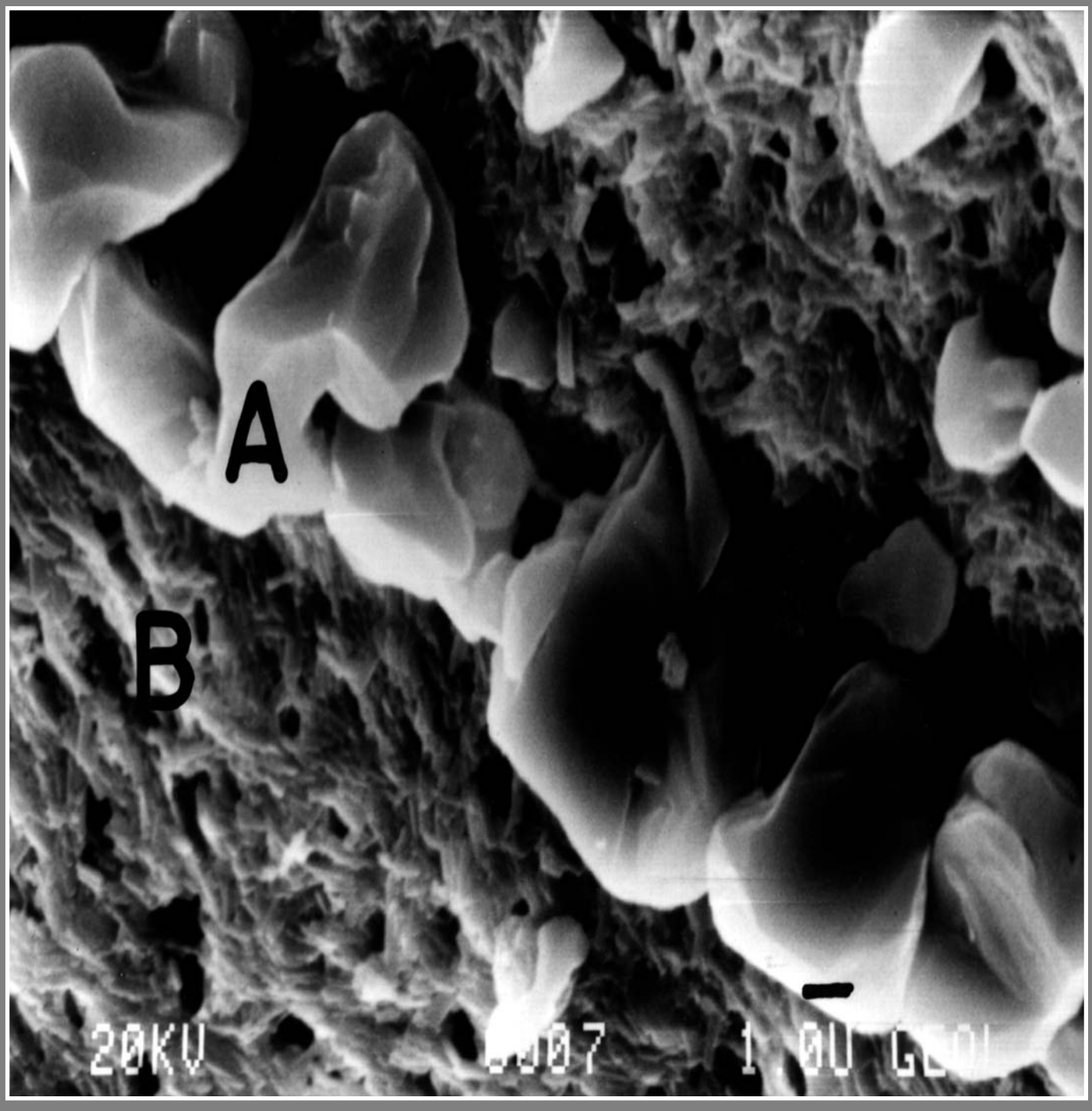

# Journal of Cave and Karst Studies of the National Speleological Society

Volume 64 Number 2 August 2002

**CONTENTS**



The *Journal of Cave and Karst Studies* (ISSN 1090-6924) is a multi-disciplinary, refereed journal published three times a year by the National Speleological Society, 2813 Cave Avenue, Huntsville, Alabama 35810-4431 USA; (256) 852-1300; FAX (256) 851-9241, e-mail: nss@caves.org; World Wide Web: http://www.caves.org/~nss/. The annual subscription fee, worldwide, by surface mail, is $18 US. Airmail delivery outside the United States of both the *NSS News* and the *Journal of Cave and Karst Studies* is available for an additional fee of $40 (total $58); The *Journal of Cave and Karst Studies* is not available alone by airmail. Back issues and cumulative indices are available from the NSS office. POSTMASTER: send address changes to the *Journal of Cave and Karst Studies*, 2813 Cave Avenue, Huntsville, Alabama 35810-4431 USA.

Copyright © 2002 by the National Speleological Society, Inc. Printed on recycled paper by American Web, 4040 Dahlia Street, Denver, Colorado 80216 USA

Front cover: SEM image of blue-greenish bone showing calcite crystals (A) over phosphasized bone (B). Scale bar on lower right side equals 1 µ. See Robles, Arroyo-Cabrales, Johnson, Allen, and Izquierdo page 145.

**Editor**
**Louise D. Hose**
Department of Physical Sciences
Chapman University
Orange, CA 92866
(714) 997-6994 Voice
(714) 532-6048 FAX
hose@chapman.edu

**Production Editor**
**James A. Pisarowicz**
Wind Cave National Park
Hot Springs, SD 57747
(605) 673-5582
pisarowicz@alumni.hamline.edu

**BOARD OF EDITORS**
**Anthropology**
**Patty Jo Watson**
Department of Anthropology
Washington University
St. Louis, MO 63130
pjwatson@artsci.wustl.edu

**Conservation**
**Julian J. Lewis**
J. Lewis & Associates, Biological Consulting
217 West Carter Avenue
Clarksville, IN 47129
(812) 283-6120
lewisbioconsult@aol.com

**Earth Sciences-Journal Index**
**Ira D. Sasowsky**
Department of Geology
University of Akron
Akron, OH 44325-4101
(330) 972-5389
ids@uakron.edu

**Exploration**
**Andrea Futrell**
987 Dow Creek Road
Pembroke, VA 24136
(540) 626-5349
karstmap@hotmail.com

**Life Sciences**
**Steve Taylor**
Center for Biodiversity
Illinois Natural History Survey
607 East Peabody Drive (MC-652)
Champaign, IL 61820-6970
(217) 333-5702
sjtaylor@inhs.uiuc.edu

**Social Sciences**
**Marion O. Smith**
Rt. 1, Box 462A
Bone Cave Rd.
Rock Island, TN 38581
931-686-2320
sharon42689@blomand.net

**Book Reviews**
**Ernst H. Kastning**
P.O. Box 1048
Radford, VA 24141-0048
ehkastni@runet.edu

**Proofreader**
**Donald G. Davis**

**JOURNAL ADVISORY BOARD**
David Ashley — Rane Curl
Malcolm Field — Andrew Flurkey
John Ganter — Donald MacFarlane
Diana Northup — Art Palmer
William White

Nicholas J. Czaplewski, William L. Puckette, and Clayton Russell - A Pleistocene tapir and associated mammals from the southwestern Ozark Highland. *Journal of Cave and Karst Studies 64*(2): 97-107.

# A PLEISTOCENE TAPIR AND ASSOCIATED MAMMALS FROM THE SOUTHWESTERN OZARK HIGHLAND

NICHOLAS J. CZAPLEWSKI
*Oklahoma Museum of Natural History, 2401 Chautauqua Avenue, Norman, OK 73072 USA,* nczaplewski@ou.edu
WILLIAM L. PUCKETTE
*Poteau High School, Poteau, OK 74953 USA*
CLAYTON RUSSELL
*Rt. 1 Box 1459, Stilwell, OK 74960 USA*

*A mud deposit in Sassafras Cave near Stilwell, Oklahoma, produced a small assemblage of fossil vertebrates including an unidentified salamander and the mammals* Myotis *sp.*, Lasionycteris noctivagans, Pipistrellus subflavus, Tamias striatus, Peromyscus *sp.*, Reithrodontomys *sp.*, Microtus *sp., and* Tapirus veroensis. *The fossiliferous mud deposit is a stream terrace containing abundant red clay accumulated behind roof fall and breakdown boulders that temporarily dammed the main stream-passage of the cave. The tapir fossils indicate a late Rancholabrean (late Pleistocene) age for the deposit. This is the first report of a tapir from the Oklahoma Ozark Highland and only the second report of Pleistocene megafauna from a cave in eastern Oklahoma. The tapir is represented by a partial skeleton with some of the distal leg bones articulated in life position in the deposit. The animal probably died while it was standing or lying in the mud, possibly after falling into the cave or walking in through an entrance that had a different configuration in the Pleistocene than the present sinkhole entrance.*

The Ozark Highland is an old remnant of a dissected plateau in southern Missouri, northern Arkansas, and northeastern Oklahoma. Today, much of the area is covered by steep-sided hills with intervening valleys cut by many clear streams that originate in the higher elevations. Numerous limestone caves occur throughout the Ozark Highlands, most of which in Oklahoma have developed within rocks of lower Pennsylvanian (Hale Formation) or Mississippian (Pitkin Formation, Keokuk Formation, or St. Joe Group) age. Sassafras Cave is one of seven known caves that occur in a point of a hill in central Adair County. The point has an area of ~20 hectares and is underlain by the Hale Formation in which the caves formed. Most of the caves were probably connected at one time but are currently separated by breakdown, clastic fills, or erosion. The total combined length of the known caves is over 4 km.

Sassafras Cave (OMNH locality V566), Adair County, Oklahoma, is at the southwestern edge of the Ozark Highland. The mapped length of the cave is 365 m (Fig. 1). The passages average 2 m wide and 6 m high. Cavers dug open the present entrance, a 10-m-deep sinkhole, in 1969-1970 while searching for new caves. However, chert flakes (cultural materials from pre-Columbian Indians) found inside the cave indicated that there was a prehistoric entrance in the vicinity of the present entrance. The cave, on the property of the NSS Donald R. Russell Cave Preserve, was donated for purposes of research and preservation.

In 2001, one of the authors (CR) and Sylvia Russell collected parts of a fossil tapir skeleton in a mud bank on the floor of a main passage in Sassafras Cave (Fig.1). The mudbank is a remnant deposit of unconsolidated sediments that possibly accumulated in an ephemeral subterranean pond behind a pile


**Figure 1. Location map and plan view of Sassafras Cave, showing discovery site of tapir skeleton in a Pleistocene terrace. NSS standard map symbols follow Hedges *et al.* (1979). Ceiling heights (encircled numbers) are given in feet.**

of breakdown boulders that presently occupies the passage, forming a dam. Today, this pile of boulders rises 2.2 m above the floor of the passage on the downstream side of the dam. The fossiliferous deposit, no greater than 30 m long and 3 m wide, occupies a short, roughly linear section of cave passage. The greatest depth of the deposit is undetermined but is probably not more than 2 m. Based on core samples we made (by pushing in PVC pipe by hand or with a sledge hammer), the sediments had accumulated behind the dam to a depth of at least 1.6 m upon the limestone bedrock (Fig.2). Apparently the breakdown dam was later breached and the stream in the cave

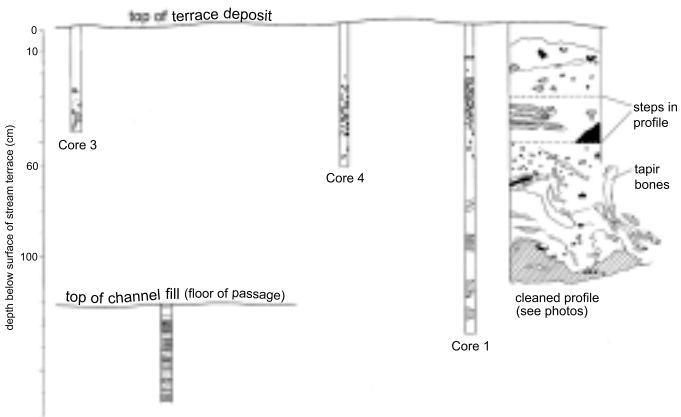


**Figure 2. Diagram of cleaned profile and cores showing stratigraphy in a Pleistocene stream terrace and a more recent stream deposit in Sassafras Cave, Oklahoma. Lateral distance is foreshortened to save space; actual distance from Core 3 to Core 1 was ~25 m. Hatching indicates red clay. In Core 2, black indicates organic layer; in the other cores and profile black indicates rocks. The profile was cut adjacent to the spot where the articulated left lower leg bones of the tapir were found. As shown by the cleaned profile and cores 1, 3, and 4, essentially the entire terrace deposit consists of sandy clays.**

incised these sediments, leaving a very short (2-m-long) remnant mudbank along the base of the south wall immediately upstream from the breakdown dam, and a much longer (12-m-long) terrace along the base of the north wall that begins 17 m from the dam.

The terrace forms a firm ledge along the north wall of the passage where the tapir skeleton was found. Stratification is visible where we cut profiles in the terrace deposit adjacent to the tapir skeleton (Figs. 2 & 3). The unit in which the tapir skeleton occurred is composed primarily of red brown, yellow brown, and dark brown sandy clay interspersed with structureless blebs of bright red clay that become more frequent in the deeper part. Dispersed through the deposit are occasional cobbles and pebbles of weathered limestone and shale originating from the cave walls and ceiling, as well as a few isolated Paleozoic invertebrate and vertebrate fossils. The deeply weathered shale cobbles within the mud were unconsolidated to poorly consolidated when wet and very friable. The Paleozoic invertebrates are tiny snails (Mollusca: Gastropoda) and columnal ossicles of crinoid stalks (Echinodermata: Crinoidea); the vertebrate remains are tiny shark teeth of several types (Chondrichthyes; W. May 2001, pers. comm.). These Paleozoic fossils entered the Pleistocene deposit as residue weathered from the surrounding limestone. The tapir skeleton and other vertebrate bones occurred in the upstream (east) end of the north terrace about 27 m from the dam. Subsequent further collecting in the deposit yielded more bones of the tapir, and screenwashing of the encasing mud produced—in addition to the Paleozoic animal fossils—the remains of a few small vertebrates including bats and rodents.

**Figure 3. Photograph of profile cut into the mud deposit in which the fossils occurred. This is the same profile as shown in Figure 2. The hind leg and foot bones of the tapir occurred in the area at the lower right in this photograph (below the person and immediately to the right side of the bottom of the cleaned profile). The photo was taken after the tapir bones were removed.**

Color and texture of the muds in which the tapir was preserved were field-judged under wet conditions (as the samples were taken from the cave) in order to assess the relative proportions of sand, silt, and clay particles. Donald G. Wyckoff did the field-judging in the lab at the Oklahoma Museum of Natural History (OMNH). The mud encasing the tapir's foot bones appeared in a profile cut to be a weakly stratified, possibly bioturbated unit of sandy clay that was very sticky, mottled red and yellowish red when wet (2.5YR 4/8 and 5YR 4/6; Munsell Soil Color Charts, 1998 revised edition, New Windsor, New York). This unit also contained frequent blebs and chunks of fine red clay (2.5YR 4/6). Immediately adjacent to the bright red clay around the left hind foot skeleton was a "stringer" of manganese oxide. This stringer was a thin sedimentary feature that swept around the front and sides of the tapir's left foot skeleton, sub-parallel to the contour of the foot and between the red and mottled red, yellowish red, and brown

muds. The bacterial decay of animal flesh sometimes leaves behind manganese oxides (B. Schubert 2001, pers. comm.). There was a small void (air space) in the mud over the top of the metatarsals of the left foot. Above the red and yellowish red mud on top of the left hind foot was a small mass of stratified dark brown mud (clay fine sand; 7.5YR 3/3 when wet) that appeared grayish in caving headlights. This stratified dark brown mud contained a bat radius. Other than these *in situ* deposits, much of the surrounding deposit from which other fossils were recovered consisted of variegated red, yellowish red, and brown muds that were disturbed by foot traffic in the cave and by efforts to recover the fossils. In places, these disturbed muds also contained flat, subangular pebbles derived from the country rock making up the cave walls.

The red clay that forms a major component of the terrace deposit in Sassafras Cave is a common feature of cave sediments throughout the Ozark Highland (Bretz 1942; Jennings 1985; Brod 1999; Reams, no date). Brod (1999) reported that no sediment information—especially on the red clay—was available for Oklahoma caves, but the occurrence of red clay there is expected because of its widespread occurrence in Missouri and Arkansas Ozark caves. In Sassafras Cave, the red clay blebs might not be in their primary depositional context in the muds in which the tapir bones occurred, but they clearly were present when the tapir died in the late Pleistocene. These Ozark red clays consist of very fine quartz particles, clay minerals (kaolinite and illite), and iron minerals that give them their red color (Brod 1999). The clay was primarily derived from surface weathering and was originally emplaced in Ozark caves probably under phreatic conditions during cave development (Brod 1999).

Clay minerals such as kaolinite are important to herbivorous mammals because the clays are ideal for adsorbing many kinds of biochemical toxins produced by the plants they eat (Barlow 2000). Tapirs and many other herbivorous vertebrates eat clay-rich soils, a behavior known as geophagy (Barlow 2000). The clay deactivates the toxins in foliage and other plant tissues. In a predominantly limestone region such as much of the Ozark Highland, clay minerals may not have been widely available to geophagous megaherbivores. It is feasible that tapirs were attracted to Ozark caves such as Sassafras Cave as a source of clay for detoxifying their intestines.

A 44-cm core taken from the center of the passage in the bed of the stream cut between the north and south terraces did not reach bedrock. It revealed a very different column from the terrace and was comprised entirely of thinly layered, unconsolidated, cross-bedded sands and silty sands (Fig. 2, core no. 2) that represent an active channel or cut-and-fill deposit, probably of Holocene age.

A small sample of the well-preserved tapir bone was sent to Beta Analytic, Miami, Florida, for AMS dating. Unfortunately, the bone did not yield a reliable collagen fraction for dating the time of death of the tapir. All its collagen appeared to have been replaced or removed, and it contained only organic molecules probably from the soil and/or humus that invaded the bone after its burial (R.E. Hatfield 2001, pers. comm.). Thus, the numerical age of the bone could not be determined.

## SYSTEMATIC PALEONTOLOGY

Class Amphibia
Order Caudata (salamanders)
Family indeterminate
Material.–OMNH 70976, caudal vertebra.

Discussion.–This vertebra measures 2.5 mm in centrum length. It is somewhat abraded (stream-worn?) and the hemal arch and delicate processes are broken. It bears an ossified cap on the anterior cotyle, forming a small condyle; in temperate North America, this condition is typical of members of the family Salamandridae (newts) and is known to occur in a few species of Plethodontidae (lungless salamanders) (Holman 1995; Hulbert 2001). The Sassafras Cave specimen probably pertains to one of these two families, but a caudal vertebra is insufficient for a familial identification.

Class Mammalia
Order Chiroptera
Family Vespertilionidae
*Myotis* sp. indeterminate

Material.—OMNH 59520, edentulous left dentary fragment with root of p3 and alveoli for all teeth except the incisors; OMNH 70972, right premaxilla with I1-I2; OMNH 70971, right maxilla and premaxilla fragment with I1-P4; OMNH 70961, left half of rostrum with C1-M3; OMNH 70970, right maxilla with P3-M3; OMNH 70968, left maxilla with P2 and P4-M3; OMNH 70969, left maxilla fragment with M2-M3; OMNH 70973, right maxilla fragment with P2-P4; OMNH 70966, right dentary with p4-m3; OMNH 70967, left dentary with i1-m3; OMNH 70965, right dentary with p4-m3; OMNH 70964, right dentary with p3-m3; OMNH 70974, left dentary with p3-p4 and m2; OMNH 70975, left dentary fragment with p2-p4; OMNH 59519, left proximal humerus; OMNH 70962, right distal humerus; OMNH 70963, right distal humerus.

Discussion.–Five species of *Myotis* (*M. grisescens*, *M. leibii*, *M. lucifugus*, *M. septentrionalis*, and *M. sodalis*) occur in the modern fauna of the Ozark Highland. Of these, we compared the Sassafras Cave fossils with skulls and humeri of all species except *M. leibii*, for which no comparative skeletons were available, and *M. septentrionalis*, for which skulls but no postcranial materials were available. We used one or two skulls and humeri each of *M. grisescens*, *M. lucifugus*, and *M. sodalis*, as well as a skull and humerus of *M. austroriparius*. The last species does not occur today in the Ozark Highlands but does occur to the south in southeastern Oklahoma. We also compared dental measurements of the fragmentary fossils with those of our comparative specimens and with numerous standard measurements provided by Miller and Allen (1928). In lieu of comparative specimens of *M. leibii*, we judged the specimens against the measurements provided by van Zyll de Jong (1984).

The various rostral and mandibular fragments preserve different portions of the upper and lower tooth rows. Different species of *Myotis* greatly resemble one another morphologically, making the identification of fragmentary fossils extremely difficult or impossible. Not all Sassafras Cave specimens were complete enough to yield standard measurements that could potentially be useful for determining the species to which the skull and jaw fragments belonged. However, the fossils are consistent with one another in their morphology and appear to represent a single species. The measurements indicate a medium-sized to small species of *Myotis* (Tables 1 & 2) in the size range of *M. lucifugus* and *M. leibii*, and also broadly over-

**Table 1. Measurements (to the nearest 0.05 mm) of the upper tooth rows of Pleistocene *Myotis* from Sassafras Cave, Oklahoma, and several Recent species of *Myotis*.**

| specimen | length of maxillary tooth row (C1-M3) | | length of P4-M3 |
|---|---|---|---|
| Fossils | | | |
| OMNH 70961 | 5.10 | | 3.75 |
| OMNH 70970 | | | 4.00 |
| OMNH 70968 | | | 3.95 |
| Modern comparative specimens | | | |
| *Myotis septentrionalis*[1] | 6.10 | 4 | |
| *Myotis lucifugus* | 5.2 | | |
| *Myotis grisescens* | 5.9 | | |
| *Myotis austroriparius* | 5.20 | 3 | |
| *Myotis sodalis* | 5.4 | | |
| *Myotis leibii*[2] | 5.0 | | |

[1] Means of 2 specimens.
[2] Means of 32 specimens (from van Zyll de Jong 1984).

lapping but less well-centered within the size ranges of *M. sodalis* and *M. austroriparius*. The measurements of the fossils definitely represent a bat smaller than *M. grisescens* and *M. septentrionalis*. Few salient details of dental morphology exist that are helpful in distinguishing among the eastern US species of *Myotis*. One such feature is a weak lingual cingulum on the upper molars that disappears completely around the base of the protocone. This type of lingual cingulum is present in the Sassafras Cave *Myotis* and in the upper molars of all modern species with which we made comparisons except *M. septentrionalis. Myotis septentrionalis* has M1-M3 with strong lingual cingula that continue all the way around the bases of the protocones of these molars.

Like the jaw fragments and teeth, the Sassafras Cave humerus fragments are morphologically indistinguishable from those of several species of *Myotis*. Measurements of the two distal humerus fragments are: width of distal articular surface (from lateral ridge of capitulum to medial edge of trochlea), 2.15 mm and 2.10 mm; greatest width of distal humerus, 2.80 mm and 2.83 mm, respectively. In size, the distal humeri most closely match those of *M. lucifugus* and *M. austroriparius*; they are smaller than one specimen of *M. grisescens* and slightly larger than two of *M. sodalis*. Nevertheless, these small samples do not represent the variability in the species. The morphology of the distal humerus is virtually identical in all the species of *Myotis* examined. Therefore, this element is of no help in distinguishing them, and it is not possible to determine the species to which the Sassafras Cave fragments belong based on the fossils presently available.

The toothless lower jawbone (OMNH 59520) has alveoli for a single-rooted p2 and p3, and a double-rooted p4. Only three genera of bats in the USA, *Myotis*, *Corynorhinus*, and *Lasionycteris*, have this lower alveolar formula. OMNH 59520 matches the morphology of *Myotis* and *Corynorhinus* most closely. It is smaller than the dentary of *Lasionycteris* discussed below, and further differs from *Lasionycteris* in having a lateral mental foramen that opens on the side of the dentary between the roots of the canine and p2 instead of between the roots of p2 and p3. The jawbone appears to be less sinuous in dorsal view than in *Corynorhinus*.

In summary, our size and shape comparisons of rostral fragments, jaws, and teeth indicate that the Sassafras Cave *Myotis* is most similar to *M. lucifugus*, *M. sodalis*, and *M. austroriparius*. The fossils definitely do not represent *M. grisescens* or *M. septentrionalis*. We cannot distinguish further among these species based on the sample of fossils that is presently available.

**Table 2. Measurements (to the nearest 0.05 mm) of the lower jaws of Pleistocene *Myotis* from Sassafras Cave, Oklahoma, and several Recent species of *Myotis*. Dash indicates broken specimen on which measurement could not be made.**

| specimen | length of p4-m3 | length of m1-m3 | alveolar length of c1-m3 | length of dentary | height of coronoid |
|---|---|---|---|---|---|
| Fossils | | | | | |
| OMNH 70966 | 4.10 | 3.50 | 5.55 | 10.30 | 3.15 |
| OMNH 70967 | 4.15 | 3.55 | 5.45 | — | — |
| OMNH 70965 | 3.80 | 3.20 | — | — | — |
| OMNH 70964 | 4.00 | 3.40 | — | — | — |
| OMNH 70974 | 4.10 | 3.20 | 5.35 | — | — |
| Modern comparative specimens | | | | | |
| *Myotis septentrionalis*[1] | 4.50 | 3.65 | 6.40 | 10.82 | 3.17 |
| *Myotis lucifugus* | 4.20 | 3.55 | 5.80 | 10.40 | 2.95 |
| *Myotis grisescens* | 4.70 | 3.95 | 6.25 | 11.90 | 3.25 |
| *Myotis austroriparius* | 4.00 | 3.35 | 5.40 | 10.20 | 2.80 |
| *Myotis sodalis* | 4.20 | 3.50 | 5.55 | 10.40 | 2.80 |
| *Myotis leibii*[2] | | | | | 2.79 |

[1] Means of 2 specimens.
[2] Mean of 32 specimens (from van Zyll de Jong 1984, who did not make the other lower jaw measurements used here).

*Lasionycteris noctivagans* (silver-haired bat)

Material.—OMNH 59526, right dentary with c1-p2 and m1-3; OMNH 59527, left dentary fragment with p2-m2 (crown of c1 broken) and alveoli for other teeth (Fig. 4A).

Discussion.–These two jaws were found separately by screen-washing but show similar degrees of tooth wear and similar preservation; they may represent the two sides of the mandible of a single bat.

Morphologically, these jaws are virtually identical to those of modern specimens of *L. noctivagans*. In occlusal outline, p2 and

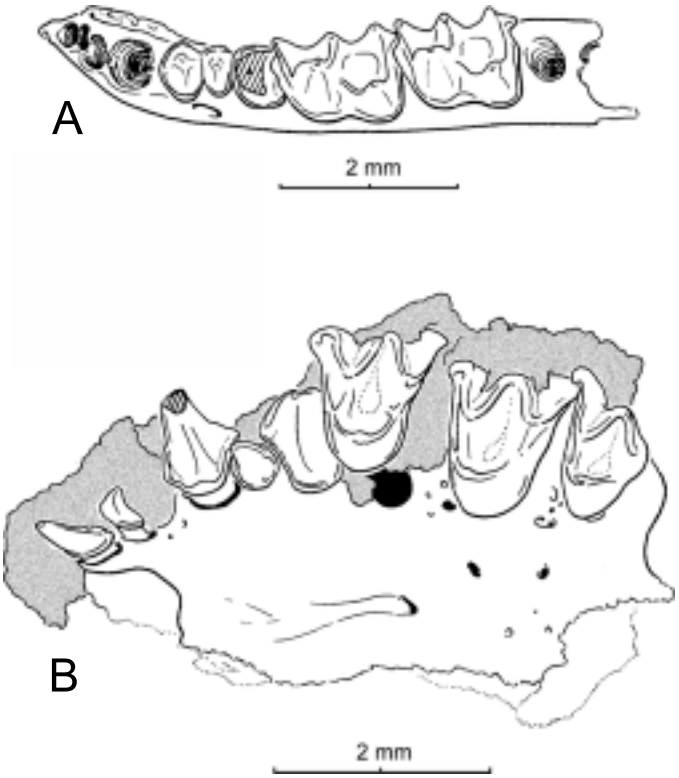


**Figure 4. Fossil remains of bats found in association with *Tapirus veroensis* in Sassafras Cave, Oklahoma. A, *Lasionycteris noctivagans*, OMNH 59527, left dentary fragment with p2-m2 in occlusal view; B, *Pipistrellus subflavus*, OMNH 59523, left half of rostrum with all upper teeth in occlusal view. Hatching indicates breakage; shading in B indicates adhering concretion.**

p3 are transversely wider than their anteroposterior length, so that these teeth appear anteroposteriorly compressed. This condition differs from *Myotis* in which the width and length are subequal in both p2 and p3. In the fossils and in modern *L. noctivagans*, the occlusal outline of p4 is very short—about as wide as it is long—and appears rather trigonal. This contrasts with *Myotis*, in which all North American species have a p4 that is longer than wide and rather rectangular in occlusal outline. *Corynorhinus* species also have a short p4, but this tooth in *Corynorhinus* has a prominent anterolingual cusp that is absent in the fossil, as well as a relatively straight lingual margin in contrast to the rounded margin in the single p4 available in the fossils. The molar teeth in the fossil also have cusps that are more robust than the distinctively slender cusps and ridges seen in *Corynorhinus*, and the m1 has a much straighter lingual outline in occlusal view than in *Corynorhinus*, which has a strong bend in m1 along the lingual border between the bases of the metaconid and paraconid. The fossils have a lateral mental foramen located between the roots of p2 and p3. In modern specimens of *L. noctivagans*, the lateral mental foramen is situated between the roots of p2 and p3 or is below the canine. By contrast, in *Myotis* the lateral mental foramen opens between the roots of c1 and p2.

*Lasionycteris noctivagans* has a poor fossil record. The species was previously known from only four localities as a Quaternary fossil or subfossil. These localities are Bell Cave, Wyoming (Zeimens & Walker 1974), Little Box Elder Cave, Wyoming (Anderson 1968), Upper Sloth Cave, Texas (Logan & Black 1979), and a cave in the Sylamore Ranger District in Ozark National Forest, Arkansas (Saugey *et al*. 1978). Although all these records are from caves, in modern times the species rarely enters caves, preferring to roost in trees. This is the first fossil record of the silver-haired bat in Oklahoma.

*Pipistrellus subflavus* (eastern pipistrelle)

Material.–OMNH 59523, left half of rostrum with I1-M3 (Fig. 4B).

Discussion.–*Pipistrellus subflavus*, the eastern pipistrelle, is a common and widespread bat across much of the eastern half of the United States and eastern Mexico. It occurs from southeastern Canada to Honduras in a very wide variety of habitat types (Fujita & Kunz 1984). The western and northern limits of its modern distribution are defined by areas lacking caves. In addition, the present northern limit of the species is approximately coincident with the Pleistocene southern limit of the Wisconsinan glaciation; north of this limit, riparian foraging habitat is unsuitable for pipistrelles (Brack & Mumford 1984). *Pipistrellus subflavus* is probably the most common bat in the Ozark Highlands, at least in caves in which it hibernates (Sealander & Young 1955). The species also roosts in trees and other situations outside caves, particularly in the summertime. It occurs in Sassafras Cave in the present day.

*Pipistrellus subflavus* occurs as a Quaternary fossil or subfossil in at least 31 cave sites scattered across 11 states in the eastern United States. The Sassafras Cave occurrence is the first record of *P. subflavus* as a fossil in Oklahoma and only the second fossil record for the species in the Ozark Highland. The other is from a cave in the Sylamore Ranger District in Ozark National Forest, Arkansas (Saugey *et al*. 1978).

Order Rodentia

Family Sciuridae

*Tamias striatus* (eastern chipmunk)

Material.–OMNH 59511, partial skeleton recovered by screenwashing as several separated elements, but probably representing the associated parts of an individual skeleton, including: left dentary with partial i1, anterior roots of p4, and all roots of m1 (Fig. 5A); two lumbar vertebrae; partial sacrum; partial right and left ilia; complete left femur and shaft of right femur; complete left tibia; right tibia lacking proximal end; and left navicular. OMNH 70980, left dentary with p4-m2; OMNH 70983, right femur; OMNH 70982, left partial lower molar; OMNH 70981, right M1 or M2.

Discussion.–The dentary associated with OMNH 59511 lacks cheek teeth but retains a portion of the lower incisor. The diastemal region of the dentary drops only slightly anterior to the p4 (as is characteristic of the Tamiini [Black 1963], whose only known Pleistocene representatives belong to the genus *Tamias*). The enamel on the anterior face of the lower incisor is faintly ridged with five to six low ridges and shallow grooves in between. Among tamiines, the cheek teeth preserved in the second dentary (OMNH 70980) match the morphology of modern specimens of *T. striatus*. Although there is the possibility that a western or unrecognized extinct species of chipmunk could be represented by these specimens, *T. striatus* is the only chipmunk that today occurs east of the Great Plains, where it is widespread. All other known chipmunks are montane species of the western USA; none occurs any closer to Sassafras Cave today than 690 km away and on the other side of the Great Plains, which are generally unsuitable habitat for these woodland sciurids. Alveolar lengths of the cheek tooth rows (p4-m3 alveoli) for the two specimens are 6.4 and 6.8 mm. In OMNH 59511, the lower incisor measures 2.1 mm in anteroposterior diameter and 1.1 mm in transverse diameter. In

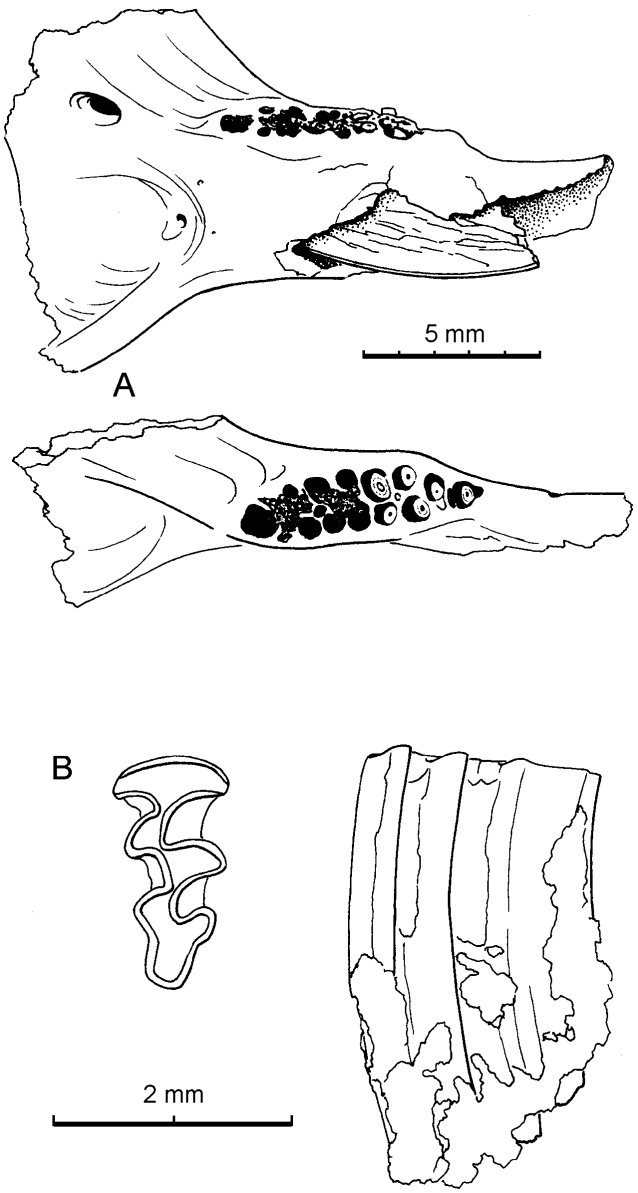


**Figure 5. Rodent fossils found in Pleistocene deposit in Sassafras Cave, Oklahoma. A, *Tamias striatus*, OMNH 59511, edentulous left dentary containing broken i1 and alveoli for other teeth; shown in lingual and occlusal views. B, *Microtus* sp., OMNH 59512, right upper third molar with adhering concretion; in occlusal and labial views.**

OMNH 70980, the anteroposterior length and transverse width of each of the cheek teeth (to the nearest 0.5 mm; measured according to the method of Gordon & Czaplewski 2000) are: p4, 1.35 x 1.45; m1, 1.70 x 1.75; m2, 1.95 x 1.90. The partial lower molar (OMNH 70982) is broken posteriorly but its transverse width is 1.70 mm. The upper molar is 1.60 mm in anteroposterior length and 1.95 mm in transverse width. These measurements compare very closely with those of modern *Tamias striatus pipilans* provided by Ray (1965). The Sassafras Cave specimen is much smaller than *Tamias aristus*, a large extinct chipmunk known only by a skull, jaw, and isolated cheek tooth from the Pleistocene of Georgia (Ray 1965). The chipmunk postcranial bones from Sassafras Cave compare favorably with those of *T. striatus*, and do not pertain to *Neotoma*, *Sigmodon*, or other rodents.

In modern times, this species is common in the eastern Ozark Highland but seems to be relatively less common to the west. Its modern distribution extends westward to the eastern edge of the Great Plains, including about the eastern one-third of Oklahoma (Caire *et al.* 1989). In a late Pleistocene context, it has been reported as far west as Beaver County, Oklahoma, where it occurred in the Elm Creek local fauna (Dalquest & Baskin 1992).

Family Muridae

Subfamily Sigmodontinae

*Reithrodontomys* sp. indeterminate (harvest mouse)

Material.–OMNH 70979, left I1; OMNH 70978, left maxilla fragment with M1-M2.

Discussion.–The upper incisor is small, strongly grooved and broken at its base. It has the following measurements (in mm): anteroposterior diameter, 1.10; transverse width, 0.60; radius of curvature (measured according to the method of Akersten, 1981), 2.75. The maxilla fragment has moderately worn teeth that are very low-crowned. Tooth measurements are: M1 anteroposterior length, 1.40; M1 transverse width, 0.85; M2 anteroposterior length, 0.90; M2 transverse width, 0.85. The cheek teeth bear no accessory lophs or cusps. Although we refer the Pleistocene specimens from Sassafras Cave to the genus *Reithrodontomys* based on size and incisor and molar morphology, we cannot refer them to a species based on the currently available material.

*Peromyscus* sp. indeterminate (white-footed mouse)

Material.–OMNH 70960, right maxilla fragment with M1-M2; OMNH 70959, left m1.

Discussion.–The maxillary molars are relatively high-crowned—much more so than in the specimens referred to *Reithrodontomys*—and in a stage of light wear. There is a poorly developed mesoloph on M1 but none on M2. The M1 has a strong parastyle connected to the posterolabial portion of the anterocone. Otherwise, no accessory lophs or cusps are present. The lower first molar is lightly worn, moderately high-crowned, and lacks accessory cuspids and lophids. Measurements (in mm) of these molars are as follows: M1 anteroposterior length, 1.85; M1 transverse width, 1.15; M2 anteroposterior length, 1.45; M2 transverse width, 1.15; m1 anteroposterior length, 1.70; m1 transverse width, 0.95. As in the case of the *Reithrodontomys* specimens mentioned above, we can readily assign these specimens to the genus *Peromyscus* based on size, crown height, and molar morphology, but the sample is too small and incomplete to assign them to a species.

Subfamily Arvicolinae

*Microtus* sp. (vole)

Material.–OMNH 59512, right M3 (Fig. 5B).

Discussion.–The tooth measures 1.9 mm in anteroposterior length and 1.1 mm in transverse width. It has an anterior loop, two closed triangles, and a posterior loop with one weak reentrant labially and one lingually. The rootless (evergrowing) tooth overall has two labial and two lingual reentrant folds filled with cementum; no cementum occurs in the weak folds of the posterior loop.

The tooth is similar to *Microtus* (*Pitymys*) *pinetorum* and *M.* (*Pedomys*) *ochrogaster*, which tend to be distinct from most other voles in having M3 usually with only two closed triangles. Distinguishing these two species on dental characters is difficult or impossible, even when complete tooth rows are available (Guilday *et al.* 1978). Nor is it possible to differentiate among the numerous

species of *Microtus* with only an isolated M3. Both *M. pinetorum* and *M. ochrogaster* are common as Pleistocene fossils in the eastern United States.

Woodland voles (*M. pinetorum*) occur in the cave area today. As the name implies, they live in woodlands, especially in dry, mature deciduous forests where they make burrows on the forest floor in leaf litter (Semken 1984). Prairie voles (*M. ochrogaster*) are known in the general region of Sassafras Cave (in Cherokee County, immediately west of Adair County). There they select dry grasslands with enough grass to cover their runways and enough soil for their burrows; they never utilize wooded regions (Semken 1984).

Order Perissodactyla
Family Tapiridae
*Tapirus veroensis* (extinct tapir)

Material.–OMNH 59528, partial skeleton (Figs.6-10) including: left dentary with p2-m3; mandibular symphysis with right alveolus for i1, broken i2, root for i3, and intact c1; anterior fragment of right maxilla with C1-P2; posterior fragment of right maxilla with M1 and separate crown of M2 or M3; right and left petrosals; partial atlas; several other vertebral fragments; small fragments of ribs; partial head and distal fragment with trochlea of left humerus; distal portions of left radius and ulna; nearly complete right humerus (proximal end damaged); complete right radius and ulna; shaft of left femur missing both ends; entire left leg skeleton distal to the middle of the tibia and fibula (found in articulation; Fig.7); partial left manus including scaphoid, lunar, trapezoid, unciform, and metacarpals II, IV, and V (metacarpal IV is rodent-gnawed and chipped); partial right manus including scaphoid, cuneiform, pisiform, fragment of magnum, metacarpal III; several phalanges; sesamoids.

Discussion.– The bones are all part of one associated skeleton of a young adult. The epiphyses of all preserved bones are fully fused, and the m3 is erupting but its cross-crests are unworn. The cross-lophs of m2 are very lightly worn. Strong facets are worn into the anterior face of the c1 and the lateral side of i2 where these teeth occluded with the I3. The crown of the i2 is not *in situ* but is preserved separately. The M2 is lightly worn and M1 moderately worn.

The P1, preserved in an anterior fragment of the maxilla, is roughly triangular in occlusal outline and is not molariform. The P2 is subquadrate and fully molariform. In a separate, posterior fragment of the right maxilla, the two remaining molars can be identified as M1 and M2 based on their position relative to the anterior base of the zygomatic arch and the fact that the tooth identified as M2 has an interdental contact facet on its posterior side. The M3 was not recovered. The interdental contact facet on the anterior side of the M2 fits perfectly against the facet on the posterior of the M1 when these teeth are manually fitted together, although the M2 is not *in situ* and the remnants of its roots no longer reach their alveoli in the maxilla because of breakage and abrasion that occurred to the tooth after death and decomposition of the carcass.

Portions of the appendicular skeleton (distal parts of the arms and legs) were articulated, vertically oriented (more or less in a standing position), and well preserved where they were embedded in the cave mud. In strong contrast, the axial skeleton, girdle elements, and proximal segments of the limbs are much more poorly preserved or absent. The left rear leg was intact and articulated from the middle of the tibia and fibula distad, but the proximal halves of the tibia and fibula are absent (Figs.7 & 8). The left femur is represented by a large portion of the shaft but is missing both ends. Judging from the lighter color of the joint areas on the right forelimb (which match the preservation in the hind limb bones), it, too, was articulated or nearly so from the humerus distad. The proximal end of the right humerus is damaged

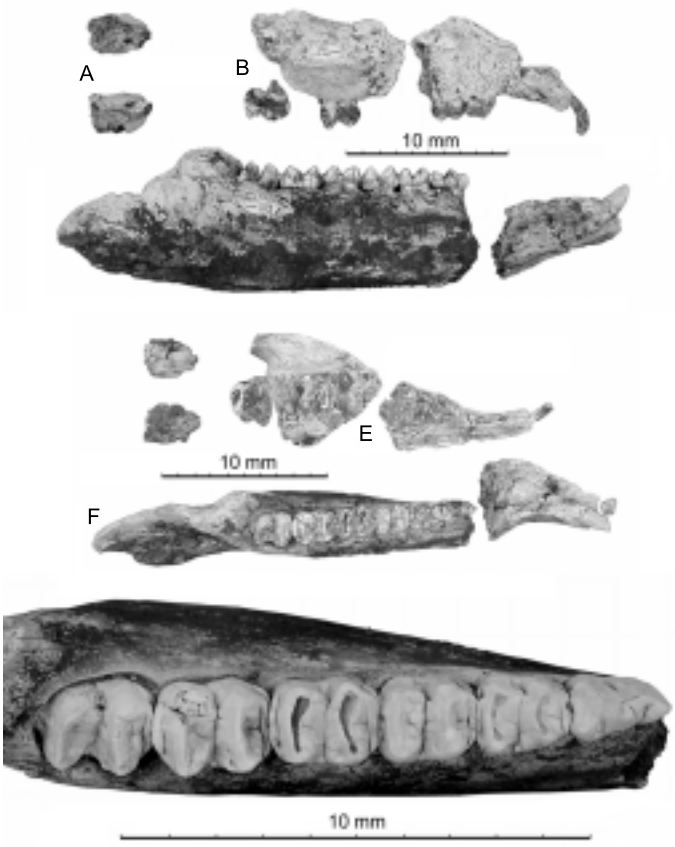


**Figure 6. *Tapirus veroensis*, OMNH 59528, cranial and jaw fragments in lateral view (A-C), and occlusal view (D-G). Photos show (A, D) right and left petrosals, (B, E) right M2 or M3, and right maxilla fragments with M1 and C1-P2, (C, F) left mandibular ramus with p2-m3, and mandibular symphysis with right i2 and c1. G, close-up occlusal view of lower left cheek teeth; the teeth were coated with ammonium chloride to show surface details.**

but the remainder of the bone is well preserved.

Unquestionably, this mode of preservation indicates that the animal died where its remains were found. The limbs were embedded in mud at or near the time of death and, after decomposition of the flesh the bones, remained in "life position" to the present day. It is unlikely that an animal that habitually spends much of its life wading and foraging in pools and ponds would have died from being entrapped by the sticky, fine cave mud. More likely it died of starvation, or perhaps of injuries sustained in a fall in the cave, while standing or lying in the mud or in a pool of water. The torso of its carcass and the proximal segments of its limbs were probably above the surface of this mud when it died. After the flesh decomposed, the distal limb bones embedded in the mud were preserved well, but the axial skeleton and proximal limb bones were apparently exposed to weathering within the cave. This resulted in the washing away of many axial skeletal elements and poor preservation of the few remaining pieces, which were later buried by additional mud until they were discovered and excavated.

In reviews of late Cenozoic tapirs of North America, Ray and Sanders (1984) and Jefferson (1989) each recognized a large and a small species of tapir based mainly on dental and cranial remains. In

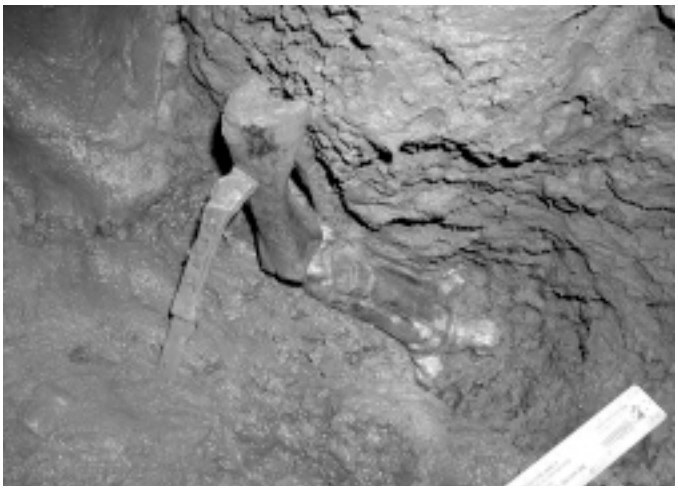

**Figure 7. *Tapirus veroensis*, OMNH 59528, lower portion of left hind leg skeleton as found articulated in the terrace deposit in Sassafras Cave. Distal halves of tibia and fibula are vertical. Knife propped against distal tibia is 18 cm long.**


**Figure 8. *Tapirus veroensis*, OMNH 59528, bony elements of the left hind limb. Distal limb elements are well preserved, but the femur (at right) is weathered and missing both ends.**

the central and eastern United States, Ray and Sanders (1984) called the larger early Pleistocene (Irvingtonian land mammal age) species *Tapirus haysii* and the smaller late Pleistocene (late Irvingtonian and Rancholabrean land mammal ages) one *T. veroensis*. In western North America, west of the Rocky Mountains, Jefferson (1989) called the large Plio-Pleistocene species *Tapirus merriami* and the smaller one *Tapirus californicus*. *Tapirus veroensis* is indistinguishable in size from *T. californicus*, and *T. veroensis* may eventually become a junior synonym of *T. californicus* if more diagnostic specimens of *T. californicus* are found (Jefferson 1989). Several cryptic species of fossil tapirs could actually be represented by the numerous fragmentary teeth and jaws found in Pleistocene deposits in the USA if living

**Table 3. Cranial measurements in mm of *Tapirus veroensis* (OMNH 59528) from Sassafras Cave, Oklahoma. Measurements follow those made by Hulbert (1995). Measurements in parentheses represent estimates of broken specimens.**

| | |
|---|---|
| Upper canine alveolar length | 6.7 |
| Upper canine alveolar width | 6.5 |
| Mandibular depth measured anterior to p2 | (54.7) |
| Mandibular depth measured posterior to m3 | 72.9 |
| Length of lower cheek tooth series (p2-m3 length) | 134.7 |
| Length of lower premolar series (p2-p4 length) | 62.6 |
| Length of lower molar series (m1-m3 length) | 72.2 |
| Lower canine alveolar length | 13.7 |
| Lower canine alveolar width | 12.4 |
| Symphysial width across the lower canines | (46.2) |
| Length of the mandibular symphysis | (75.0) |
| Diastema length between C1 and P1 alveoli | (48.4) |

Central and South American *Tapirus* species are used as examples. As pointed out by Ray and Sanders (1984), the three species of tapirs living today in northern Colombia are easily differentiated in the flesh and by cranial characters, but they overlap broadly in most dental characters (Hershkovitz 1954). Numerous species names have already been applied to relatively abundant tapir fossils across the USA and Mexico, but most of the material is inadequate for specific identification. In the meanwhile, *T. veroensis* is the name that has been widely applied to small eastern U.S. tapirs.

The Sassafras Cave tapir compares favorably in the dimensions of its teeth and jaws with the small Pleistocene tapirs of the central and eastern United States (Tables 3-5). There is only one other adult tapir from the Ozark Highland that includes parts of the postcranial skeleton (Oesch 1967; Parmalee *et al.* 1967), and that specimen is larger than the Sassafras Cave specimen in most available measurements (Tables 4 & 5). Accordingly, we tentatively assign the Sassafras Cave specimen to *T. veroensis*. *Tapirus veroensis* is primarily known from sites of Rancholabrean age (Ray & Sanders 1984; Hulbert 1995); therefore, we also tentatively assign the Sassafras Cave faunal assemblage to the Rancholabrean.

## DISCUSSION

The Sassafras Cave faunule is the first Pleistocene mammalian assemblage to be described from the Ozark Highland in Oklahoma. In fact, previous authors recorded only one Pleistocene vertebrate, the giant short-faced bear, *Arctodus simus*, from a cave in this part of Oklahoma (Puckette 1976; Smith & Cifelli 2000). Martin and Naples (1999) noted that there was a gap in the distribution of tapirs in eastern North America in the late Pleistocene. At that time, tapirs occurred nearly to the continental glacier front except for an area more-or-less centered along what is now the Oklahoma-Arkansas political boundary. They suggested that Pleistocene tapirs in North America were more limited by the density of aquatic-margin vegetation than by temperature. In any case, this record from Sassafras Cave, Oklahoma, and that of Martin and Naples (1999) from Kansas now fill the former gap in the


**Figure 9. *Tapirus veroensis*, OMNH 59528, bony elements of the forelimbs including complete right humerus, radius, and ulna, distal left radius and ulna, and several carpals, metacarpals, and manual phalanges.**

Pleistocene distribution of tapirs.

Outside of caves, there were three previous localities in which Pleistocene tapirs occurred in Oklahoma. Two of these localities yielded early Pleistocene (Irvingtonian) specimens and one is of unknown age. One Irvingtonian record is at Bowles gravel pit near Chickasha, Grady County, where a palate with all the cheek teeth (OMNH 9568) and an isolated left metatarsal III (OMNH 16504) were found (Stovall & Johnston 1934; Strain 1937). The other Irvingtonian record of

**Table 4. Tooth measurements in mm of *Tapirus veroensis* (OMNH 59528) from Sassafras Cave, Oklahoma, and of another adult specimen (CM 159; Central Missouri State College, Warrensburg, Missouri) from Crankshaft Cave, Missouri, as provided by Oesch (1967) and Parmalee *et al.* (1967).**

| | length | | anterior width | | posterior width | |
|---|---|---|---|---|---|---|
| Tooth | OMNH 59528 | CM 159 | OMNH 59528 | CM 159 | OMNH 59528 | CM 159 |
| P1 | 18.3 | 21.2 | 12.0 | 12.5 | 15.7 | 18.8 |
| P2 | 19.0 | 20.0 | 21.2 | 23.4 | 23.1 | 15.0 |
| M1 | 23.2 | 22.7 | 26.6 | 27.3 | 23.8 | 25.0 |
| M2 | 26.0 | 25.3 | 28.6 | 30.9 | 24.9 | 27.0 |
| p2 | 21.4 | 24.7 | 11.2 | — | 14.3 | 16.5 |
| p3 | 20.3 | 22.3 | 15.6 | 16.8 | 17.1 | 19.3 |
| p4 | 21.1 | 21.3 | 18.4 | 20.4 | 18.5 | 21.3 |
| m1 | 23.0 | 28.7 | 18.9 | 19.9 | 17.6 | 19.2 |
| m2 | 25.2 | 26.3 | 19.8 | 21.8 | 18.9 | 21.3 |
| m3 | 24.8 | — | 19.2 | — | 17.1 | — |

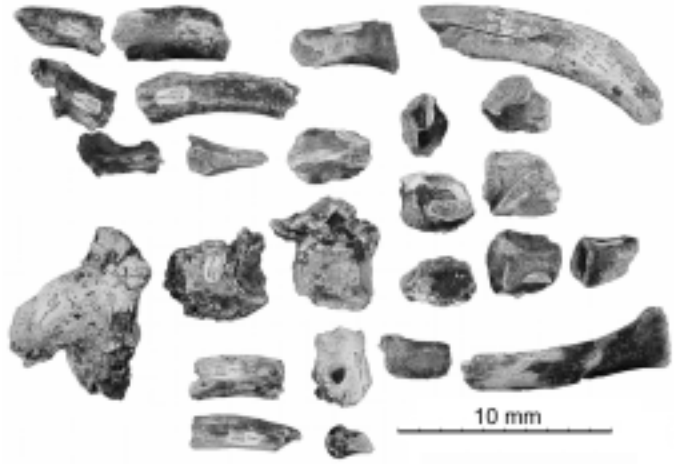


**Figure 10. *Tapirus veroensis*, OMNH 59528, selected elements from the axial skeleton showing poor preservation. Atlas fragment at lower left.**

*T. haysii* is from the Holloman gravel pit near Frederick, Tillman County, where a right dentary containing dp3, dp4, p3, p4, and m1 was found (Midwestern State University specimen no. 9238, now housed at the Texas Memorial Museum; Hay & Cook 1930; Dalquest 1977; Ray & Sanders 1984). All three of these specimens represent *Tapirus haysii* and are larger than the Sassafras Cave tapir. The third locality was reported by Troxell (1917), who merely included "tapir" among a list of other fossil vertebrates from a channel-fill deposit near Mulhall, Logan County, but gave no other information. The whereabouts of the Mulhall specimen, the skeletal element and species represented, and age of this specimen are unknown.

Beyond Oklahoma, other Ozark Highland records of Pleistocene tapirs include Peccary Cave and Ten Mile Rock in Arkansas, and Crankshaft Cave, Boney Spring, Jones Spring, and Enon Sink in Missouri (Mehl 1962; Oesch 1967; Parmalee *et al.* 1967; Saunders 1977; Faunmap Working Group 1994), but records of the genus *Tapirus* are widespread elsewhere in Pleistocene localities across the southern half of the United States (except in mountainous regions of the West) and Mexico (Kurtén & Anderson 1980; Jefferson 1989; Faunmap Working Group 1994; Arroyo-Cabrales *et al.* 1996).

## ACKNOWLEDGMENTS

We thank Sylvia Russell for help in collecting and for generously donating fossils to OMNH, Steve Hensley for help in field work and logistics, and William Caire for initial contacts. Kyle Davies enthusiastically aided in the field work and Bill May picked and sorted the screenwashed matrix. Don G. Wyckoff kindly gave his time to field-judge the sediment samples from the cave. The OMNH provided funds for the analysis preliminary to attempting AMS radiometric dating. Chris Bell and Frederick Grady provided thoughtful and helpful reviews that improved the paper.

**Table 5. Measurements of postcranial bones (in mm) of *Tapirus veroensis* (OMNH 59528) from Sassafras Cave, Oklahoma. Measurements follow those made by Hulbert (1995), where preserved in the Oklahoma specimen. Abbreviations: trw = transverse width; apl = anteroposterior length. Measurements of another adult specimen (CM 159; Central Missouri State College, Warrensburg, Missouri) from Crankshaft Cave, Missouri, as given by Oesch (1967) and repeated by Parmalee *et al.* (1967), are provided in brackets for comparison, where available.**

| | Humerus | Radius | Femur | Tibia |
|---|---|---|---|---|
| Greatest length | | 222.2 | | |
| Midshaft transverse width | 31.5 [34.0] | 29.6 | 39.0 | 30.2 |
| Midshaft anteroposterior length | 37.4 | 21.0 | 35.3 [34] | 32.5 |
| Proximal articular width | | 54.1 | | |
| Proximal articular apl | | 30.1 | | |
| Greatest distal width | 70.8 | 60.8 | | 52.7 |
| Width of distal articular surface | 54.9 | | | |
| Distal apl | | 37.9 | | 43.5 |

| Metacarpal | II | III | IV | V |
|---|---|---|---|---|
| Greatest length | 99.3 [111.7] | 120.8 [135.2] | 97.1 [106.9] | 74.2 [83.4] |
| Midshaft trw | 20.3 | 28.6 | 19.8 | 12.2 |
| Midshaft apl | 12.0 | 13.4 | 12.3 | 10.8 |
| Proximal articular width | 22.9 | 31.7 | 21.3 | 15.1 |
| Proximal articular apl | 20.5 | 24.0 | 23.0 | 20.8 |
| Distal articular width | 20.7 | 29.1 | 21.0 | 17.7 |
| Distal articular apl | 23.1 | 22.8 | 21.9 | 19.2 |

| | Astragalus | Calcaneus |
|---|---|---|
| Greatest length | | 106.6 [110] |
| Medial length | 53.3 | |
| Lateral length | 61.6 [64] | |
| Medial length of trochlea | 43.7 | |
| Greatest transverse width | 56.4 [53] | 49.3 |
| Greatest apl | | 49.1 |
| Distal articular width | 49.2 | |
| Distal articular apl | 27.2 | |

| Metatarsal | II | III | IV |
|---|---|---|---|
| Greatest length | 102.3 [114] | 120.1 [133] | 103.6 [114] |
| Midshaft trw | 19.6 | 26.3 | 18.7 |
| Midshaft apl | 13.8 | 16.3 | 14.0 |
| Proximal arcticular width | 18.5 | 31.9 | 23.4 |
| Proximal arcticular apl | 25.9 | 33.9 | 25.4 |
| Distal articular width | 21.4 | 30.2 | 21.4 |
| Distal apl | 25.6 | 25.2 | 25.5 |

## REFERENCES


Akersten, W.A., 1981, A graphic method for describing the lateral profile of isolated rodent incisors: Journal of Vertebrate Paleontology, v. 1, p. 231-234.

Anderson, E., 1968, Fauna of the Little Box Elder Cave, Converse County, Wyoming: University of Colorado Studies, Series of Earth Sciences, v. 6, p. 1-59.

Arroyo-Cabrales, J., Polaco, O.J., Alvarez, T., & Johnson, E., 1996, New records of fossil tapir from northeastern Mexico: Current Research in the Pleistocene, v. 13, p. 93-95.

Barlow, C., 2000, The ghosts of evolution: Nonsensical fruit, missing partners, and other ecological anachronisms: New York, Basic Books, 291 p.

Black, C.C., 1963, A review of the North American Tertiary Sciuridae: Bulletin of the Museum of Comparative Zoology, Harvard University, v. 130, p. 109-248.

Brack, V., Jr., & Mumford, R.E., 1984, The distribution of *Pipistrellus subflavus* and the limit of the Wisconsinan glaciation: An interface: American Midland Naturalist, v. 112, p. 397-401.

Bretz, J H., 1942, Vadose and phreatic features of limestone caverns: Journal of Geology, v. 50, p. 675-811.

Brod, L.G., Jr., 1999, Sedimentation in Missouri caves: Missouri Speleology, v. 39, p. 1-51.

Caire, W., Tyler, J.D., Glass, B.P., & Mares, M.A., 1989, Mammals of Oklahoma: Norman, University of Oklahoma Press, 567 p.

Dalquest, W.W., 1977, Mammals of the Holloman local fauna, Pleistocene of Oklahoma: The Southwestern Naturalist, v. 22, p. 255-268.

Dalquest, W.W., & Baskin, J.A., 1992, Mammals of the Elm Creek local fauna, late Pleistocene of Beaver County, Oklahoma: American Midland Naturalist, v. 127, p. 13-20.

Faunmap Working Group 1994, Faunmap: A database documenting late Quaternary distributions of mammal species in the United States: Illinois State Museum Scientific Papers no. 25(1-2), p. 1-670.

Fujita, M.S., & Kunz, T.H., 1984, *Pipistrellus subflavus*: Mammalian Species no. 228, p. 1-6.

Gordon, C.L., & Czaplewski N.J., 2000, A fossil marmot from the late Miocene of western Oklahoma: Oklahoma Geology Notes, v. 60, p. 28-32.

Guilday, J.E., Hamilton, H.W., Anderson, E., & Parmalee, P.W., 1978, The Baker Bluff Cave deposit, Tennessee, and the late Pleistocene faunal gradient: Bulletin of Carnegie Museum of Natural History no. 11, p. 1-67.

Hay, O.P., & Cook, H.J., 1930, Fossil vertebrates collected near or in association with human artifacts at localities near Colorado, Texas; Frederick, Oklahoma; and Folsom, New Mexico: Proceedings of the Colorado Museum of Natural History, v. 9, p. 17-18.

Hedges, J., Russell, B., Thrun, B., & White, W.B., 1979, The 1976 NSS standard map symbols: National Speleological Society Bulletin, v. 41, p. 35-43.

Hershkovitz, P., 1954, Mammals of northern Colombia, preliminary report no. 7: Tapirs (genus *Tapirus*), with a systematic review of American species: Proceedings of the United States National Museum, v. 103, p. 465-496.

Holman, J.A., 1995, Pleistocene amphibians and reptiles of North America: New York, Oxford University Press, 243 p.

Hulbert, R.C., Jr., 1995, The giant tapir, *Tapirus haysii*, from Leisey Shell Pit 1A and other Florida Irvingtonian localities: Bulletin of the Florida Museum of Natural History, v. 37 Part II, p. 515-551.

Hulbert, R.C., Jr., 2001, The fossil vertebrates of Florida: Gainesville, University Press of Florida, p. 350.

Jefferson, G.T., 1989, Late Cenozoic tapirs (Mammalia: Perissodactyla) of western North America: Contributions in Science, Natural History Museum of Los Angeles County no. 406, p. 1-22.

Jennings, J.N., 1985, Karst geomorphology: New York, Basil Blackwell, 293 p.

Kurtén, B., & Anderson, E., 1980, Pleistocene mammals of North America: New York, Columbia University Press, 443 p.

Logan, L.E., & Black, C.C., 1979, The Quaternary vertebrate fauna of Upper Sloth Cave, Guadalupe Mountains National Park, Texas, *in* Genoways, H.H., & Baker, R.J., eds., Biological investigations in the Guadalupe Mountains National Park, Texas: National Park Service, Proceedings and Transactions Series no. 4, p. 141-158.

Martin, L.D., & Naples, V., 1999, A sabre-tooth tiger and the first record of a tapir from the Pleistocene of Kansas: Current Research in the Pleistocene, v. 16, p. 126-127.

Mehl, M.G., 1962, Missouri's Ice Age animals: Rolla, Missouri, Missouri Department of Business and Administration, Division of Geological Survey and Water Resources, 104 p.

Miller, G.S., Jr., & Allen, G.M., 1928, The American bats of the genera *Myotis* and *Pizonyx*: United States National Museum Bulletin, v. 144, p. 1-218.

Oesch, R.D., 1967, A preliminary investigation of a Pleistocene vertebrate fauna from Crankshaft Pit, Jefferson County, Missouri: National Speleological Society Bulletin, v. 29, p. 163-185.

Parmalee, P.W., Oesch, R.D., & Guilday, J.E., 1969, Pleistocene and Recent vertebrate faunas from Crankshaft Cave, Missouri: Illinois State Museum Reports of Investigations no. 14, p. 1-37.

Puckette, W.L., 1976, Notes on the occurrence of the short-faced bear (Arctodus) in Oklahoma: Proceedings of the Oklahoma Academy of Science, v. 56, p. 67-68.

Ray, C.E., 1965, A new chipmunk, *Tamias aristus*, from the Pleistocene of Georgia: Journal of Paleontology, v. 39, p. 1016-1022.

Ray, C.E., & Sanders, A.E., 1984, Pleistocene tapirs in the eastern United States, *in* Genoways, H.H., and Dawson, M. R., ed., Contributions in Quaternary vertebrate paleontology: A volume in memorial to John E. Guilday: Pittsburgh, Special Publication of Carnegie Museum of Natural History no. 8, p. 283-315.

Reams, M.W., Undated [probably 1999], Cave sediments and the geomorphic history of the Ozarks: Missouri Speleology, v. 38, no. 1-4, p. 1-97.

Saugey, D.A., Baber, R.H., & McDaniel, V.R., 1978, An unusual accumulation of bat remains from an Ozark cave: Proceedings of the Arkansas Academy of Sciences, v. 32, p. 92-93.

Saunders, J.J., 1977, Late Pleistocene vertebrates of the western Ozark Highland, Missouri: Illinois State Museum Reports of Investigations no. 33, p. 1-118.

Sealander, J.A., & Young, H., 1955, Preliminary observations of the cave bats of Arkansas: Proceedings of the Arkansas Academy of Sciences, v. 7, p. 21-31.

Semken, H.A., Jr., 1984, Paleoecology of a late Wisconsinan/Holocene micromammal sequence in Peccary Cave, northwestern Arkansas, *in* Genoways, H.H., & Dawson, M.R., eds., Contributions in Quaternary vertebrate paleontology: A volume in memorial to John E. Guilday: Pittsburgh, Special Publication of Carnegie Museum of Natural History no. 8, p. 405-431.

Simpson, G.G., 1945, Notes on Pleistocene and Recent tapirs: Bulletin of the American Museum of Natural History no. 86, p. 37-81.

Smith, K.S., & Cifelli, R.L., 2000, A synopsis of the Pleistocene vertebrates of Oklahoma: Oklahoma Geological Survey Bulletin, v. 147, p. 1-36.

Stovall, J.W., & Johnston, C.S., 1934, *Tapirus haysii* of Oklahoma: American Midland Naturalist, v. 15, p. 92-93.

Strain, W.L., 1937, The Pleistocene geology of part of the Washita River Valley, Grady County, Oklahoma [Masters thesis]: University of Oklahoma, 102 p.

Troxell, E.L., 1917, An Oklahoma Pleistocene fauna: Bulletin of the Geological Society of America, v. 28, p. 212.

van Zyll de Jong, C.G., 1984, Taxonomic relationships of Nearctic small-footed bats of the *Myotis leibii* group (Chiroptera: Vespertilionidae): Canadian Journal of Zoology, v. 62, p. 2519-2526.

Zeimens, G., & Waller, D.N., 1974, Preliminary archaeological and paleontological investigations, *in* Wilson, M., ed., Applied geology and archaeology. The Holocene history of Wyoming: Geological Survey of Wyoming Reports of Investigations v. 10, p. 88-90.

L. Bruce Railsback, Adel A. Dabous, J.K. Osmond, and C.J. Fleisher - Petrographic and geochemical screening of speleothems for U-series dating: An example from recrystallized speleothems from Wadi Sannur Cavern, Egypt. *Journal of Cave and Karst Studies 64*(2): 108-116.

# PETROGRAPHIC AND GEOCHEMICAL SCREENING OF SPELEOTHEMS FOR U-SERIES DATING: AN EXAMPLE FROM RECRYSTALLIZED SPELEOTHEMS FROM WADI SANNUR CAVERN, EGYPT

L. Bruce Railsback[1], Adel A. Dabous[2], J.K. Osmond[2], and C.J. Fleisher[1]
[1]*Department of Geology, University of Georgia, Athens, Georgia 30602-2501 USA*
[2]*Department of Geological Sciences, Florida State University, Tallahassee, Florida 32306-4100 USA*

*Petrographic and geochemical analyses of four speleothems from Wadi Sannur Cavern in eastern Egypt show that petrography and geochemistry can provide a useful way to screen speleothems prior to dating via U-series analysis. The speleothems vary from inclusion-rich zoned calcite to clear featureless calcite. U concentrations (ranging from 0.01-2.65 ppm) and Sr concentrations (ranging from 0.00-0.11 wt%) are greater in inclusion-rich zoned calcite. U concentrations are also greater in speleothems with small (<1.2 mm wide) columnar calcite crystals than in speleothems with larger crystals. Mg concentrations in the speleothems range from 0.2-2.3 mol% $MgCO_3$ and show no significant relationship to petrography at the microscopic scale. Geochemical considerations suggest that the Wadi Sannur speleothems were originally mostly aragonite, and that all four have undergone recrystallization. More generally, they suggest that coarse clear columnar calcite and large (>1.0 ppm) ranges of U concentration are warning signs of recrystallization and U loss. However, even finer grained, inclusion-rich columnar calcite may be the result of recrystallization while retaining U contents less depleted than those of associated clear calcite.*

Radiometric dating is an essential component in the application of speleothems to paleoenvironmental studies. Such dating, when applied to entire speleothems, allows determination of speleothem growth periods that have been interpreted as wetter phases (e.g., Brook *et al.* 1997). It also allows calibration of paleoenvironmental conditions based on time-series records within individual speleothems (e.g., Dorale *et al.* 1992, 1998). U-series dating is one of the most valuable dating methods, because it yields ages up to roughly 500 ka (Edwards *et al.* 1987) that are readily applicable to Quaternary studies and particularly to the last few glacial-interglacial cycles (Imbrie *et al.* 1993).

Accurate U-series dating requires that isotopic compositions evolve under closed chemical conditions. Loss of U during recrystallization of aragonite, high-Mg calcite, or fine-grained calcite may result in calculated $^{230}Th/U$ dates that do not represent true depositional ages. The $UO_2^{2+}$ cation, like most oxocomplexes of cations of high ionic potential, is relatively soluble (Langmuir 1978). It is, therefore, readily mobilized by diagenetic solutions and can be leached from speleothems. On the other hand, $Th^{4+}$ is effectively insoluble in most aqueous environments (Kaufman 1969) and commonly remains in carbonates undergoing recrystallization. As a result, diagenetically modified speleothems may have chemically altered $^{230}Th/^{234}U$ ratios that yield anomalously old radiometric ages. For example, Dabous and Osmond (2000) analyzed 32 samples from 8 speleothems from Wadi Sannur Cavern in Egypt and found that 11 of the samples had $^{230}Th/^{234}U$ activity ratios greater than 1 at the 95% confidence level, indicative of U loss in the past. The obvious enhancement of $^{230}Th/^{234}U$ ratios in those samples and likely enhancement of the rest allowed Dabous and Osmond only to infer that the remaining samples were also affected by secondary U mobility and that the dates calculated from $^{230}Th/^{234}U$ - $^{234}U/^{238}U$ activity ratios were probably maximum depositional ages. Other workers commonly report similar problems with U loss and resulting questionable radiometric ages (e.g., Openshaw *et al.* 1996; Whitehead *et al.* 1999). Such problems do not, of course, mean that all U-series ages are suspect, because U-series data can be checked using the $\gamma_0$ test (e.g., Ludwig *et al.* 1992; Szabo *et al.* 1994; Ludwig & Paces 2002).

The possibility of U loss in some speleothems during recrystallization makes methods to recognize such speleothems very desirable. This paper reports the petrography and geochemistry of some of the speleothems studied by Dabous and Osmond (2000), with the goal of identifying telltale characteristics of recrystallized speleothems. The results suggest that petrography and geochemistry can indeed be useful in recognizing recrystallized material and in avoiding wasted effort in dating of that material. They further suggest that recrystallization yielding columnar, and seemingly primary, calcite may be more common than frequently thought.

## Materials, methods, and previous reports

Speleothems 7, 9, 12, and 13 from Wadi Sannur Cavern in northeastern Egypt were described and analyzed previously for U-series isotopes by Dabous and Osmond (2000) and provided the material studied in this project. Dabous and Osmond (2000) divided each speleothem into at least three samples of


Copyright © 2002 by The National Speleological Society

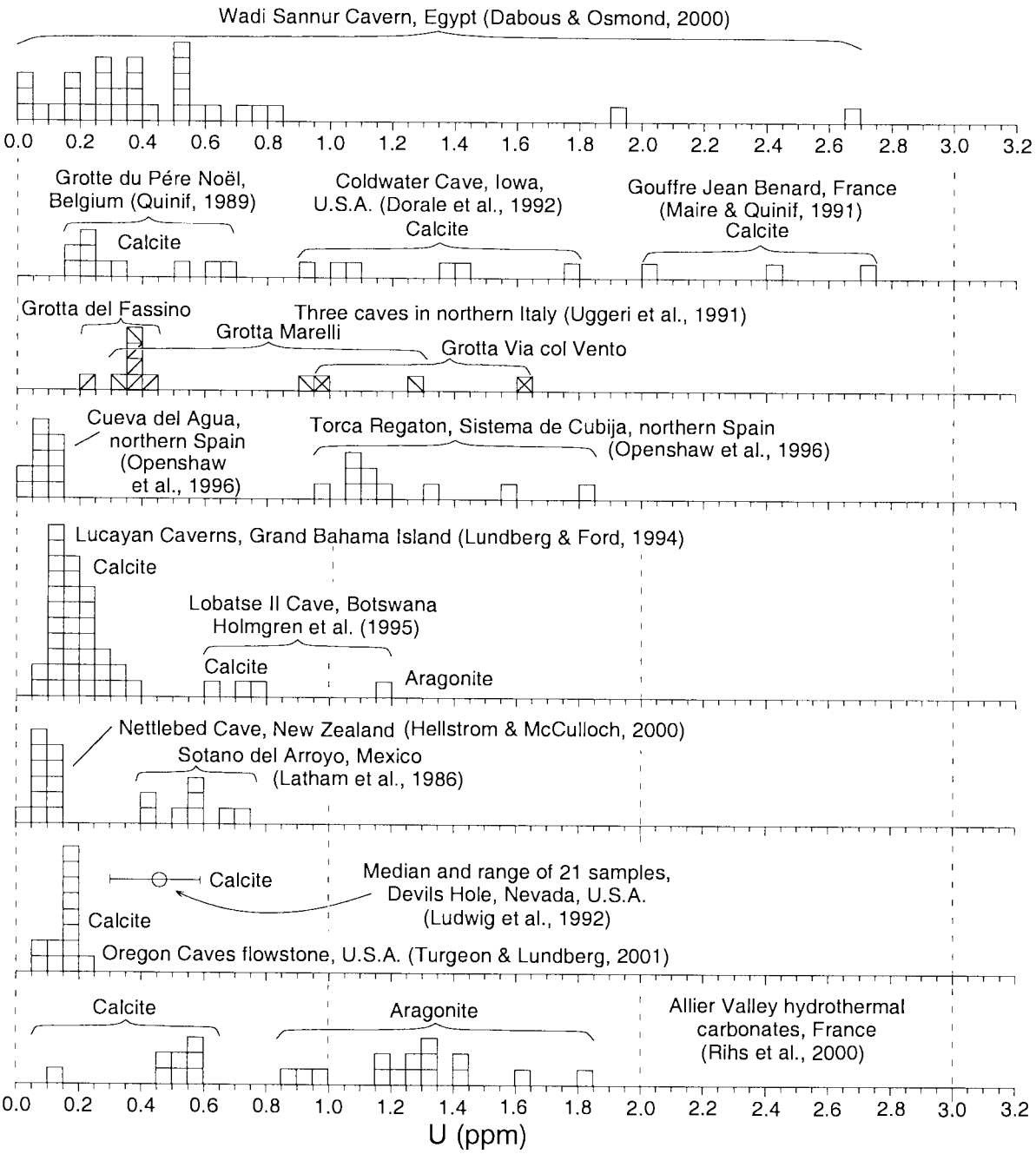


**Figure 1. Histograms of U concentrations in speleothems (upper 7 histograms) and other terrestrial carbonates (lowest histogram) reported in various studies. Each square represents one analysis. Mineralogy is indicated where reported in the original reference. Note broad range of concentrations from Wadi Sannur samples.**

10-20 gm each, and they recorded the position of those samples as "inner" (i.e., near the core of the speleothem), "middle", and "outer". Their Table 1 listed U and Th concentrations, $^{234}U/^{238}U$ and $^{230}Th/^{234}U$ activity ratios determined by alpha spectrometry, and apparent ages for 32 samples from eight speleothems.

Detailed chemical analyses of polished C-coated thin sections of the speleothems were performed on a JEOL JXA 8600 electron microprobe using wavelength-dispersive spectrometers. All analyses were performed using a 15 kV accelerating voltage, a 10 nanoamp beam current, 20 second counting times, and natural carbonate standards (Jarosewich & Macintyre 1983; Jarosewich & White 1987). A 10 μm beam diameter was used to minimize volatilization during analysis. Our microprobe's software reports a minimum detection limit of ~0.05 wt% Sr, but our previous work (Brook *et al.* 1999: Fig. 4) indicates an MDL of ~0.02 wt% Sr and a 95% confidence interval of ~0.014 wt% Sr.

Samples of roughly 50 mg were drilled from each of the four speleothems with a dental drill. Mineralogy of these powders was determined by X-ray diffractometry using a Scintag XDS 2000 X-ray diffractometer. Hydrochloric acid dissolved 3.0 mg subsamples of the powders and the resulting solutions were analyzed using a Thermo Jarrell-Ash 965 inductively coupled argon plasma (ICP) spectrometer in the University of Georgia Chemical Analysis Laboratory. Results have standard

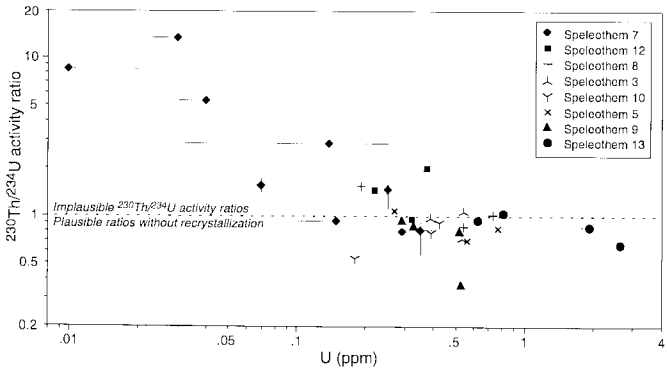


**Figure 2. Log-log plot of U concentrations and $^{230}Th/^{234}U$ activity ratios of 32 samples from eight speleothems from Wadi Sannur Cavern, Egypt. Filled symbols indicate data from speleothems examined in this study. Error bars are shown where uncertainties significantly exceed size of symbols. Note that a $^{230}Th/^{234}U$ activity ratio greater than 1 requires loss of U from the system or addition of Th to it. Data are from Dabous and Osmond (2000).**

errors of 0.46% for Ca, 0.30% for Mg, and 0.48% for Sr and have minimum detection limits of 0.001 wt% for Sr and 0.005 mol% $MgCO_3$ for Mg.

### U CONCENTRATIONS AND $^{230}TH/^{234}U$ ACTIVITY RATIOS

The U concentrations reported by Dabous and Osmond (2000) range from 0.01-2.65 ppm in a distribution with two outliers at its upper end (Fig. 1). The large range of these U concentrations contrasts sharply with ranges typically observed in speleothems and other terrestrial carbonates (Fig. 1). Consideration of data sets from several speleothems or suites of speleothems reveals a maximum range of only 0.87 ppm (Dorale *et al.* 1992), or only one third of the range in the Wadi Sannur samples. Uranium concentrations from aragonitic hydrothermal near-surface carbonates in France have a range of 0.94 ppm (Rihs *et al.* 2000), but even that range does not approach the range of U concentrations in the samples from Wadi Sannur Caverns.

$^{230}Th/^{234}U$ activity ratios show an inverse correlation with U concentrations in the Wadi Sannur samples (Fig. 2). Only (but not all) samples with U concentrations greater than 0.15 ppm have plausible $^{230}Th/^{234}U$ activity ratios (i.e., ratios ≤ 1.0), whereas the three samples with U concentrations less than 0.05 have $^{230}Th/^{234}U$ activity ratios in excess of 5.0. These observations are compatible with post-depositional U loss.

Uranium concentrations show no strong relationship to position within speleothems (Fig. 3). The mean concentrations of inner, middle, and outer samples are statistically unresolvable. Middle samples, which might be hypothesized to be most protected from recrystallizing waters, have both the highest U concentration reported and the three lowest values reported (Fig. 3).

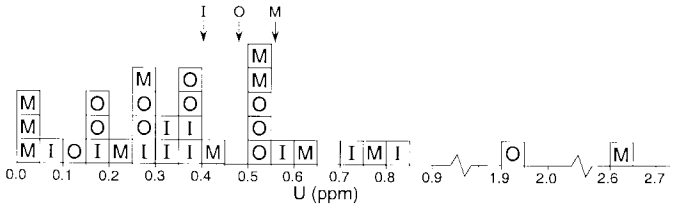


**Figure 3. Histogram of U concentrations of 32 samples from eight speleothems from Wadi Sannur Cavern, Egypt. Samples are coded by location within each speleothem: "I" = inner, "M" = middle, and "O" = outer. Arrows above histogram indicate means for each group. Data are from Dabous and Osmond (2000).**

### PETROGRAPHY

Petrography and X-ray diffraction indicate that the four speleothems examined in this study are all calcite, but their fabrics vary from inclusion-rich and zoned to clear and featureless. Macroscopically, transverse sections of Speleothem 13 show mostly light brown calcite with pronounced fine-scale zonation (Railsback 2000: Fig. B2). Microscopically, Speleothem 13 consists of elongate or columnar calcite crystals radiating from the speleothem's center. The columnar crystals are as much as 12 mm long and vary in width from 0.15 to 1.2 mm. They are inclusion-rich, rather than clear, and the inclusions consist of at least two types (Figs. 4A & 4B). One type is small (0.1 to 0.4 mm) subequant inclusions of opaque to translucent material. The other type is elongate to linear (typically 0.01 by 0.1 mm) liquid or gaseous inclusions oriented parallel to the long direction and extinction direction of the calcite crystals. Both kinds of inclusions define apparent growth zones that extend across calcite crystals and that can commonly be traced in concentric circles all the way around the central canal. None of the edges of the columnar calcite crystals coincide with the growth zones defined by inclusions.

Macroscopically, Speleothem 9 consists mostly of finely zoned light brown calcite, but the center is clear and vitreous (Railsback 2000: Fig. B2). A single crystal of clear calcite extends outward from the center of the speleothem across concentric zonations that appear to define the original wall of the central canal (Figs. 4C & 4D). Euhedral boundaries of that crystal extend across and into growth zones in inclusion-rich columnar calcite. Columnar calcite crystals that are 0.07 to 1.55 mm wide and as much as 10.1 mm long radiate outward from the central crystal. The interior portions of those columnar crystals are rich in both of the kinds of inclusions described with regard to Speleothem 13, and those inclusions likewise define concentric growth zones (Figs. 4C & 4D). The outer portions (i.e., nearest the outside of the speleothem) are generally inclusion-poor and locally clear. Some patterns of inclusions in the outer areas have the form of euhedral calcite terminations, whereas others appear to follow growth zonations that, if continuous, would define large concentric circles

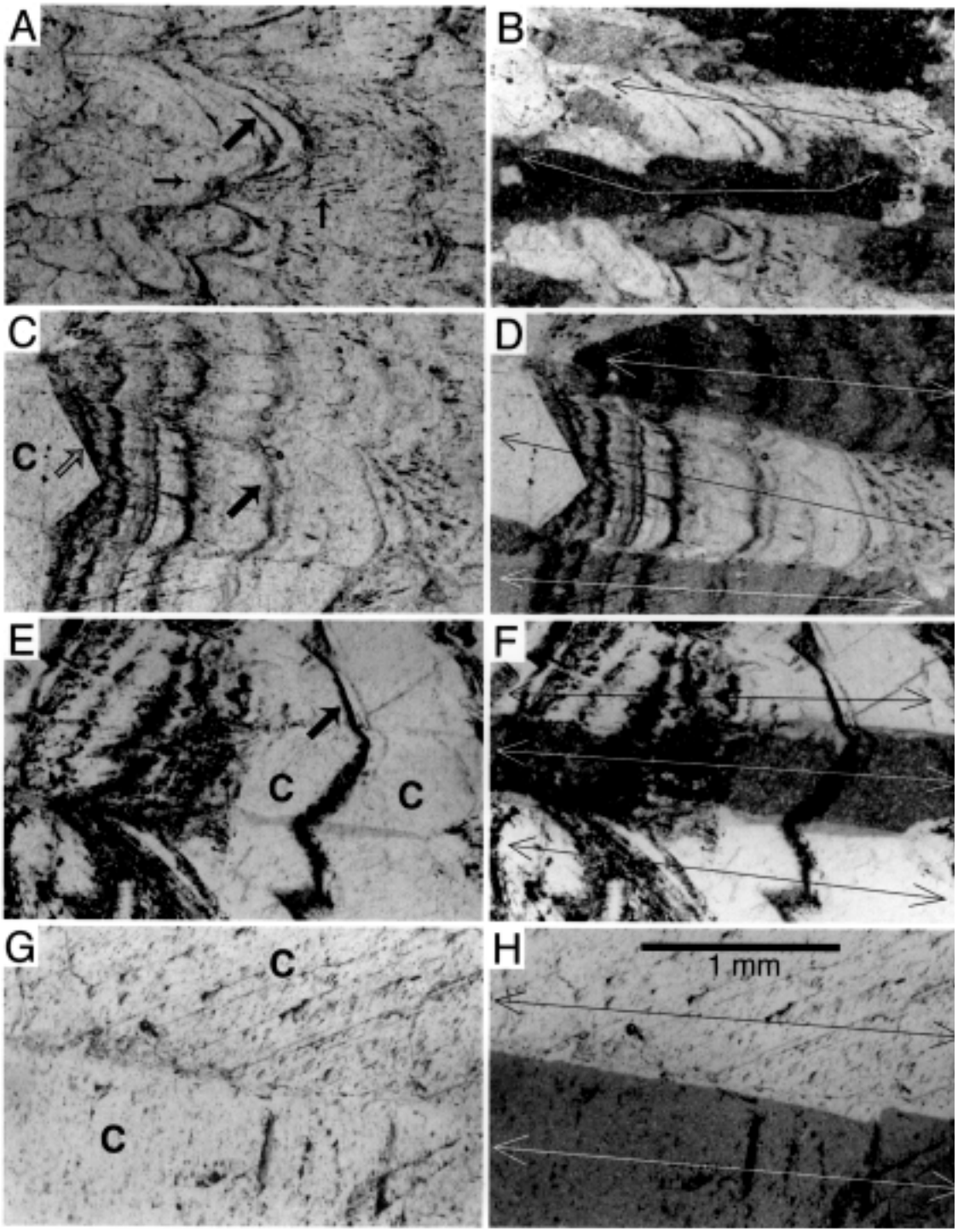


**Figure 4. Photomicrographs of speleothems studied. A and B: Speleothem 13. C and D: Speleothem 9. E and F: Speleothem 7. G and H: Speleothem 12. Photomicrographs in left column are in plane-polarized light; photomicrographs in right column are of same areas in cross-polarized light. Larger filled arrows in left column point to layers defined by small subequant inclusions; smaller filled arrows on left point to elongate to linear inclusions parallel to length of crystals; open arrow in C points to euhedral boundary in crystal that extends to left into central canal. "C" indicates clear calcite. Long thin arrows in right column indicate extent of single optically continuous crystals. In A through F, central canal is to left, just out of field of view. Scale bar in H applies to all eight photomicrographs.**

around the central canal.

Speleothem 7 macroscopically consists partly of light brown calcite with weakly defined zones and partly of clear to white calcite that is only locally zoned (Railsback 2000: Fig. B2). A few crystals of clear calcite extend outward across zones of inclusions that apparently define the original edge of the central canal. Columnar calcite crystals that are as much as 22 mm long and 0.2 to 1.8 mm wide radiate from the central canal (Figs. 4E & 4F). One zone within them is rich in small subequant inclusions of opaque to translucent material; that zone is ~3 mm thick. The rest of the columnar calcite is generally clear with at most a few linear and small subequant inclusions.

Speleothem 12 consists macroscopically of vitreous calcite in which zonation is only faintly recognizable. The speleothem consists of large crystals of columnar calcite that are up to 2.7 mm wide and some of which are at least 34 mm long. This calcite is almost entirely clear with only a few thin (≤ 0.15 mm) zones that contain inclusions (Figs. 4G & 4H).

In summary, the sequence of speleothems from 13 to 9 to 7

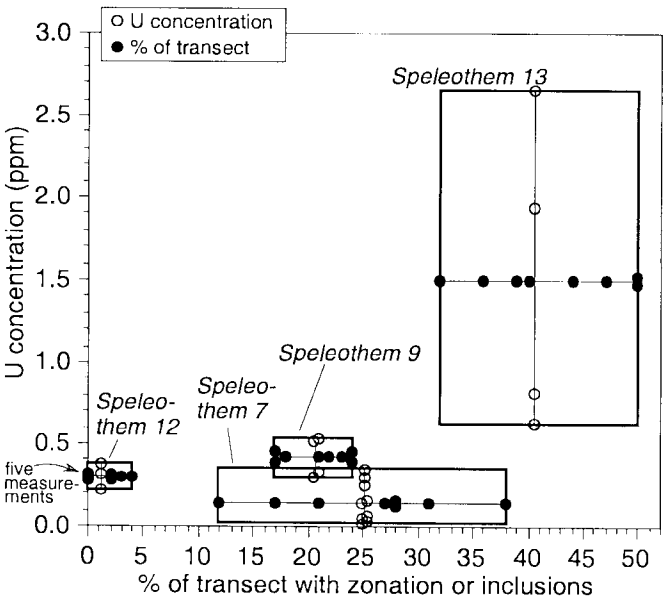


**Figure 5. Plot of U concentration (open symbols, on vertical axis) and extent of textural preservation (filled symbols, plotted on horizontal axis) of four speleothems from Wadi Sannur Cavern. Textural preservation was measured by examination of linear transects across thin sections and measurement of the proportion of each transect characterized by inclusion-rich or zoned calcite. Locations of U analyses did not coincide with locations of transects, so each variable is plotted against the average of the other (thin lines) to generate rectangles encompassing range for each speleothem. Some filled symbols have been moved vertically and some open symbols have been moved horizontally to avoid overlap. U concentration data are from Dabous and Osmond (2000).**

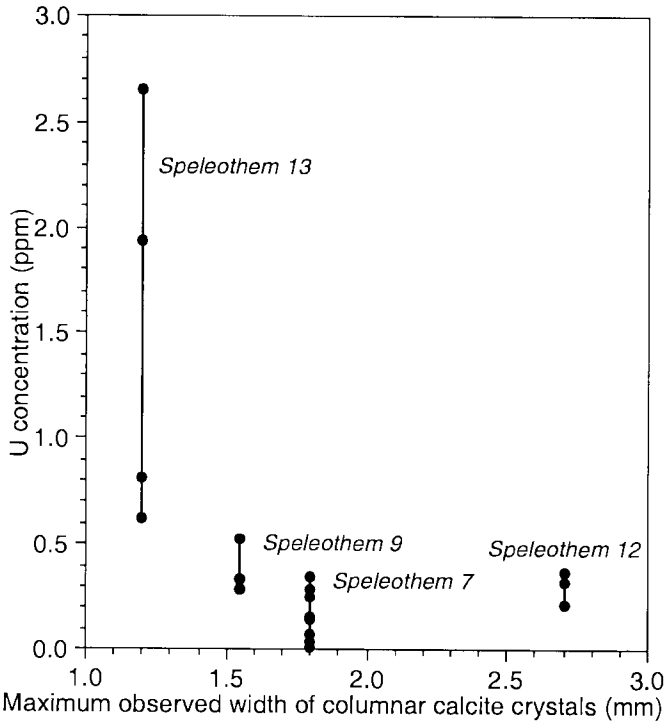


**Figure 6. Plot of U concentration (filled circles, on vertical axis) and maximum observed width of columnar crystals (vertical lines, on horizontal axis) of four speleothems from Wadi Sannur Cavern. U concentration measurements are from different parts of speleothems, whereas widths are one maximum from each speleothem, so multiple values of U concentration are plotted against one value of width for each speleothem. Widths are "maximum observed" because widths were measured in thin sections that may have not encountered the greatest crystal width in the entire speleothem. U concentration data are from Dabous and Osmond (2000).**

to 12 represents a spectrum from relatively small inclusion-rich crystals across which growth zonation is evident to relatively coarse clear crystals across which growth zonation is indistinct. None of the speleothems have detectable cathodoluminescence.

## RELATIONSHIPS BETWEEN PETROGRAPHY AND GEOCHEMISTRY

The trends in petrography described above are related to U concentration. For example, if randomly chosen linear transects are made across the speleothems and the percentage of each transect crossing zonation or inclusion-rich zones is measured, U concentration of the speleothems is less in speleothems with lower percentage of zoned and/or inclusion-rich material (Fig. 5). (Note that the scale of observation in the petrographic transects is similar to that of sampling to determine U concentrations). Uranium concentration also is less in speleothems with greater width of columnar calcite crystals (Fig. 6).

Petrography is also related to concentration of Sr at the microscopic scale. Microprobe analysis reveals that Sr concentration in inclusion-rich or zoned calcite ranges from 0.00-0.11 wt%, with a mean of 0.046 wt% (Fig. 7). Sr concentration in clear calcite ranges from 0.00-0.11 wt%, with a mean of 0.027 wt% (Fig. 7). Although the ranges are identical, a Student's t-test reveals that the means differ with statistical significance ($p$=0.002, where $p$ is the probability that the observed difference arose randomly). Means of Sr concentrations in the two kinds of calcite differ with even greater statistical significance ($p$=0.001) in Speleothem 13 (Fig. 8), the petrographically best-preserved speleothem.

Petrography is related to concentration of both Mg and Sr at the macroscopic scale (Fig. 9). ICP analysis of drilled powders yields a Sr concentration of 0.053 wt% and Mg concentration of 0.450 mol% $MgCO_3$ in Speleothem 12, the speleothem with the coarsest crystals and the least zonation and fewest inclusions. In contrast, Speleothems 7, 9, and 13, which have finer crystals and more zonation and inclusions, have Sr concentrations of 0.058-0.069 wt% and Mg concentrations of 0.803-0.920 mol% $MgCO_3$. These ICP results fall in

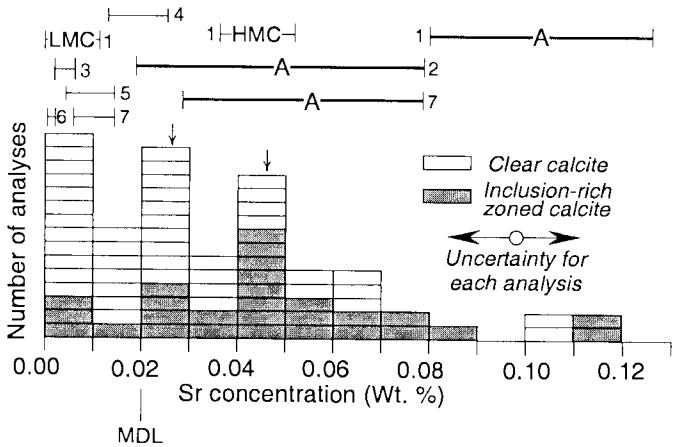


**Figure 7. Histogram of microprobe measurements of Sr concentration in four speleothems from Wadi Sannur Cavern. Shading indicates degree of textural preservation; arrows indicate mean Sr concentration for each group. At top, thick horizontal bars labeled "A" are ranges of Sr concentration in aragonite in speleothems reported in literature; thin unlabeled bars show ranges of Sr concentration in calcite in speleothems reported in literature; "LMC" and "HMC" indicate reported ranges for low-Mg calcite and high-Mg calcite. Sources of data are 1: Bar-Matthews *et al.* (1991); 2: Brook *et al*. (1999); 3: Gascoyne (1983); 4: Goede & Vogel (1991); 5: Goede *et al*., (1998); 6: Huang & Fairchild (2001); 7: Railsback *et al*. (1997).**

the middle of the ranges of the microprobe results, which is to be expected because they represent larger samples that necessarily include a greater range of petrographic characteristics.

Petrography is not correlative with concentration of Mg at the microscopic scale. Mg concentration in inclusion-rich zoned calcite ranges from 0.19-2.30 mol% $MgCO_3$ with a mean of 0.87 mol% $MgCO_3$, and Mg concentration in clear calcite ranges from 0.04-2.30 mol% $MgCO_3$ with a mean of 0.78 mol% $MgCO_3$ (Fig. 8). Those means do not differ with statistical significance ($p$=0.25). Only in data from Speleothem 12 does the mean Mg concentration of inclusion-rich zoned calcite differ with statistical significance from that of clear calcite ($p$=0.043). Even that significance is eliminated if one notes that four sets of data (Fig. 8) are tested and, therefore, uses a Bonferroni correction and divides $\alpha$ by 4, reducing $\alpha$ from 0.05 to 0.0125. A Bonferroni correction is required because repeated tests of one hypothesis are made. If four tests were made with $\alpha$=0.05, the probability that random numbers would yield $p$<0.05 in one of those tests would be 0.20 (an unacceptably high probability of a faulty inference) rather than 0.05 (the standard value in the earth sciences).

## CONCLUSIONS AND DISCUSSION

### CONCLUSIONS SPECIFIC TO THE WADI SANNUR SPELEOTHEMS

The relatively high Sr concentrations in inclusion-rich portions of the Wadi Sannur speleothems (Fig. 7, 8, & 9) and the high U concentrations of some of the samples from the speleothems (Fig. 1) suggest that some, and perhaps much, of the material in these speleothems was originally aragonite. Sr concentrations in inclusion-rich portions of the speleothems are equal to Sr concentrations of spelean aragonite, whereas they exceed Sr concentrations in primary spelean calcites (Fig. 7). In fact, most Sr concentrations in *clear* calcite from the Wadi Sannur speleothems also exceed those reported in primary spelean calcites (Fig. 7). High U concentrations similarly argue for an original aragonite mineralogy, because the distribution coefficient for U is much larger in aragonite than in calcite (Kitano & Oomori 1971; Meece & Benninger 1993).

Although the Wadi Sannur speleothems were probably partly to mostly aragonite when they formed, the Mg content of their calcite suggests that the speleothems also originally contained calcite with a non-trivial Mg content. The distribution coefficient for incorporation of Mg in aragonite (0.002) reported by Brand and Veizer (1983) would imply aragonite precipitation from a water with Mg/Ca = 11.8 to allow the greatest Mg concentrations observed in the speleothems (2.3 mol% $MgCO_3$). Mg/Ca ratios are typically not that great in cave waters (Fig. 10), suggesting that the Mg was not incorporated in primary aragonite. The distribution coefficient for incorporation of Mg in spelean calcite (~0.03) (Gascoyne 1983; Huang & Fairchild 2001) would, on the other hand, imply calcite precipitation from a water with Mg/Ca = 0.8 to allow the greatest Mg concentrations observed in the speleothems (2.3 mol% $MgCO_3$). Cave waters with Mg/Ca = 0.8 are relatively common (Fig. 10), so that the Mg concentrations of the calcites could have resulted from precipitation of primary magnesian calcite. Two conclusions are possible: 1) Some of the original material of the Wadi Sannur speleothems was Mg-bearing calcite; 2) Recrystallization of aragonite to calcite took place in waters sufficiently Mg-rich to result in the present Mg content.

The geochemical considerations discussed above and the petrographic character of the Wadi Sannur speleothems combine to suggest that all four speleothems underwent significant recrystallization. Petrographic evidence (preservation of zonation and relative fine calcite crystal size) and geochemical evidence (high U concentration and distinct Sr-rich zones) indicate that Speleothem 13 underwent the least recrystallization. However, even Speleothem 13 appears to have undergone recrystallization, because its high Sr content is incompatible with an original calcite mineralogy and because the boundaries of all of the elongate calcite crystals have no relationship to zonation defining the speleothem's growth layers. The coarser crystals and lesser preservation of original fabric in Speleothems 9, 7, and 12 suggest that they underwent even more recrystallization than Speleothem 13.

### CONCLUSIONS GENERALLY APPLICABLE TO SPELEOTHEMS

The most general conclusion from this work is that microscopic petrography is a valuable tool in evaluating

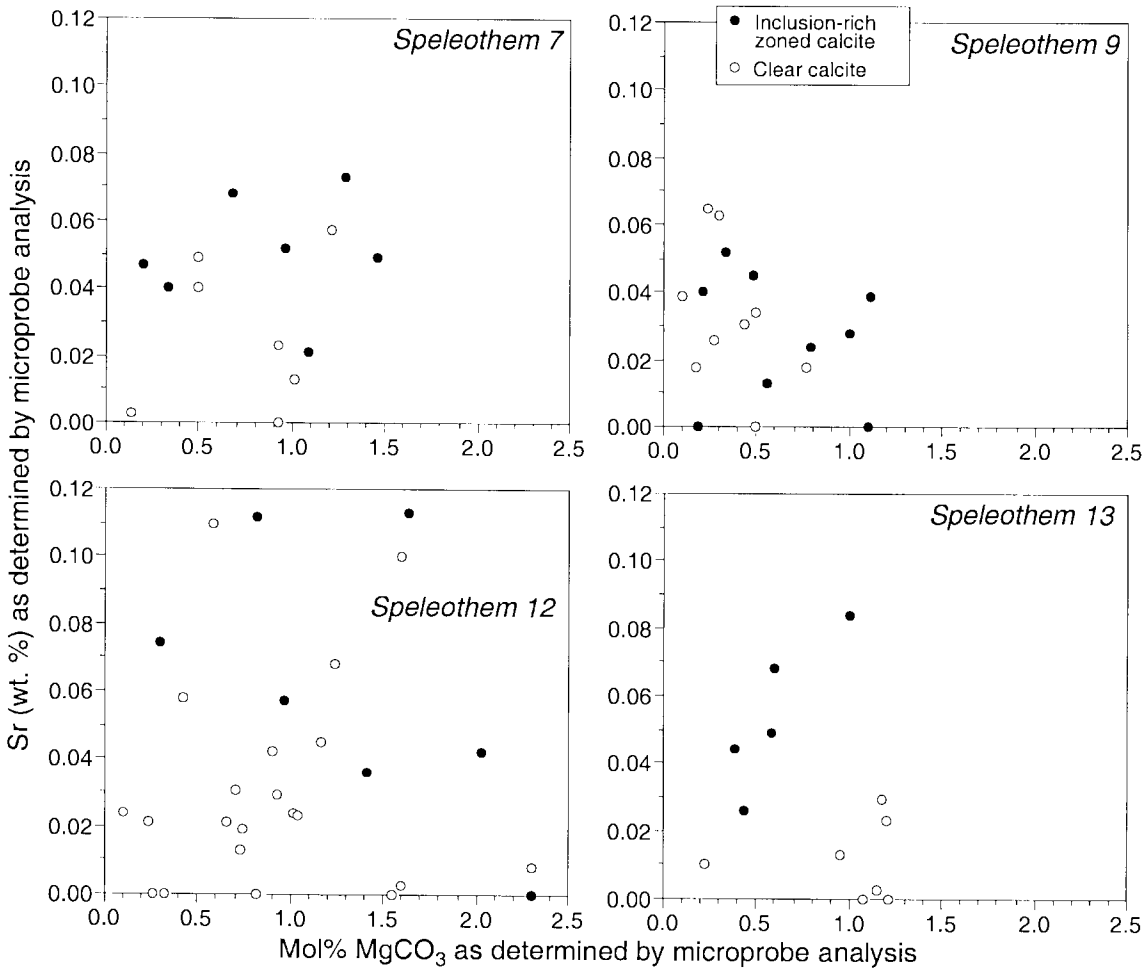


**Figure 8. Plots of Sr and Mg concentration determined by microprobe analysis of four speleothems from Wadi Sannur Cavern.**

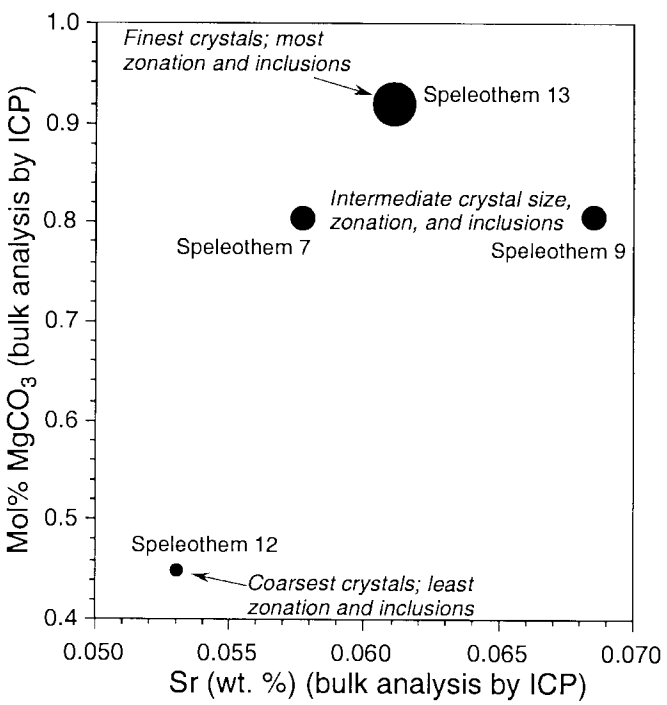


**Figure 9 (Right). Plot of Sr and Mg concentration determined by ICP analysis of drilled powders of four speleothems from Wadi Sannur Cavern. Symbol size reflects petrographic parameters (see horizontal axes of Figs. 5 & 6) and is proportional to inferred degree of preservation of original texture. Analytical uncertainty is less than size of smallest symbol. Sample sizes for these analyses were much larger than for the microprobe analyses reported in Figures 7 and 8, but the minimum detection limits were much lower (offscale to left and bottom of this figure).**

speleothems for potential U-series dating. Visual examination of hand samples is often used by practitioners of speleothem geochemistry as their sole means to evaluate preservation. However, Speleothem 13 demonstrates that macroscopic observation of well-defined concentric zonation is not sufficient to disprove possible recrystallization. Instead, positive relationships of U concentration with quantified measures of petrography (Figs. 5 & 6) and differences in Sr concentration with petrography (Figs. 7, 8, & 9) indicate that thin-section petrography provides an effective method to evaluate the preservation of speleothems for U-series dating and perhaps for other geochemical applications as well.

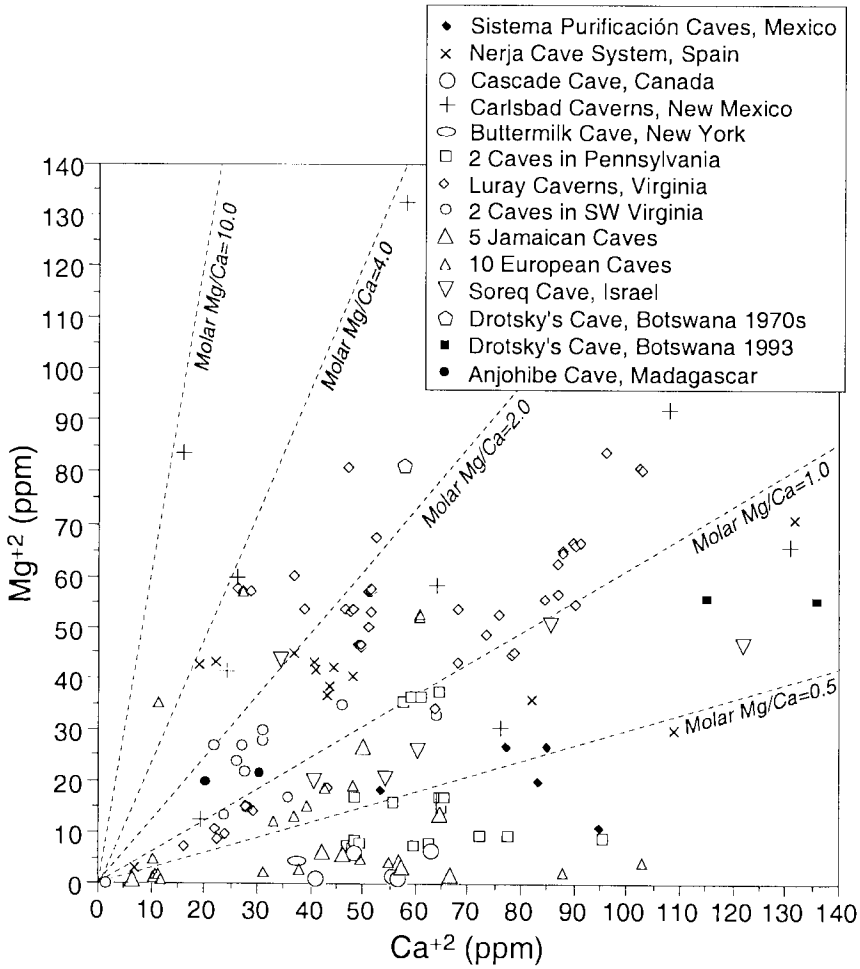


**Figure 10. Plot of $Ca^{+2}$ and $Mg^{+2}$ concentrations in waters reported from caves around the world. Sources of data are Carrasco *et al.* (1995) (Spain), Cooke (1975) (Botswana), Even *et al.* (1986) (Israel), Feeney (1997) (New York), Fischbeck (1976) (Europe), Gascoyne (1983) (Canada & Jamaica), Gonzalez and Lohmann (1988) (New Mexico), Holland *et al.* (1964) (Luray Caverns & Pennsylvania), Hose (1996) (Mexico), and Murray (1954) (southwest Virginia). Only a selection of samples from Figure 3.7 of González and Lohmann (1988) are shown because their data were not tabulated. Data from caves near marine shorelines have been excluded to preclude inclusion of waters with Mg-enrichment from seawater.**

The large range of U concentration in the Wadi Sannur speleothems and the smaller ranges reported in other terrestrial carbonates shown in Figure 1 suggest that large ranges of U concentration in monomineralic speleothems may also serve as a warning that at least some of the material has undergone recrystallization and loss of U. The condition "in monomineralic speleothems" must be added because the distribution coefficient for U is much larger in aragonite than in calcite (Kitano & Oomori 1971; Meece & Benninger 1993). Lev *et al.* (2000) likewise argued that a large range in U concentration is evidence of post-depositional remobilization in shales.

Finally, the presence of Sr-rich, inclusion-rich columnar calcite in some of the Wadi Sannur speleothems is evidence that inclusion-rich columnar calcite in speleothems can be secondary, rather than primary. The origin of columnar calcite in speleothems has been the subject of vigorous debate (e.g., González *et al.* 1992, 1993; Kendall 1993; Frisia *et al.* 2000). The results of this study cannot lead to a general statement about the origin of all columnar calcites, but they do provide an example in which spelean columnar calcite with inclusion-rich and inclusion-poor bands preserving original zonation seems to be the result of recrystallization of aragonite (and perhaps magnesian calcite).

## ACKNOWLEDGMENTS

We thank Paul Schroeder of the University of Georgia Department of Geology for his help with X-ray diffractometry. We thank James B. Paces of the US Geological Survey and an anonymous *JCKS* reviewer for comments that greatly improved the manuscript.

## REFERENCES

Bar-Matthews, M., Matthews, A., & Avalon, A., 1991, Environmental controls of speleothem mineralogy in a karstic dolomitic terrain (Soreq Cave, Israel): Journal of Geology, v. 99, p. 189-207.

Brand, U., & Veizer, J., 1983, Origin of coated grains: Trace element constraints, *in* Peryt, T.M., ed., Coated grains: Berlin, Springer Verlag, p. 9-26.

Brook, G.A., Cowart, J.B., Brandt, Steven A., & Scott, L., 1997, Quaternary climatic change in southern and eastern Africa during the last 300 ka: The evidence from caves in Somalia and the Transvaal region of South Africa: Zeitschrift für Geomorphologie, v. 108, p. 15-48.

Brook, G.A., Rafter, M.A., Railsback, L.B., Sheen, S.-W., & Lundberg, J., 1999, A high-resolution proxy record of rainfall and ENSO since AD 1550 from layering in stalagmites from Anjohibe Cave, Madagascar: The Holocene, v. 9, p. 695-705.

Carrasco, F., Andreo, B., Bena Vente, J., & Vadillo, I., 1995, Chemistry of the water in the Nerja Cave System, Andalusia, Spain: Cave and Karst Science, v. 21, p. 27-32.

Cooke, H.J., 1975, The palaeoclimatic significance of caves and adjacent landforms in western Ngamiland, Botswana: Geographical Journal, v. 141, p. 430-444.

Dabous, A.A., & Osmond, J.K., 2000, U/Th study of speleothems from the Wadi Sannur Cavern, Eastern Desert of Egypt: Carbonates and Evaporites, v. 15, p. 1-6.

Dorale, J.A., González, L.A., Reagan, M.K., Pickett, D.A., Murrell, M.T., & Baker, R.G., 1992, A high-resolution record of Holocene climate change in speleothem calcite from Cold Water Cave, northeast Iowa: Science, v. 258, p. 1626-1630.

Dorale, J.A., Edwards, R.L., Ito, E., & González, L.A., 1998, Climate and vegetation history of the Midcontinent from 75 to 25 ka: A speleothem record from Crevice Cave, Missouri, USA: Science, v. 282, p. 1871-1874.

Edwards, R.L., Chen, J.H., & Wasserburg, G.J., 1987, $^{238}U$-$^{234}U$-$^{230}Th$-$^{232}Th$ systematics and the precise measurement of time over the past 500,000 years: Earth and Planetary Science Letters, v. 81, p. 175-192.

Even, H., Carmi, I., Magaritz, M., & Gerson, R., 1986, Timing the transport of water through the upper vadose zone in a karstic system above a cave in Israel: Earth Surface Processes and Landforms, v. 11, p. 181-191.

Feeney, T.P., 1997, The geomorphic evolution of limestone pavements and alvar grasslands in northwestern New York state, USA [PhD thesis]: University of Georgia, 311 p.

Fischbeck, R., 1976, Mineralogie und Geochemie carbonatischer Ablagerungen in europäischen Höhlen - ein Beitrag zur Bildung und Diagenese von Speleothemen: Neues Jahrbuch Mineralogie Abhandlungen, v. 126, p. 69-291.

Frisia, S., Borsato, A., Fairchild, I.J., & McDermott, F., 2000, Calcite fabrics, growth mechanisms, and environments of formation in speleothems from the Italian Alps and southwestern Ireland: Journal of Sedimentary Research, v. 70, p. 1183-1196.

Gascoyne, M., 1983, Trace-element partition coefficients in the calcite-water system and their paleoclimatic significance in cave studies: Journal of Hydrology, v. 61, p. 213-222.

Goede, A., & Vogel, J.C., 1991, Trace element variations and dating of a Late Pleistocene Tasmanian speleothem: Palaeogeography, Palaeoclimatology, Palaeoecology, v. 88, p. 121-131.

Goede, A., McCulloch, M., McDermott, F., & Hawkesworth, C., 1998, Aeolian contribution to strontium and strontium isotope variations in a Tasmanian speleothem: Chemical Geology, v. 149, p. 37-50.

González, L.A., & Lohmann, K.C., 1988, Controls on mineralogy and composition of spelean carbonates: Carlsbad Caverns, New Mexico, *in* James, N.P., & Choquette, P.W., ed., Paleokarst: New York, Springer-Verlag, p. 81-101.

González, L.A., Carpenter, S.J., & Lohmann, K.C., 1992, Inorganic calcite morphology: Roles of fluid chemistry and fluid flow: Journal of Sedimentary Petrology, v. 62, p. 382-399.

González, L.A., Carpenter, S.J., & Lohmann, K.C., 1993, Columnar calcite in speleothems: Reply: Journal of Sedimentary Petrology, v. 63, p. 553-556.

Hellstrom, J.C., & McCulloch, M., 2000, Multi-proxy constraints on the climatic significance of trace element records from a New Zealand speleothem: Earth and Planetary Science Records, v. 179, p. 287-297.

Holland, H.D., Kirispu, T.V., Huebner, J.S., & Oxburgh, U.M., 1964, On some aspects of the chemical evolution of cave waters: Journal of Geology, v. 72, p. 36-67.

Holmgren, K., Karlén, W., & Shaw, P.A., 1995, Paleoclimatic significance of the stable isotopic composition and petrology of a Late Pleistocene stalagmite from Botswana: Quaternary Research, v. 43, p. 320-328.

Hose, L.D., 1996, Hydrology of a large, high relief, subtropical cave system: Sistema Purificación, Tamaulipas, México: Journal of Cave and Karst Studies, v. 58, p. 22-29.

Huang, Y., & Fairchild, I.J., 2001, Partitioning of $Sr^{2+}$ and $Mg^{2+}$ into calcite under karst-analog experimental conditions: Geochimica et Cosmochimica Acta, v. 65, p. 47-62.

Imbrie, J., & 18 others, 1993, On the structure and origin of major glaciation cycles; 2, The 100,000-year cycle: Paleoceanography, v. 8, p. 698-735.

Jarosewich, E., & Macintyre, I.G., 1983, Carbonate reference samples for electron microprobe and scanning electron microscope analyses: Journal of Sedimentary Petrology, v. 53, p. 677-678.

Jarosewich, E., & White, J.S., 1987, Strontianite reference sample for electron microprobe and SEM analyses: Journal of Sedimentary Petrology, v. 57, p. 762-763.

Kaufman, A., 1969, The Th-232 concentration of surface ocean water: Geochimica et Cosmochimica Acta, v. 33, p. 717-724.

Kendall, A.C., 1993, Columnar calcite in speleothems: Discussion: Journal of Sedimentary Petrology, v. 63, p. 550-552.

Kitano, Y., & Oomori, T., 1971, The coprecipitation of uranium with calcium carbonate: Journal of the Oceanographic Society of Japan, v. 27, p. 34-43.

Langmuir, D., 1978, Uranium solution-mineral equilibria at low temperatures with applications to sedimentary ore deposits: Geochimica et Cosmochimica Acta, v. 42, p. 547-570.

Latham, A.G., Schwarcz, H.P., & Ford, D.C., 1986, The paleomagnetism and U-Th dating of Mexican stalagmite, DAS2: Earth and Planetary Science Letters, v. 79, p. 195-207.

Lev, S.M., McLennan, S.M., & Hanson, G.N., 2000, Late diagenetic redistribution of uranium and disturbance of the U-Pb whole rock isotope system in a black shale: Journal of Sedimentary Research, v. 70, p. 1234-1245.

Ludwig, K.R., Simmons, K.R., Szabo, B.J., Winograd, I.J., Landwehr, J.M., Riggs, A.C., & Hoffman, R.J., 1992, Mass-spectrometric $^{230}Th$-$^{234}U$-$^{238}U$ dating of the Devils Hole calcite vein: Science, v. 258, p. 284-287.

Ludwig, K.R.P., J.B., 2002, Uranium-series dating of pedogenic silica and carbonate, Crater Flat, Nevada: Geochimica et Cosmochimica Acta, v. 66, p. 487-506.

Lundberg, J., & Ford, D.C., 1994, Late Pleistocene sea level change in the Bahamas from mass spectrometric U-series dating of submerged speleothem: Quaternary Science Reviews, v. 13, p. 1-14.

Maire, R., & Quinif, Y., 1991, Mise en evidence des deux derniers interglaciaires (Stades 5 and 7) dans les Alpes Francaises du Nord d'après l'étude des remplissages endokarstiques (Haut-Giffre, Platé, Chartreuse): Speleochronos, no. 3, p. 3-10.

Meece, D.E., & Benninger, L.K., 1993, The coprecipitation of Pu and other radionuclides with $CaCO_3$: Geochimica et Cosmochimica Acta, v. 57, p. 1447-1458.

Murray, J.W., 1954, The deposition of calcite and aragonite in caves: Journal of Geology, v. 62, p. 481-492.

Openshaw, S.J., Latham, A.G., & Shaw, J., 1996, Palaeosecular variation observed in speleothems from western China and northern Spain: http://www.liv.ac.uk/~steveo/mat/front.html.

Quinif, Y., 1989, Datation d'un interstade au sein de la derniere glaciation: la séquence stalagmatique de la Galerie Gillet (Grotte du Père Noël, Massif de Han-sur-Lesse, Belgique): Speleochronos, no. 1, p. 23-28.

Railsback, L.B., Sheen, S.-W., Rafter, M.A., Brook, G.A. & Kelloes, C., 1997, Diagenetic replacement of aragonite by aragonite in speleothems: Criteria for its recognititon from Botswana and Madagascar: Speleochronos, no. 8, p. 3-11.

Railsback, L.B., 2000, An atlas of speleothem microfabrics: http://www.gly.uga.edu/railsback/speleoatlas/SAindex1.html.

Rihs, S., Condomines, M., & Poidevin, J.-L., 2000, Long-term behaviour of continental hydrothermal systems: U-series study of hydrothermal carbonates from the French Massif Central (Allier Valley): Geochimica et Cosmochimica Acta, v. 64, p. 3189-3199.

Szabo, B.J., Kolesar, P.T., Riggs, A.C., Winograd, I.J., & Ludwig, K.R., 1994, Paleoclimatic inferences from a 120,000-yr calcite record of water-table fluctuation in Browns Room of Devils Hole, Nevada: Quaternary Research, v. 41, p. 59-69.

Turgeon, S., & Lundberg, J., 2001, Chronology of discontinuities and petrology of speleothems as paleoclimatic indicators of the Klamath Mountains, southwest Oregon, USA: Carbonates and Evaporites, v. 16, p. 53-167.

Uggeri, A., Bini, A., & Quinif, Y., 1991, Contribution of isotope geochemistry to the study of the climatic and environmental evolution of Monte Campo die Fiori Massif (Lombardy, Italy): Speleochronos, no. 3, p. 17-28.

Whitehead, N.E., Ditchburn, R.G., Williams, P.W. & McCabe, W.J., 1999, 231Pa and 230Th contamination at zero age: A possible limitation on U/Th series dating of speleothem material: Chemical Geology, v. 156, p. 359-366.

D.A. McFarlane, J. Lundberg, and A. G. Fincham - A late Quaternary paleoecological record from caves of southern Jamaica, West Indies. *Journal of Cave and Karst Studies 64*(2): 117-125.

# A LATE QUATERNARY PALEOECOLOGICAL RECORD FROM CAVES OF SOUTHERN JAMAICA, WEST INDIES

D. A. MCFARLANE
*W. M. Keck Science Center, The Claremont Colleges, Claremont, CA 91711 USA*
J. LUNDBERG
*Department of Geography and Environmental Studies, Carleton University, Ottawa, ON K1S 5B6, CANADA*
A. G. FINCHAM
*Center for Craniofacial Molecular Biology, University of Southern California, Los Angeles, CA 90089, USA*

*Studies of an unusual and diverse system of caves in coastal southern Jamaica have yielded a paleoclimatic record associated with a fossil vertebrate record that provides useful insights into the poorly documented paleoecology of latest Wisconsinan and Holocene Jamaica. Episodes of significantly increased precipitation during the Holocene have left characteristic deposits of speleothems, and have supported both faunal and archaeological communities that were dependent on these mesic conditions. Deposits of fossil bat guano preserved in the caves provide a $\delta^{13}C$ record of alternating mesic and xeric climatic episodes that supports the interpretation of the faunal and archaeological record.*

A diverse assemblage of late Pleistocene and Holocene vertebrate remains (Table 1) have been recovered from the ~10 km Jacksons Bay cave system on the south coast of Portland Ridge, Clarendon, Jamaica (Fig. 1). Portions of this cave system have been known since at least 1897 (Duerden 1897), but difficult terrain meant that the full extent of the caves did not begin to be appreciated until the discovery of Drum Cave in 1976 (Wadge *et al.* 1979). Significant new cave discoveries continue to be made; Potoo Hole was first explored in 1993 as an adjunct to the paleontological work described here (Fincham 1997). Concurrent with the collection of vertebrate remains, collections of fossil bat guano and other materials were made. As well as providing the context for a unique record of vertebrate extinctions, these materials offer insights into the paleoclimate of the area during the latest Pleistocene and Holocene, of which relatively little is currently known.

Portland Ridge (77° 13' W, 17° 44' N) is a carbonate peninsula in the most southerly part of Jamaica. It consists of some 2200 m of Eocene-Miocene limestones resting on volcanic rocks (Wadge *et al*. 1979). As currently known, the Jacksons Bay system consists of some 9200 m of mapped passages, the inland ones running less than 40m below the modern karst surface. The much shallower coastal sections extend at a very gradual dip to an unknown depth below modern sea level and emerge in one of the offshore terraces; many of the (undived) coastal passages sump seaward in slightly brackish water. The caves (Fig. 2) are essentially an interconnecting phreatic system of trunk passages following two major joint systems now modified by several big collapses. Although the Portland Ridge Peninsula behaves geomorphologically as a carbonate island, it is of interest that these caves do not appear to follow the flank-margin model described by Mylroie and Carew (2000) for carbonate islands. The caves are equilibrated to a lower sea level than today: it is possible that, at low sea levels, allogenic groundwater may have reached the peninsula from further north.

**Table 1. Birds and mammals from the fossil and subfossil record, Jacksons Bay Caves (domesticated species omitted)**
@ = endemic # = extinct

*Tyto alba* (barn owl)
*Leptotila jamaicensis* (White Belly)
*?Milvago* sp (caracara*) @#*
*Pelicanus occidentalis* (brown pelican)
*Cathartes aura* (John crow)
*Amazona cf. agilis* (Amazon parrot)
*Xenicibis xympithecus* (flightless ibis) @#
*Rattus rattus* (black rat)
*Geocapromys brownii* (hutia) @
*Oryzomys antillarum* (Jamaican rice rat) @#
Undescribed rodent. @#
*Xenothrix mcgregori* (primate) @#
*Homo sapiens* (man)
*Herpestes auropunctatus* (mongoose)
*Artibeus jamaicensis* (Jamaican fruit bat)
*Ariteus flavescens* (naseberry bat) @
*Erophylla sezekorni* (buffy flower bat)
*Monophyllus redmani* (Redman's flower bat) @
*Eptesicus lynni* (Lynn's brown bat) @
*Brachyphylla nana* (brown flower bat) #
*Macrotus waterhousii* (leaf-nosed bat)

Some 14 nominally separate but developmentally interconnected caves can be divided into an "upper" cave group that developed well above the present water table, and a "lower" group developed at or below the modern water table. The lower caves contain standing water (but no active streams or flows) and have not proved to be of paleontological significance. The "upper" caves are older and drier, with a distinctive sequence of secondary deposits. They are frequently breached by collapse pits 10 - 20 m deep, most notably in Arrow, Somerville, Drum, and Lloyds Caves. These features provide

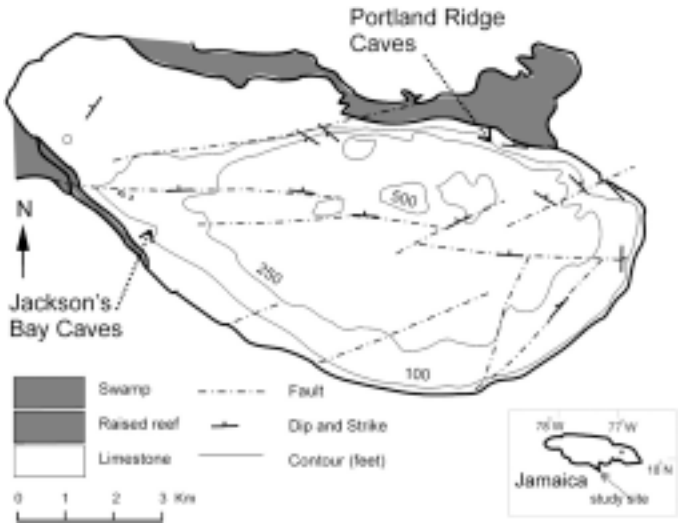


**Figure 1. Location map of Portland Ridge Peninsula, the southernmost part of Jamaica, Jacksons Bay Cave site. Modified from Wadge *et al*. 1979. The Blue Mountains are shown on the inset (*).**


**Figure 2. The Jacksons Bay Cave System, plan view. Grid lines are at 500 m intervals. Drum Cave, which overlies Jacksons Bay Cave, is shown in lighter shading. Modified from Fincham (1997), which should be consulted for more detailed mapping. Important passage locations are Bone Hall (A), Brown Dust Passage (B), The Map Room (C), Mantrap Hole (D), Arawak Gallery (E) and Big Chamber (F).**

points of ingress for secondary deposits including lateritic karst residuum (red cave fill), limestone breakdown clasts, and notable accumulations of owl (*Tyto alba*) vomitus. The very dry, powdery, indistinctly stratified, red paleosol-derived cave fill floors large areas of these caves, reaching a depth up to 1.5 m in places. Many of the vertebrate remains were in this material. These sediments are frequently capped by a thin (< 2 cm) but laterally extensive flowstone deposit that commonly forms the walls of rimstone pools (gours). Typically, these pools contain large numbers of cave pearls–speleothems formed by the concentric accretion of calcite from dripping water around crystallization nuclei. In the Jacksons Bay caves, gastropods commonly provide these nuclei (McFarlane 1987), although vertebrate bones also form cores. Largely inactive but very clean and uncorroded speleothems that are at least partially contemporaneous with the rimstone pools extensively ornament ceilings and walls. In some areas of the caves, 1-5 m deep accumulations of subfossil bat guano bury the floors. Archaeological remains are common in the caves, including Amerindian skeletal remains dated at 710 ±60 $^{14}$C yrs BP (Mizutani *et al.* 1992), cassava griddles, pottery, petroglyphs and pictographs (Fincham & Fincham 1997). These remains are always superficial to the sediment and flowstone capping, and are either unmodified or occasionally thinly veneered with calcite (Wadge *et al.* 1979).

Portland Ridge is located in the rain shadow of the Blue Mountains (~2300 m) and supports a xerophyllic, sclerophyllous vegetation described by Asprey and Robbins (1953) as the arid coastal facies of dry limestone scrub forest, and more graphically by Seifriz (1943) "...as superb a picture of the eternal persistence of life under the most adverse conditions nature can produce". Annual precipitation averages 1014 mm with a pronounced dry season of 6-10 months having <100 mm-month (data from Amity Hall, 91 year averages; Anonymous 1950). The precipitation-evapotranspiration (PET) ratio is 1.58, placing the area in the "Dry Forest" Holdridge Life Zone (Holdridge 1967). These conditions are apparently too xeric to support major bat populations, with the ubiquitous *Pteronotus parnelli* and *Macrotus waterhousii* occurring in minimal populations of 10-100 individuals, in contrast to populations of $10^4$-$10^5$ individuals commonly occurring in comparable caves elsewhere in the more mesic areas of the island (Goodwin 1970; McFarlane 1986). The presence of extensive deposits of subfossil bat guano in several of the Jacksons Bay caves, unrelated to modern populations, is therefore of considerable paleoecological import.

## SAMPLING AND METHODS

In addition to a general study of all the caves of the area, four main field sites were studied: Brown Dust Passage in Drum Cave; Bone Hall Chamber in Drum Cave; Lloyds Cave; and Map Room in Skeleton Cave. Vertebrate remains were collected from the red cave fill, from the dry gour pools, from the owl vomitus, and occasionally from the fossil bat guano. Guano samples were collected from several layers exposed in the walls of excavated pits. Sample sites were documented *in situ* before removal of samples for lab analysis. Guano volumes were determined by survey of their lateral extent and measurement of thickness in test pits and by probing with a steel rod.

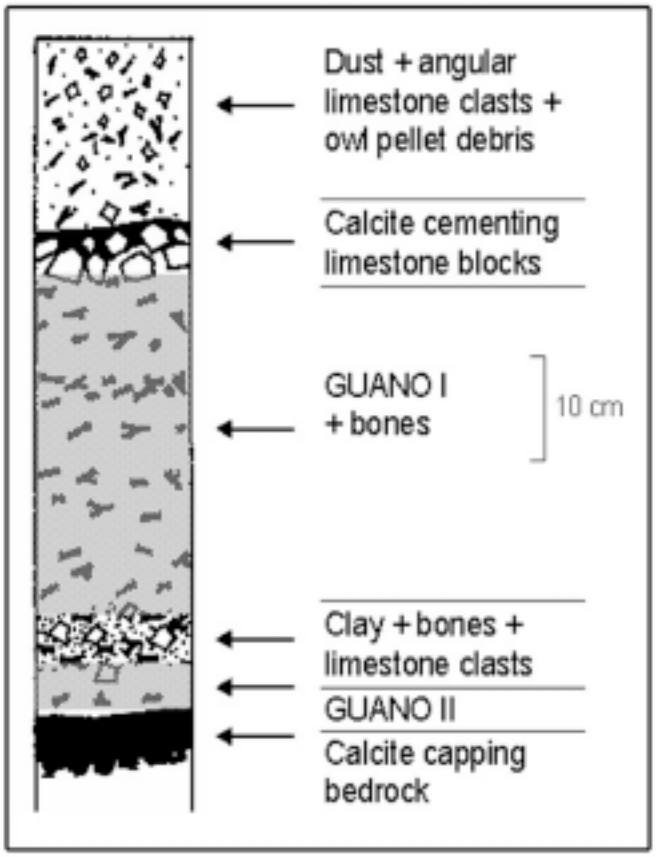


**Figure 3 Diagrammatic profile of Brown Dust Passage Excavation Pit.**

Vertebrate specimens were dated directly by $^{14}C$ dating of their bone collagen, or indirectly by $^{14}C$ dating on the associated guano (acid insoluble chitin residue) or gastropods (inorganic shell carbonate). Gastropods were radiocarbon dated following manual removal of calcite as necessary, and acid etching. Because gastropods can acquire some of their carbon from old, radiogenically dead carbonate bedrock, the measured dates were then corrected for the 'limestone effect' (Goodfriend & Stipp 1983) by subtracting a pseudo-age of 320 ±60 yrs BP obtained from modern (dead) *Pluerodonte* collected in the forest above Birthday Cave. Although we cannot establish the relative contribution of post-bomb radiocarbon (if any) in our modern sample, this 320 year correction factor is in general concordance with that published for other Jamaican specimens and based on modern, pre-bomb *Pluerodonte* (Goodfriend & Stipp 1983). Bone dates are based on collagen fractions prepared by decalcification in excess 1M HCl and alkali washes in 5% NaOH. Fossil guanos were treated with excess 6M HCl at 90° C for 24 hrs, then repeatedly washed in de-ionized water to remove soluble organics and secondary carbonates. Stable isotope mass spectrometry was performed by Beta Analytic (Miami, Florida).

All the original radiocarbon dates reported in this work are obtained by beta counting or accelerator mass spectrometry by Beta Analytic; they are corrected for fractionation using $\delta^{13}C$ values, but are not corrected for $^{14}C$ flux to facilitate comparison with older published dates. Dates are therefore quoted in radiocarbon years before present ($^{14}C$ yrs BP), not calendar years. All quoted errors are 1σ. Radiocarbon data are summarized in Appendix 1.

## Results

Excavation of the Brown Dust Passage sediments in Drum Cave began in January 1995, and was further extended and deepened in July 1995 and September 1996. Stratigraphy is clear and distinctive (Fig. 3). A 20 cm surface deposit of light-colored dust, angular fragments of limestone breakdown, and modern owl-pellet debris overlies a thin (<2 cm) calcite floor, which cements larger limestone breakdown blocks. This unit caps a rather uniform, 34 cm thick layer of dark brown, subfossil bat guano (36% acid-insoluble organics by ignition), hereafter designated 'Guano I'. This is underlain by a 6 cm thick layer of limestone fragments, clay and finely comminuted bone, and then the 3 cm thick 'Guano II'. Below, more clay and degraded bone fragments continue to a solid calcite floor at -125 cm, presumed to be developed directly on the bedrock. Bone occurs throughout the section, often in concentrations so thick as to warrant the description 'bone cake'. Numerous 'hardgrounds' formed by calcite induration of the sediments are scattered throughout the section. Guano II was deposited 11,980 ±80 $^{14}C$ yr BP, followed by a short hiatus and the deposition of Guano I beginning at 11,260 ±80 $^{14}C$ yr BP and terminating at 10,250 ±80 $^{14}C$ yr BP. The Guano I deposit is laterally extensive, forming a deep, 250+ $m^3$ accumulation. It is deepest in Brown Dust Passage and extends laterally to the Bone Hall chamber (below).

Bone Hall, Drum Cave, is a large, flat-floored chamber receiving vertebrate remains from the same collapse pit as Brown Dust Passage. Accumulation rates have been lower than in Brown Dust Passage (BDP), but the stratigraphy is quite similar. The Guano I stratum of BDP appears in Bone Hall as three thin guano layers: G1a, G1b, and G1c. The latter dates to 11,220 ±100 $^{14}C$ yrs BP, statistically indistinguishable from the initiation of Guano 1 in Brown Dust Passage. Guano II is not present in Bone Hall. The Bone Hall pit was terminated at -30 cm where solid calcite overlies the presumed bedrock floor. A gastropod date from this basal calcite yielded 13,220 ±150 $^{14}C$ yrs BP.

Mantrap site, an 8 m deep pit entrance to Lloyds Cave, yielded several vertebrate remains, the most interesting of which was an uncalcited skull of the endemic primate, *Xenothrix mcgregori*, (unfortunately undateable due to the uniqueness of the specimen) recovered from the surface of the cave fill. The 100+ cm deep guano deposit from the Guano Crawl, further south in Lloyds Cave, gave a basal date of 16,400 ±110 yrs BP, a date of 10,440 ±100 $^{14}C$ yrs BP at 30-40 cm depth, and a date of 1750 ±80 $^{14}C$ yrs BP at the surface.

The Map Room, Skeleton Cave, has red paleosol-derived

sediments 1.5 m deep, with no identifiable stratification, filling the back of the chamber to the roof, where it intercalates with small stalactites on the roof. The top surface of this deposit against the roof is marked by a distinct layer of uncalcited gastropods dating to 3910 ±70 $^{14}$C yrs BP. An excavation dug one meter from the wall yielded a bone (*Geocapromys*) from the top 0 – 30 cm layer dating to 1870 ±50 $^{14}$C yrs BP. Gastropods from a depth of ~30 cm date to 6410 ±110 $^{14}$C yrs BP. This level also yielded a hemi-mandible of *Xenothrix*. Gastropods from 1.5 m date to 3420 ±60 $^{14}$C yrs BP.

Potoo Hole has extensive deposits of bat guano in the Arawak Gallery and the Big Chamber. The thickest part of the deposit forms a guano "mountain," rising some 6 m in height above the general guano floor covering; is at least a meter deep, but was not excavated. Samples taken from the top of the "mountain" date to 950 ± 50 $^{14}$C yrs BP but the date of the start of deposition is not known.

High Dome Cave, located on the northeastern side of the Portland Ridge, (Portland Ridge Caves group; Fig. 1) also preserves extensive deposits of stratified fossil guano; a sample from 115 cm depth exposed by guano mining yielded a date of 10,850 ±100 $^{14}$C yrs BP.

## CHRONOLOGY AND PALEOENVIRONMENTAL SIGNIFICANCE OF THE CAVE DEPOSITS

The origin of the Jacksons Bay caves is poorly understood. The caves formed within the Miocene host rock. The oldest dated cave calcite, a U-Th date on flowstone from Shamrock Passage, a lower level passage in the Jacksons Bay New Cave, gave an age of 278 +57,-37 ka. The weighted mean of four samples (Wadge *et al.* 1979) from the same flowstone is 202 ±16 ka, so that section of the cave must have been already formed before that date. The 'upper' caves pre-date the New Cave, and may have their origins in the earliest Pleistocene or late Pliocene as did comparable caves on Isla de Mona, Puerto Rico (Panuska *et al.* 1998). Regardless of the timing of speleogenesis, the caves did not become paleontologically important until the opening of the collapse pit entrances, which admit vertebrate remains. The radiocarbon date of 13,220 ±150 $^{14}$C yrs BP on the calcited gastropod cemented to the bedrock floor of the Bone Hall Excavation, Drum Cave, pre-dates all fossil and sediment deposits in this cave and probably marks the opening of the Drum Cave #3 collapse pit.

The late Pleistocene and Holocene was marked in these caves by the progressive emplacement of the red cave fill, vertebrate deposits, and calcite floors. These extensive deposits provide *prima facie* evidence that these caves were much wetter at intervals in the recent past. In many cases, the characteristics of the deposits and the relationships between dated materials give additional information about the environmental conditions of formation.

## EVIDENCE FOR WET PHASES

In Lloyds Cave, bat guano deposition began at least as early as 16,400 ±110 $^{14}$C yrs BP and continued until at least 1750 ±120. In Brown Dust Passage, Drum Cave, guano deposition began more than 11,980 ±80 $^{14}$C yrs BP but terminated around 10,350 ±70 $^{14}$C yrs BP. The thickest guano deposits are Late Holocene; e.g., deposition of the very large guano deposits in Potoo Hole (~ 4000 m$^3$) terminated around 950 ±50 BP. The preservation of laminations (seasonal?) in the 10,850 ±100 $^{14}$C yrs BP guano deposit of High Dome Cave (north side of Portland Ridge) evidences that the relatively thin late Pleistocene deposits in the Jacksons Bay caves are not simply the result of decomposition deflation. This suggests that conditions were more favorable for bats in the Jacksons Bay caves during the late Holocene.

A U-Th date on the top of an inactive stalagmite from the Coliseum, Jacksons Bay Great Cave, of 1.9 +2.9,-2.8 ka and a basal date of 27.9 +12,-11 ka (Wadge *et al.* 1979) is consistent with Late Pleistocene to Holocene wet intervals. The solid calcite beneath the guano in Brown Dust Passage, Drum Cave, and the numerous calcite-indurated layers scattered throughout the section indicate wetter conditions than now pertain in the cave; these wet conditions began an unknown time before ~13 ka and continued (perhaps intermittently) until some time after 10 ka. In Bone Hall, Drum Cave, the gastropod core of a cave pearl dated to 3700 ±120 yrs BP. From this we infer that conditions were at least seasonally wet enough to account for the extensive development (~1500 m² in Drum Cave alone) of gour pools that have never been observed to fill in 25 years of speleological investigations in the cave.

At present water levels, crocodiles are not found in any of the Jacksons Bay Caves: discoveries of undated, but superficial, crocodile remains, *Crocodylus acutus*, on top of the cave fill in Mantrap Hole, Lloyds Cave, indicate wetter conditions in the middle to late Holocene when the cave supported extensive bodies of standing water.

Archaeological remains are extensive in both the upper and lower Jacksons Bay caves, but are always superficial to the paleosols and calcite floors. Broken water jars in Water Jar Cave have been taken as evidence that Amerindians collected fresh water from now-dry gour pools (Fincham & Fincham 1997). A date on Amerindian bone intimately associated with these ceramics indicate that this practice continued until at least 710 ±80 $^{14}$C yrs BP.

These data suggest intermittently wetter-than-today conditions in the interval from at least 28 ka, isotope stage 2, the Late Glacial Maximum, until about AD 1300, the Medieval Warm Period of Northern Europe (Lamb 1995). The wettest, or longest, wet interval was probably coincidental with the thickest guano deposits, which terminated at ~950 $^{14}$C yrs BP.

**Table 2. Stable carbon isotope record of the Jacksons Bay Cave guanos.**

| Sample ID | Age ($^{14}$C kyr BP) | d $^{13}C_{PDB}$ |
|---|---|---|
| 95-24, 95-25, ** | 0 | -21.6, -22.8, -21.6 |
| 85-02 | 0.70 +/- 0.05 | -25.0 |
| 95-16 | 0.95 +/- 0.05 | -26.8 |
| 93-03 | 1.75 +/- 0.08 | -27.7 |
| 95-21 | 10.25 +/- 0.08 | -21.7 |
| 95-04 | 10.35 +/- 0.07 | -16.6 |
| 95-07 | 10.44 +/- 0.10 | -20.7 |
| 96-15 | 10.85 +/- 0.1 | -20.6 |
| 95-03 | 11.05 +/- 0.07 | -17.5 |
| 96-16 | 11.22 +/- 0.1 | -21.3 |
| 95-22 | 11.26 +/- 0.08 | -18.6 |
| 95-23 | 11.98 +/- 0.08 | -20.9 |
| 95-08 | 16.40 +/- 0.11 | -22.4 |

** indicates a replicate analysis

## Evidence for flood activity

The dates from the uncalcited gastropods and bone in the red sediment of the Map Room, Skeleton Cave, need to be examined: the top layer beside the cave wall dates to 3910 ±70 $^{14}$C yrs BP, while the 0–30 cm layer of the excavation dates to 1870 ±50 $^{14}$C yrs BP; the 30 cm level dates to 6410 ±110 $^{14}$C yrs BP, but the 150 cm level dates to 3420 ±60 $^{14}$C yrs BP. From this chronological jumble, we conclude that the Skeleton Cave fill and its contents were catastrophically emplaced, probably by severe flooding, sometime after ~3600 $^{14}$C yrs BP and most probably after 1870 $^{14}$C yrs BP during the same Late Holocene wet phase responsible for massive guano deposition in Potoo Hole and Amerindian water collection in Water Jar Cave.

## Paleoecological significance of stable isotopic records of guano deposits

The utility of subfossil bat guano deposits as a source of a $^{13}$C/$^{12}$C stable isotope proxy record of climate has been demonstrated by Mizutani *et al.* (1992). Insectivorous bat guano consists of finely commutated insect exoskeletons, of which some 25-40% by dry weight may be chitin (polymerized N-acetylglucosamine) (Jeuniaux 1971). Chitin is highly resistant to chemical and physical degradation, although it is readily digested by fungal and bacterial chitinases under aerobic and anaerobic conditions respectively (Miller *et al.* 1993; Koval & Kharkevich 1983). However, under conditions of low pH (Logan *et al.* 1991) or desiccation, decomposition is extremely slow. Last Interglacial insect remains from Nova Scotian sediments contain as much as 28% dry weight of chitin (Miller *et al.* 1993). We have found subfossil guano from a dry site in Bat Cave, Grand Canyon (Arizona, USA) radiocarbon dated at 12,400 ±90 yrs BP (DAM 96-03) that preserves 31.9% dry weight of chitin (unpublished data).

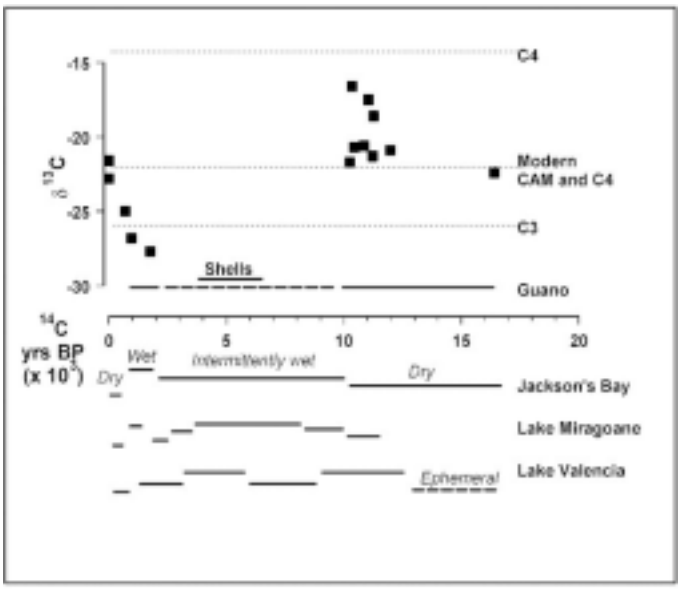


**Figure 4 $\delta^{13}$C values for fossil bat guano samples are graphed against time; the horizontal line just above the x-axis indicates the span of guano deposition, the unbroken part showing dated continuous deposition and the dashed part showing probable continuous deposition. The line marked "Shell" marks the cluster of cave pearl dates. A summary of inferred climatic conditions for Jacksons Bay and lake levels for Lake Mirogoane and Valencia, are shown below the x-axis.**

Although decomposition undoubtedly proceeds much faster in moist tropical environments, the low pH of fresh deposits (~pH 3.8) can preserve chitinous residues for extended periods of time. Subfossil bat guanos of a degraded nature can be conclusively identified by deacetylation of the chitin to chitosan followed by colorimetric assay using the van Wisselingh test (Muzzarelli 1977), or following enzymatic digestion using chitosanases and assay of the N-acetylamino sugars by the method of Reissig *et al.* (1955). Degradation of chitin progresses by depolymerization, but does not introduce significant shifts in the $^{13}$C/$^{12}$C ratio (Schimmelmann & DeNiro 1986).

Modern insectivorous bat (*Pteronotus* and *Macrotus*) guano accumulating in small quantities in the Jacksons Bay caves has a mean $\delta^{13}$C signature of -21.7, consistent with its origin in a food chain based on xerophyllic C4 and CAM plant taxa (Des Marais 1980). The Late Holocene fossil bat guanos from these caves have divergent $\delta^{13}$C signatures that are independent of diagenesis or age (Table 2), which we interpret as resulting from an increased C3 plant component in the food chain during more mesic climatic excursions (indicated by $\delta^{13}$C values around -26). Figure 4 shows the changes in $\delta^{13}$C against time. These data suggest a xerophytic period similar to today at around 16,000 $^{14}$C yrs BP and again at around 12,000–10,000 $^{14}$C yrs BP with perhaps more C4 vegetation. The shift to C3 signatures at around 1,750-700 $^{14}$C yrs BP (250

- 1300 AD) indicate wetter conditions, followed by an obvious trend up to modern CAM values showing increased aridity.

## BIOGEOGRAPHIC SIGNIFICANCE OF THE PALEONTOLOGICAL REMAINS

A perennial and unresolved debate that has long been central to Caribbean biogeography addresses the manner in which terrestrial vertebrate colonists first reached the islands (Williams 1989). In the specific case of Jamaica, putative land bridges have been decisively eliminated on geologic grounds (Buskirk 1985); but see recalcitrant opinions in MacPhee and Iturralde-Vinent (1999). For several West Indian mammals, humans are thought to be the vectors. For this to be true, the dates on the oldest remains must be consistent with the earliest dates of human colonization. The Jacksons Bay Caves record throws some light on the origin of one endemic species of mammal, *Oryzomys antillarum*, the extinct Jamaican Rice Rat.

Although it has been shown that the Jamaican rice rat is apparently distinct from other *Oryzomys* (Morgan 1993), it has not previously been demonstrated that *O. antillarum* was present in the Pleistocene of Jamaica. The BDP excavation in Drum Cave yielded several mandibles of *O. antillarum* from above, and more importantly from within, the undisturbed Guano I horizon, which is tightly constrained to have been deposited between 11,260 ±80 $^{14}$C yrs BP and 10,250 ±80 $^{14}$C yrs BP. The bone bears the characteristic staining seen in all Guano I material, and the interface between Guano I and the overlying sediments is so distinct as to preclude any reasonable possibility that *Oryzomys* could be intrusive. *Oryzomys* is, thus, established as a *bona fide* member of the latest Pleistocene fauna of Jamaica. It has long been established that *O. antillarum* is little differentiated from its mainland sister taxon and, therefore, of relatively recent tenure on Jamaica (Morgan 1993). This Pleistocene record, therefore, also eliminates any possibility that *O. antillarum* was an accidental traveler on an Amerindian canoe, and adds it to the roster of native Antillean mammals whose arrival in the Antilles can be definitively ascribed to over-water disperal. Eustatic sea level between the Late Glacial Maximum (~20 ka) and 11-10 ka would have been between ~-120 and ~-40 m (Bard *et al.* 1990), considerably shortening the distance to be covered by exposing the Mosquito, Rosalind and Pedro Banks.

## PALEOCLIMATIC RECONSTRUCTION

These records suggest that the paleoenvironment of Portland Ridge was significantly different from today during the latest Pleistocene and most of the Holocene. Wetter periods throughout the record (~16.5 ka to ~0.7 ka) are suggested by:

- extensive deposits of now largely inactive calcite
- extensive deposits of sub-fossil bat guano, no longer being deposited in such quantities
- archaeological remains indicating water collection in now dry caves
- crocodile remains in now dry caves
- evidence for mid- to Late Holocene flood activity
- Late Holocene guano $\delta^{13}$C values indicating formerly more mesic conditions

The presence of guano in Lloyds Cave at 16.4 – 10.44 $^{14}$C kyrs BP, and the layers of calcite of unknown depth overlying bedrock in BDP and Bone Hall suggest wetter conditions at least periodically from ~16–10 $^{14}$C kyrs BP. Guano from 11.98 –11.44 $^{14}$C kyrs BP, the cluster of guano dates 10.26–10.25 $^{14}$C kyrs BP, and the calcite plus breakdown capping on the 10.25 $^{14}$C kyrs BP guano suggest periodic interruptions. Guano deposition continued throughout this period until ~1.7 $^{14}$C kyrs BP in Lloyds and ~0.95 $^{14}$C kyrs BP in Potoo Hole, in combination with the possible flood event after 1.8 $^{14}$C kyrs BP in Skeleton Cave, and the scattering of shell dates between 4 and 3.4 $^{14}$C kyrs BP. These data suggest only periodic interruptions rather than a prolonged dry spell.

We tentatively divide the paleoclimate into four phases:

| | |
|---|---|
| ~16.5 – 10 | $^{14}$C kyrs BP: Dry |
| ~10 – 2 | $^{14}$C kyrs BP: Intermittently wet |
| ~2 – 0.7 | $^{14}$C kyrs BP: Wet, humid |
| ~0.7 – 0 | $^{14}$C kyrs BP: Dry |

## COMPARISON WITH OTHER RECORDS OF CARIBBEAN CLIMATE CHANGE

Paleoclimatic records from the Caribbean are not abundant. One of the best-studied sites is Lake Miragoane, southern Haiti. Pollen and stable isotope records since ~10.3 $^{14}$C kyrs BP are reported in Hodell *et al.* (1991) and Higuera-Grundy *et al.* (1999). This site is in a similar south-coastal, leeward-of-highlands setting as the Jacksons Bay site. Lake levels are complicated by rising Holocene sea level but the climatic interpretations take this into account. Low lake levels indicating a dry climate at ~10.5–10 $^{14}$C kyrs BP are coincidental with the Younger Dryas period of Europe and North America. Higher lake levels at ~10–7 $^{14}$C kyrs BP coincide with the end of Termination II and the early Holocene in the marine isotopic records although some discrepancy exists between lake level data and vegetation data. The pollen record continued to show dry conditions until ~8.2 $^{14}$C kyrs BP. The highest lake levels between ~7 and 3.2 $^{14}$C kyrs BP are matched by mesic forest in the pollen record. Decline of lake levels at ~3.2–2.4 $^{14}$C kyrs BP indicate dry conditions, becoming very dry at 2.4–1.5 $^{14}$C kyrs BP. A brief return to wet conditions at ~1.5–0.9 $^{14}$C kyrs BP interrupted the drying trend to the present very dry conditions. These changes, summarized in Figure 4, are broadly comparable with the record from Jacksons Bay, although of higher resolution. The indication of higher water levels starting at ~10 $^{14}$C kyrs BP in the Jacksons Bay sediments coincides with the lake levels rather than with vegetation indices. The short-lived wet episode of ~1.5–0. 9 $^{14}$C kyrs BP is matched by

the 0.7–2.0 $^{14}$C kyrs BP wet event and the postulated <~1.8 $^{14}$C kyrs BP flood event in Jacksons Bay Caves, and the recent return to dry conditions coincides in both records.

Little information is available on comparable sites in southern Jamaica. Digerfeldt and Enell (1984) report that levee deposits and silt/clay deposits in the peat of Black River Morass (on the southern coast west of Portland Ridge) indicates increased flooding and wetness between 1.5 and 1.0 $^{14}$C kyrs BP. The other somewhat relevant Jamaican site is from the northern coast but of low resolution: Goodfriend and Mitterer (1988) present evidence of Pleistocene coolness and aridity from land snail amino acid epimerization data, moist conditions in the Late Holocene, and drier conditions beginning sometime during the last millennium. This pattern conforms to the Jacksons Bay record. Street-Perrott *et al.* (1993) report a lake core from Wallywash Great Pond, southern Jamaica, that records a cool, dry climate in the Late Pleistocene at 9.5–9.3 kyrs BP followed by three cycles of alternating wet and dry conditions during the Holocene, regrettably not directly datable.

Another lake site reported by Martin *et al.* (1997): Lake Valencia, just west of Caracas on the Venezuelan coast, is open to the NE trades at all seasons. It is not on the leeward side of highlands and, thus, has a somewhat different climatic regime, as is apparent from the differing climatic history. The lake was ephemeral before ~12.4 ka with savanna-chaparral vegetation; high during the period 12.4–8.8 ka with a shift to forest vegetation; low at ~8.88 to ~5.5 ka, high at ~5.5–3.0 ka, low at ~3.0–1.0 ka, and desiccated in historical times. These changes are summarized in Figure 4.

Higuera-Grundy *et al.* (1999) reviewed the published evidence of climatic change from the Caribbean region. All records agree that the Late Pleistocene was cool and dry with savanna vegetation and low lake levels, remaining dry until at least ~10.5 $^{14}$C kyrs BP when forest taxa appeared in Guatemala. After ~10 $^{14}$C kyrs BP the trade winds weakened, upwelling diminished and lake levels started to rise as a consequence of the higher precipitation. Early Holocene dryness apparently persisted in north coast of Jamaica, Florida, and the Yucatan; Jamaica continued to show a cool, dry climate until ~9.5 $^{14}$C kyrs BP; Florida vegetation did not show a change to mesic conditions until ~7 $^{14}$C kyrs BP. All the Caribbean records show a similar drying phase since ~1 $^{14}$C kyrs BP, which is assumed to have caused the collapse of prehistoric and early historic agriculture (Leyden *et al.* 1998).

## Controls on climate

The ocean-atmosphere system strongly influences Jamaica's climate and, thus, in many ways is very simple. Martin *et al.* (1997), in a discussion of climate controls for the Amazon basin, note that the migration of the Intertropical Convergence Zone (ITCZ) governs seasonality in the Caribbean, when it shifts south in austral summer as the continent of South America warms. While the ITCZ is in its southerly position the Caribbean climate is governed by the North Atlantic sub-tropical high. Holocene shifts displayed in climatic records from southeastern Amazonia and Bolivian Altiplano demonstrate that during the period 15.5–8.8 ka, the ITCZ did not reach as far south into the Amazon basin during the austral summer as it does today. Martin *et al.* (1997) relate this shift to the difference in orbital parameters around 11 ka compared to today. Today's situation of perihelion in December, the austral summer, causes strong seasonal differences in the southern hemisphere. The shift to perihelion in June during the period 15.5–8.8 ka reduces southern hemisphere seasonal differences at this time. Since it is the warming of the continental mass that controls excursions of the ITCZ, the climatic controls on the southern hemisphere are, therefore, significant for the Caribbean climate. Associated with the shift northwards of the ITCZ is an increase in Caribbean precipitation and a weakening of the trade winds.

Hodell *et al.* (1991) note the general agreement between Holocene climatic changes in the Caribbean and in northern Africa, and suggest that the common controlling mechanism is provided by orbital changes. However, they point out that more abrupt changes, such as the sudden change to drier conditions at ~3200 $^{14}$C yr BP in Lake Miragoane, related to ocean-atmosphere interactions, are superimposed on the simple, smooth orbital trends. The general trend of increased wetness and flood activity in the Jacksons Bay caves is probably related to the insolation high centered over 7 ka, but the sudden shift in the guano $\delta^{13}$C from forest to xeric vegetation from ~2000 $^{14}$C yrs BP to present must relate to non-orbital effects.

Jacksons Bay, almost exactly southwest of the Blue Mountains, the highest part of Jamaica, is particularly sensitive to trade wind direction. It is in a rain shadow position for NE winds but open to higher rainfall if the wind shifts to a more easterly origin. We suggest that the general pattern of mid-Holocene wetness is explicable by orbital changes controlling the position of the ITCZ. However, the frequent, rapid shifts of the last two millennia may relate more to local changes in prevailing wind direction.

## Acknowledgments

The fieldwork reported here was conducted between 1995 and 1996 with funding from the National Geographic Society (CRE Grant #5291-94 and 5660-96) to the senior author. Permission to excavate fossils was granted by the Division of Mines and Geology, Jamaica, who have been unstintingly supportive of our work.

We are especially grateful for the hospitality afforded to us by Peter Fletcher, Paul Banks, and other members of the Jacksons Bay Gun Club, without whom sustained efforts at Jacksons Bay would have been impossible. Ross MacPhee and Clare Flemming were essential contributors to the vertebrate paleontology effort. Lisa DeNault, Ray Keeler, Judy Lemire and Andrew Pearson provided invaluable contributions to the fieldwork. Finally, we are most grateful for Stephen Donovan's

interest, assistance, and hospitality at the University of the West Indies, Mona., and David Burney for a critical review of the manuscript.

## REFERENCES

Anonymous, 1950, Handbook of Jamaica, Kingston, Jamaica, Government of Jamaica.

Asprey, G.F., & Robbins, R.G., 1953, The vegetation of Jamaica: Ecological Monographs, v. 23, p. 359-412.

Bard, E., Hamelin, B., & Fairbanks, R.G., 1990, U-Th ages obtained by mass spectrometry in corals from Barbados; sea level during the past 130,000 years: Nature, v. 346, p. 456-458.

Buskirk, R.E., 1985, Zoogeographic patterns and tectonic history of Jamaica and the northern Caribbean: Journal of Biogeography, v. 12, p. 445-461.

Des Marais, D.J., 1980, The carbon isotope biogeochemistry of the individual hydrocarbons in bat guano and the ecology of the insectivorous bats in the region of Carlsbad, New Mexico: Geochimica et Cosmochimica Acta, v. 44, p. 2075-2086.

Digerfeldt, G., & Enell, M., 1984, Paleoecological studies of the past development of the negril and Black River Morasses, Jamaica, *in* Bjork, S., ed., Environmental feasibility study of peat mining in Jamaica: Kingston, Jamaica, Petroleum Corporation of Jamaica, Appendix 1., p. 1-145.

Duerden, J.E., 1897, Aboriginal Indian remains in Jamaica: Journal of the Institute of Jamaica, v. 2, p. 1-52.

Fincham, A.G., 1997, Jamaica underground. The caves, sinkholes and underground rivers of the island: Kingston, Jamaica, University of West Indies Press, 447 p.

Fincham, A.G., & Fincham, A.M., 1997, The Potoo Hole pictographs: Jamaica Journal, v. 26, p. 2-6.

Goodfriend, G.A., & Stipp, J.J., 1983, Limestone and the problem of radiocarbon dating of land snail shell carbonate: Geology, v. 11, p. 575-577.

Goodfriend, G.A., & Mitterer, R.M., 1988, Late Quaternary land snails from the north coast of Jamaica: Local extinctions and climatic change: Palaeogeography, Palaeoclimatology, Palaeoecology, v. 63, p. 293-311.

Goodwin, R.E., 1970, The ecology of Jamaican bats: Journal of Mammalogy, v. 51, p. 571-579.

Higuera-Grundy, A., Brenner, M., Hodell, D.A., Curtis, J.H., Leyden, B.W., & Binford, M.W., 1999, A 10,300 14C yr record of climate and vegetation change from Haiti: Quaternary Research, v. 52, p. 159-170.

Hodell, D.A., Curtis, J.H., Jones, G.A., Higuera-Gundy, A., & Brenner, M., 1991, Reconstruction of Caribbean climate change over the past 10,500 years: Nature, v. 352, p. 790-793.

Holdridge, L.R., 1967, Life zone ecology: San Jose, Tropical Science Center.

Jeuniaux, C., 1971, Chitinous structures, *in* Florkin, M.S., & Stotz, E.H., eds., Comprehensive Biochemistry: Amsterdam, Elsevier, p. 595-632.

Koval, E.Z., & Kharkevich, E.S., 1983, Chitin degredation by soil fungi in a wooded area: Mikrobiologicheskii Zhurnal, v. 45, p. 57-63.

Lamb, H.H., 1995, Climate, history and the modern World: London, Routledge, 433 p.

Leyden, B.W., Brenner, M., & Dahlin, B.H., 1998, Cultural and climatic history of Coba, a lowland Maya city in Quintana Roo, Mexico: Quaternary Research, v. 49, p. 111-122.

Logan, G.A., Collins, M.J., & Eglinton, G., 1991, Preservation of organic biomolecules, *in* Allison, P.A., & Briggs, D.E.G., eds., Taphonomy: Releasing the data locked in the fossil record: New York, Plenum.

MacPhee, R.D.E., & Iturralde-Vinent, M.A., 1999, Paleogeography of the Caribbean region; implications for Cenozoic biogeography: Bulletin of the American Museum of Natural History, p. 95.

Martin, L., Bertaux, J., Corrège, T., Ledru, M.-P., & Mourguiart, P., 1997, Astronomical forcing of contrasting rainfall changes in tropical South America between 12,400 and 8800 cal yr B.P.: Quaternary Research, v. 47, p. 117-122.

McFarlane, D.A., 1986, Cave bats in Jamaica: Oryx, v. 20, p. 27-30.

McFarlane, D.A., 1987, Radiant darkness - the many facets of the caves of Jacksons Bay, Jamaica: Terra (Natural History Museum of Los Angeles County), v. 25, p. 24-26.

Miller, R.F., Voss-Foucart, M.-F., Toussaint, C., & Jeuniaux, C., 1993, Chitin preservation in Quaternary Coleoptera: Palaeogeography, Palaeoclimatology, Palaeoecology, v. 103, p. 133-140.

Mizutani, H., McFarlane, D.A., & Kabaya, Y., 1992, Carbon and nitrogen isotopic signatures of bat guanos as a record of past environments: Mass Spectroscopy, v. 40, p. 67-82.

Morgan, G.S., 1993, Quaternary land vertebrates of Jamaica, *in* Wright, R.M., & Robinson, E., ed., Biostratigraphy of Jamaica: Memoirs of the Geological Society of America. Vol. 182: Denver, Geological Society of America.

Muzzarelli, R.A.A., 1977, Chitin: Oxford, Pergamon.

Mylroie, J.E., & Carew, J.L., 2000, Speleogenesis in coastal and oceanic settings, *in* Klimchouk, A.B., Ford, D.c., Palmer, A.N., & Dreybrodt, W, ed., Speleogenesis: Evolution of karst aquifers: Huntsville, AL, National Speleological Society, p. 226-233.

Panuska, B.C., Mylroie, J.M., Armentrout, D., & McFarlane, D., 1998, Magnetostratigraphy of Cueva del Aleman, Isla de Mona, Puerto Rico and the species duration of Audubon's Shearwater: Journal of Cave and Karst Studies, v. 60, p. 96-100.

Reissig, J.L., Strominger, J.L., & Leloir, F.L., 1955, A modified colorimetric method for the estimation of N-acetylamino sugars: Journal of Biological Chemistry, v. 217, p. 959-966.

Schimmelmann, A., & DeNiro, M.J., 1986, Stable isotopic studies on chitin II. The 13C/12C and 15N/14N ratios in arthropod chitin: Contributions in Marine Science, v. 29, p. 113-130.

Seifriz, W., 1943, The plant life of Cuba: Ecological Monographs, v. 13, p. 375-426.

Street-Perrott, F.A., Hales, P.E., Perrott, R.A., Fontes, J.C., Switsur, V.R., & Pearsons, A., 1993, Late Quaternary palaeolimnology of a tropical marl lake: Wallywash Great Pond, Jamaica: Journal of Paleolimnology, v. 9, p. 3-22.

Wadge, G., Fincham, A.G., & Draper, G., 1979, The caves of Jacksons Bay and the Cainozoic geology of southern Jamaica: Transactions of the British Cave Research Association, v. 6, p. 70-84.

Williams, E.E., 1989, Old problems and new opportunities in West Indian biogeography, *in* Woods, C.A., ed., Biogeography of the West Indies: Past, present and future: Gainesville, Sandhill Crane Press, p. 1-46.

**Appendix 1. Summary of radiocarbon dates from the Jacksons Bay Caves**

| ID | Site | Material | Age |
|---|---|---|---|
| 95-04 (81354) | BDP, Drum cave. Surface guano | Bat Guano | 10,350 ± 70 |
| 95-21 (83967) | BDP excavation, Drum Cave. Top of Guano I | Bat Guano | 10,250 ± 80 |
| 95-22 (83968) | BDP excavation, Drum Cave. Base of Guano I | Bat Guano | 11,260 ±80 |
| 95-23 (86687) | BDP excavation, Drum Cave, Base of Guano II | Bat Guano | 11,980 ±80 |
| 95-17 (82655) | Surface gours, Drum cave, near Entrance #3. Cave pearl. | Shell | 4,020 ±120 (3,700 ±120*) |
| 95-03 (82221) | Bone Hall, Drum cave. 'Guano I' | Bat Guano | 11,050 ± 70 |
| 96-16 (98640) | Bone Hall excavation, Drum Cave. 'G1c' layer. | Bat Guano | 11,220 ±100 |
| 96-22 (98642) | Bone Hall, Drum Cave. –30 cm, bottom of pit | Shell | 13,540 ±150 (13,220 ±150*) |
| 95-07 (83966) | Guano Crawl, Lloyds Cave. -30 to -40 cm | Bat Guano | 10,440 ±100 |
| 95-08 (82689) | Guano Crawl, Lloyds Cave. - 95 to -100 cm. | Bat Guano | 16,400 ± 110 |
| 96-18 (98641) | Map Room, Skeleton Cave. 'surface' against roof. | Shell | 4230 ±70 (3910 ±70*) |
| 95-12 (81716) | Map Room, Skeleton Cave, mixed layer, 0 to -30 cm. | Bone | 1870 ±50 (AMS) |
| 95-14 (81718) | Map Room, Skeleton Cave. - 150 to -160 cm | Shell | 3740 ± 60 (3420 ±60*) |
| 95-32 (83970) | Map Room, Skeleton Cave. Xenothrix level. | Shell | 6,730 ±110 (6,410 ±110*) |
| 95-16 (82222) | 'Guano Mountain', Potoo Hole. -5 to -10 cm. | Bat Guano | 950 ± 50 |
| 93-03 (67572) | Guano Crawl, Lloyds Cave. Surface 1 cm. | Bat Guano | 1750 ± 80 |
| 85-02 | Queen's Series, Jacksons Bay Old Cave, -1 to –3 cm | Bat Guano | 0.70 ±0.05 |
| 96-15 (98639) | High Dome Upper. Guano deposit at -115 cm. | Bat Guano | 10,850 ±100 |

* indicates shell dates corrected for the 320 year "limestone effect"
ID numbers are field numbers, with Beta Analytic laboratory codes in parentheses.

Eugene H. Studier, Kathleen H. Lavoie, and Francis G. Howarth - Leg attenuation and seasonal femur length: Mass relationships in cavernicolous crickets (Orthoptera: Gryllidae and Rhaphidophoridae). *Journal of Cave and Karst Studies 64*(2): 126-131.

# LEG ATTENUATION AND SEASONAL FEMUR LENGTH: MASS RELATIONSHIPS IN CAVERNICOLOUS CRICKETS (ORTHOPTERA: GRYLLIDAE AND RHAPHIDOPHORIDAE)

EUGENE H. STUDIER[1], KATHLEEN H. LAVOIE[1,3]
[1]*Department of Biology, University of Michigan-Flint, Flint, MI 48502-2186 USA*
FRANCIS G. HOWARTH[2]
[2]*Hawaii Biological Survey, Bishop Museum, Honolulu, HI 96817-2704 USA*
[3]*Current address: Dean, Faculty of Arts and Sciences; 101 Broad Street; State University of New York at Plattsburgh; Plattsburgh, NY 12901-2681 USA*

*We report here some factors that affect the relationship between hind femur length (HFL) to crop-empty live weight (CELW) and propose a quantitative, non-lethal measurement ratio that has potential as an index of extent of adaptation to a cavernicolous existence in "crickets". Curvilinear relationships exist between HFL and CELW for camel crickets* (Ceuthophilus stygius) *and cave crickets* (Hadenoecus subterraneus). *The relationships differ significantly between the species and also by gender within both species and, in cave crickets, by season as well. In* C. stygius, *females of small HFL are slightly lighter, and those of large HFL slightly heavier than males. In* H. subterraneus, *females have progressively greater CELW than males as HFL increases. In adult* H. *subterraneus of identical HFLs, CELW is greatest in fall and least in spring, i.e., individuals are most robust in the fall in these long-lived crickets, probably due to seasonal constraints on surface feeding. An attenuation index of CELW/HFL³ yields a ratio that ranks the extent of adaptation to cave life in these two and eight other species of variously adapted cavernicolous and epigean "crickets". Lower values of the attenuation index indicate greater adaptation to cavernicolous existence. The three gryllid species from Hawaii Island are closely related and include the blind, obligate cave cricket,* Caconemobius varius, *and two surface species, the lava flow cricket,* Caconemobius fori, *and the marine littoral cricket,* Caconemobius sandwichensis. *The latter two species are nocturnal scavengers on barren rock habitats. The lower CELW/HFL³ ratio in lava flow crickets suggest they use caves more frequently for daytime roosts than does the marine littoral species.*

Rhaphidophorids and Gryllids are found in a wide range of environments, including caves, and those that occupy deep cave habitats are often known as cave crickets. The deep cave environment is quite stable, with high humidity and nearly constant year-round temperature, although both of these conditions are more variable near entrances (Poulson & White 1969; Howarth 1982). Beyond the twilight zone, caves are characterized by complete darkness and are perceived as being food-poor, or where food is difficult to locate and exploit. Culver (1982) and Howarth (1983) summarize expected adaptations to cave life into four areas: metabolic economy, increased senses, adaptations to high moisture and humidity, and development of neoteny. These features, commonly associated with reduced eyes and bodily pigment, are collectively known as troglomorphic characteristics (Christiansen 1995) and are discussed further in Culver *et al*. (1995).

The general perception of elongated appendages and fragile appearance is widely regarded as being characteristic of cave animals, but few studies compare cave-limited species with surface relatives and ancestral species (Culver 1982). Elongated appendages, particularly antennae, could increase sensory perception, while elongated legs may be an adaptation for walking on irregular surfaces in total darkness, i.e., in a 3D dark maze where stepping across gaps may be safer than jumping or walking around. Elongated appendages also could be an adaptation for metabolic economy-with longer legs, the animal could move farther with each step.

Vandel (1965) generalizes very broadly that cavernicolous rhaphidophorids show extreme appendage elongation, even within a group that tends to have long appendages, although he states that cavernicolous *Ceuthophilus* have limbs of normal dimensions. Culver (1982) criticizes many of Vandel's conclusions, citing use of inappropriate comparisons of cave and surface species.

Holsinger and Culver (1970), in an allometric study of populations of the amphipod *Gammarus minus* in springs and caves, show that significantly longer first antennae in cave populations is not due to positive allometric effects. They also point out that the genetic basis and the role of selection in these differences is unclear. Recent studies have begun to examine the genetic basis of adaptation to cave life by North American (Caccone & Sbordoni 1987) and European cave crickets (Allegracci *et al*. 1991) and biogeography (Caccone & Sbordoni 2001)

Cave crickets that feed outside and roost in caves are important in the food budgets of cave ecosystems. When bats or seasonal flooding in upper-level passages are absent, cricket guano, eggs and carcasses are a major food resource for obligate cavernicoles (Poulson & White 1969). As part of our studies of many aspects of rhaphidophorid biology (Studier *et*

 Copyright © 2002 by The National Speleological Society

*al*. 1986; 1987a; 1987b; 1991; Northup *et al*. 1993; Studier 1996), we have collected data on hind femur length (HFL, a measure of attenuation) and crop empty live weight (CELW, a measure of mass) in several species that are variously adapted to a cavernicolous existence. We use crop-empty live mass to minimize the effects of foraging on the relationship. Some cave crickets are known to consume 100% or more of their body weight in a single night of foraging (Studier *et al*. 1986).

Species examined in this study include epigean gryllids: the house cricket (*Acheta domestica*) and field cricket (*Gryllus pennsylvanicus*), neither of which is adapted for cave life, as well as other species of both gryllids and rhaphidophorids that are variously adapted to cave life from Kentucky, New Mexico, and Hawaii.

Kentucky species include the cave cricket, *Hadenoecus subterraneus*, and camel cricket, *Ceuthophilus stygius*. Studies indicate that *H. subterraneus* is a long-lived (at least 1.5 years as an adult) species (Studier *et al*. 1988), which possesses highly attenuated appendages (Christiansen 1995), copulates and lays large eggs in caves, reproduces in all seasons (Cyr *et al*. 1991), and forages outside caves at irregular, long intervals when epigean conditions are favorable (Studier *et al*. 1986; Poulson *et al*. 1995). *Ceuthophilus stygius* completes its life cycle in a year, copulates in cave entrances in the fall, is found deeper in caves only as young instars in the winter, leaves caves nightly to forage and appears to be very robust with few adaptations to cave life (Studier *et al*. 1988).

Rhaphidophorids studied from New Mexico are *Ceuthophilis longipes*, *Ceuthophilus conicaudus*, and *Ceuthophilus carlsbadensis*. Of these, *C. longipes* appears to be the most highly adapted to cave life while *C. conicaudus* seems to be the functional equivalent of *C. stygius*. *C. carlsbadensis*, which feeds on surface material in the massively abundant guano deposited by the Mexican free-tailed bat, *Tadarida brasiliensis*, appears to be the least cave adapted. Details of their behavioral, morphological, and physiological adaptation to cave life are given in Northup (1988) and Northup *et al*. (1993).

The gryllids studied from Hawaii are the rock crickets, *Caconemobius sandwichensis*, *Caconemobius fori*, and *Caconemobius varius*. The genus *Caconemobius* is found only in Hawaii and all known species are specialized to live only in barren wet rock habitats (Howarth 1987; Otte 1994). The presumed ancestor of the island terrestrial species is *C. sandwichensis*, a nocturnal marine littoral species living in the wave splash zone of boulder beaches on all the main Hawaiian Islands (Otte 1994). This species shows no cave adaptation but will roost in deep crevices and caves if available and moistened by salt spray. On Hawaii Island, several species have evolved to live inland on similar barren wet rock habitats. *Caconemobius fori*, a nocturnal scavenger of wind-borne debris on young, unvegetated lava flows on Kilauea Volcano (Howarth 1979), colonizes new flows within a month of eruption and disappears when plants begin to colonize the flow. During the day, these crickets hide deep in fumaroles, moist cracks, and caves within the flow but exhibit no troglomorphies. In contrast, the closely related *C. varius* is troglomorphic and obligately adapted to live only in caves and associated medium-sized subterranean voids in young basaltic lava. Although *C. varius* occasionally forage among wet rocks in the twilight zone of caves, they do not occur on the surface and display no activity rhythm, being minimally active throughout each 24-hour cycle (Ahearn & Howarth 1982).

This paper examines seasonal changes in the extent of attenuation in *H. subterraneus* and explores the possibility of using relative HFL attenuation as a simple, non-lethal index of degree of cave adaptation in cavernicolous and epigean orthopterans.

## MATERIALS AND METHODS

Techniques used to determine HFL and CELW follow Studier *et a1*. (1986). HFL is measured using calipers and a metric ruler. CELW is determined by dissection and removal of the distensible crop to create a baseline curve that can then be used non-lethally to predict mass using HFL and, by difference, the amount of material in the crop. Approximately 100 *H. subterraneus* of both sexes and varying ages were collected seasonally (spring - 29 April 1986; summer - 26 July 1986; fall - 20 October 1986; and winter - 24 January 1987) from Walnut Hill Cave near Park City, Kentucky (KY). Smaller total numbers (n=247) of *C. stygius* were collected during the same time span, at nearly monthly intervals (9-36 individuals/month), from the entrances of Great Onyx and White caves, and the Frozen Niagara, Floyd Collins Crystal, and Austin entrances to Mammoth Cave in Mammoth Cave National Park, KY. In May 1989, *C. carlsbadensis* (n=29), *C. longipes* (n=21) and *C. conicaudus* (n=20) were taken from the Bat Cave and Sand Passage portions of Carlsbad Cavern and Spider Cave, respectively, in Carlsbad Caverns National Park, New Mexico (NM). In September 1989, house crickets, *A. domestica*, were purchased from a local pet store and field crickets, *G. pennsylvanicus*, were collected in Iosco Co., Michigan. In May 1988, individuals of both sexes of *C. varius* (n=19) were collected from Kaumana Cave, *C. fori* (n=19) from the 1974 Mauna Ulu and the 1987 Pu'u' 'O'o lava flows, and *C. sandwichensis* (n=14) from a rocky slope leading to the sea on the north side of Wailuku River mouth, on the island of Hawaii, (HI). Examples of the Kentucky and New Mexico crickets studied have been deposited in the insect collection, Museum of Zoology, University of Michigan-Ann Arbor. Voucher specimens of Hawaiian crickets are housed in the Bishop Museum, Honolulu, HI.

The possible relationship between CELW, HFL, $HFL^2$, $HFL^3$, sex and season was analyzed in a multiple regression (backward elimination) model using SPSSX where sex and season were included as dummy (categorical) variables (SPSS 1993). Dummy variables were assigned as follows: males = 0, females = 1; winter = 0, spring = 1, summer = 2, fall = 3. Variables were tested for normal distributions and transformed

if necessary. The critical probability value for multiple regression analyses was set at 0.10. Critical values for all other analyses were set at 0.05. Descriptive statistics and polynomial regression equations were generated with SYSTAT (Wilkinson 1988) for relationships between CELW and HFL, done separately by sex and season for *H. subterraneus.* Reproduction occurs only once on an annual cycle in *C. stygius* (Studier *et al*. 1988), thus regression analysis was done separately only by sex in this species.

## RESULTS AND DISCUSSION

Multiple regression analysis of log CELW as a function of HFL, $HFL^2$, sex, and season for *H. subterraneus* ($F = 3201.4$, d.f. = 6 and 421, $P < 0.0001$, $r^2 = 0.98$) is summarized in Table 1. Neither $HFL^3$ nor interactions between sex and season were significant and both were excluded from the model. The dummy variables for gender and season exhibit significance in the overall analysis for *H. subterraneus*, therefore separate polynomial regression analyses of the relation of CELW to HFL and $HFL^2$ were performed (Table 2). The analyses indicate that female *H. subterraneus* are larger than males in all seasons, that individuals of identical HFL are lightest in the spring and heaviest in the fall, and that the aforementioned differences are progressively greater as HFL increases.

Gonad mass is markedly greater in female than male *H. subterraneus* (Studier *et al*. 1986), thus mature females would be expected to have greater CELW than males of similar HFL. The observed seasonal differences may relate to the epigean foraging frequency and reproductive effort of *H. subterraneus*, because it exhibits extreme metabolic and water budget sensitivities to ambient relative humidity and temperature (Studier & Lavoie 1990). Epigean feeding in *H. subterraneus* appears limited to nights when above-ground relative humidity is at or near saturation and is near cave temperatures of 12-14°C (Studier & Lavoie 1990; Poulson *et al.*1995). Such conditions occur most frequently in late summer and fall in Kentucky; therefore, we expect that these cave crickets exhibit positive energy budgets, greatest secondary productivity, and greatest mass in the fall. Although *H. subterraneus* are reproductively active throughout the year, they exhibit a peak in occurrence of mature gonads and rates of egg laying in winter months (Hubbell & Norton 1978; Cyr *et al*. 1991). These activities, coupled with infrequent appropriate conditions for epigean feeding, account for the individual loss of biomass through the winter and extending into spring. The combined stress of infrequent foraging and great energy expenditure for reproductive effort, explain the loss of individual biomass and may account for the apparent marked mortality of adults that occurs in the

**Table 1. Multiple regression analysis of log CELW as a function of HFL, $HFL^2$, and the categorical variables, sex, and season of *Hadenoecus subterraneus*. Values in parentheses are standard errors (SE). Variable interactions and $HFL^3$ were not significant and not retained in the model.**

| Variables | Coefficent (SE) | Probability |
|---|---|---|
| HFL | 0.1369 (0.0039) | <0.0001 |
| $HFL^2$ | -0.001700 (0.000135) | <0.0001 |
| Female | 0.01336 (0.00810) | 0.0999 |
| Spring | -0.03381 (0.01127) | 0.0029 |
| Summer | 0.02396 (0.01091) | 0.0287 |
| Fall | 0.03810 (0.01112) | 0.0007 |
| Constant | -2.6084 (0.0263) | <0. 0001 |

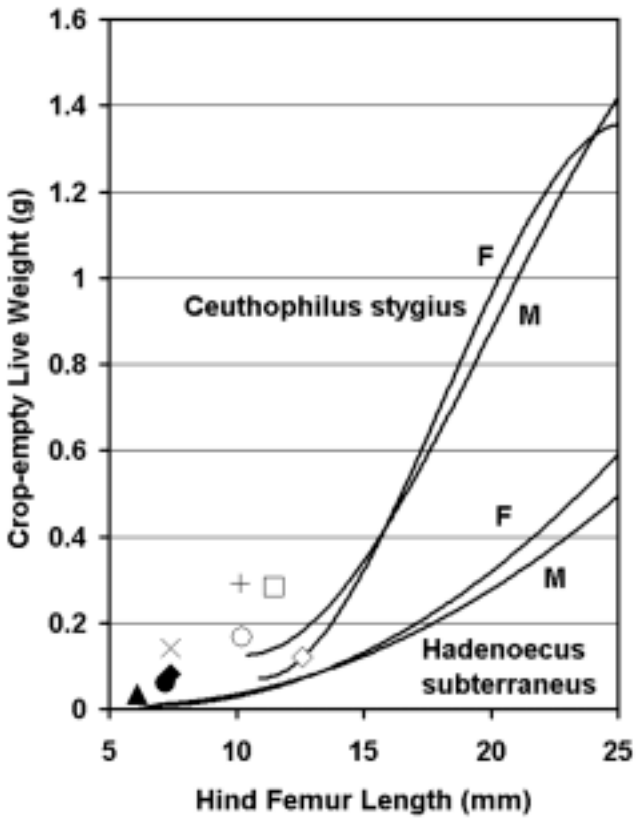


**Figure 1. Relationship between hind femur length (HFL in mm) and crop-empty live weight (CELW in g) in various aged male (M), female (F) and immature cave crickets, *Hadenoecus subterraneus*, (solid lines; equations for spring – see Table 2) and camel crickets, *Ceuthophilus stygius* (dashed lines; equation for males: $CELW = -0.0004101\ HFL^3 + 0.02481\ HFL^2 - 0.3824\ HFL + 1.881$; and, for females: $CELW = -0.0008709\ HFL^3 + 0.04734\ HFL^2 - 0.7233\ HFL + 3.459$. Both species can be separated reliably by gender at HFL ≥ 15 mm. Other species and symbols are *Ceuthophilus longipes* (open diamond), *Ceuthophilus carlsbadensis* (open square), *Ceuthophilus conicaudus* (open circle), *Caconemobius varius* (closed triangle), *Caconemobius fori* (closed circle), *Caconemobius sandwichensis* (closed diamond), *Gryllus pennsylvanicus* (+), and *Acheta domestica* (x). Data for these species are from Table 3.**

**Table 2. Polynomial regression analysis of CELW (gm) to HFL and HFL$^2$ (both in mm) for *Hadenoecus subterraneus* by sex and season. All equations are of the form CELW = a (HFL$^2$) + b (HFL) + c, where a and b are regressions coefficients and c is the intercept. Numbers in parentheses are standard errors. P < 0.0001 in all cases.**

| Sex | Season | a | b | c | $r^2$ | df | F |
|---|---|---|---|---|---|---|---|
| Males | Spring | 0.001283 | -0.01426 | 0.04856 | 0.970 | 2, 33 | 542.1 |
| | | (0.000143) | (0.00402) | (0.02320) | | | |
| | Summer | 0.001225 | -0.01238 | 0.04430 | 0.960 | 2, 48 | 570.9 |
| | | (0.000146) | (0.00414) | (0.02543) | | | |
| | Fall | 0.001662 | -0.02174 | 0.08807 | 0.933 | 2, 39 | 271.2 |
| | | (0.000268) | (0.00726) | (0.04118) | | | |
| | Winter | 0.001482 | -0.01948 | 0.08157 | 0.959 | 2, 66 | 772.3 |
| | | (0.000133) | (0.00394) | (0.02609) | | | |
| Females | Spring | 0.001699 | -0.02202 | 0.07896 | 0.942 | 2, 59 | 475.8 |
| | | (0.000188) | (0.00565) | (0.03681) | | | |
| | Summer | 0.001740 | -0.02302 | 0.08722 | 0.955 | 2, 48 | 505.6 |
| | | (0.000174) | (0.00510) | (0.03318) | | | |
| | Fall | 0.001856 | -0.02739 | 0.01178 | 0.940 | 2, 54 | 423.7 |
| | | (0.000193) | (0.00230) | (0.03420) | | | |
| | Winter | 0.001590 | -0.02120 | 0.08791 | 0.980 | 2, 54 | 1323.1 |
| | | (0.000117) | (0.00355) | (0.02333) | | | |

winter to spring time span (Studier *et al*. 1988).

Relationships between HFL and CELW are curvilinear in those species where a range of sizes of individuals were studied (Fig. 1). In both *H. subterraneus* and *C. stygius*, the ratio of CELW to HFL changes greatly with size and, therefore, does not provide a useful index of attenuation. These species reach sexual maturity when HFL $\geq$ 20 mm. Because mass and volume are related to linear measures cubed, we compared the ratio of CELW to HFL$^3$ as a potential attenuation index. In *H. subterraneus*, the ratio of CELW/HFL$^3$ averages 0.0334, is essentially constant with a total range of 0.0296-0.0380, and is independent of size. While slightly more variable in *C. stygius* (0.0508-0.1214; average=0.0996), this ratio is proposed as an index of the extent of attenuation, which is useful in species comparison.

This attenuation index (CELW/ HFL$^3$) ranks the cricket species with respect to their level of adaptation to a cavernicolous existence, with low values indicating a high degree of cave adaptation (Table 3). Comparison of the attenuation index within genera (*Hadenoecus*, *Ceuthophilus*, and *Caconemobius*) demonstrates agreement with the degree of adaptation of each group to life in caves. *Ceuthophilus* crickets from New Mexico and Kentucky cover a wide range of levels of cave adaptation and show increased attenuation indices with increased adaptation to life in caves.

The situation with the gryllids from Hawaii is particularly striking considering that the 3 closely related *Caconemobius* species studied represent an appropriate comparison between a cave-adapted species and its 2 closely related surface congeners. All 3 diverged from each other within a relatively short evolutionary time since the island of Hawaii emerged from the sea and became available for colonization between 700,000 and 1,000,000 years ago (Howarth 1982, 1991; Otte 1994). Although both surface species have similar behavior and morphology, the attenuation index data suggest that *C. fori* is more trogloxenic than *C. sandwichensis*. Because of the difficulty of sampling in their solid rock habitats, precise daytime roosting and egg-laying sites cannot be determined except indirectly by behavioral, morphological, and ecological studies. *Caconemobius sandwichensis* does not need to descend very far into its boulder habitat to roost in a permanently moist environment, whereas *C. fori* lives in a much more variable and diverse habitat and may, at times, need to descend into caves to find moisture. Ahearn and Howarth (1982) studied water balance physiology and metabolic rate of these same species and, as expected, their ability to conserve water is strongly correlated with their environment. *Caconemobius sandwichensis*, the marine littoral ancestor, is rarely, if ever, subjected to extremes in temperature or to an ambient relative humidity different from 98%, the equilibrium humidity of seawater. *Caconemobius fori*, the lava flow species, is exposed to extreme daily temperature and relative humidity fluctuations as well as to geothermal heat. The cave species, *C. varius*, lives in a constant temperature environment and is extremely sensitive to and avoids relative humidity below saturation. After 12 hours in a desiccating environment near their normal ambient temperature (19°C), the cave species lost significantly more water (14.7 ±0.7% of body mass) than did either surface species, *C. fori* (8.8 ±0.7%) and *C. sandwichensis* (11.5 ±0.6%) (Ahearn & Howarth 1982).

In summary, a relationship exists between body mass (CELW) and a linear body measurement (HFL) in those species of cavernicolous crickets where a wide range of sizes has been measured–*H. subterraneus* and *C. stygius*. In both

**Table 3. Averages or ranges [in brackets] of hind femur lengths (HFL), crop-empty live weight (CELW) and attenuation indices (CELW/HFL³) for "cricket" species, Rhaphidophoridae and Gryllidae, variously adapted to a cavernicolous or epigean environment. Values in parentheses are standard errors. Crickets are ranked specifically by attenuation index and broadly by status of cave adaptation in decreasing order indicated as TB = troglobite, TP = troglophile, TX = trogloxene, EP = epigean.**

| Species | Status in caves | Number location | CELW (mg) | HFL (mm) | CELW HFL³ |
|---|---|---|---|---|---|
| **Rhaphidophoridae** | | | | | |
| *Hadenoecus subterraneus* | TP | 425 KY | [11.3-556.8] | [7-25] | 0.0334 [0.0296-0.0380] |
| *Ceuthophilus longipes* | TP | 21 NM | 120.2 (0.1) | 12.6 (0.1) | 0.0602 |
| *Ceuthophilis stygius* | EP/TX | 247 KY | [108.5-1338] | [10-25] | 0.0996 [0.0508-0.1214] |
| *Ceuthophilus conicaudus* | EP/TX | 20 NM | 166.0 (9.3) | 10.2 (0.2) | 0.1546 |
| *Ceuthophilus carlsbadensis* | EP/TX | 29 NM | 283.6 (0.1) | 11.5 (0.1) | 0.1879 |
| **Gryllidae** | | | | | |
| *Caconemobius varius* | TB | 19 HI | 34.0 (2.4) | 6.1 (0.1) | 0.1474 |
| *Caconemobius fori* | EP/TX | 19 HI | 59.4 (0.1) | 7.2 (0.2) | 0.1571 |
| *Caconemobius sandwichensis* | EP | 14 HI | 80.9 (4.0) | 7.4 (0.2) | 0.1998 |
| *Gryllus pennsylvanicus* | EP | 20 MI | 291.7 (0.1) | 10.1 (0.1) | 0.2831 |
| *Acheta domestica* | EP | 20 — | 142.2 (4.0) | 7.4 (0.2) | 0.3543 |

species, the relationships differ between sexes with adult females routinely being heavier than adult males of similar HFL. In *H. subterraneus*, relationships additionally differ with season where individuals of similar HFL are lightest in the spring and heaviest in the fall. An attenuation index (CELW/HFL³) inversely ranks the studied cricket species to their level of adaptation to a cavernicolous existence and is proposed as a potentially useful non-lethal quantitative indicator of extent of cave adaptation in orthopterans.

ACKNOWLEDGMENTS

We thank Diana Northup, Ken Ingham, William Ziegler, Dave Barclay, Steve Sevick, Dennis Viele, and the staff of the Cave Resources Office at Carlsbad Caverns National Park for aid in collection and Diana Northup for identification of crickets in New Mexico. Jim Lavoie and Fred Stone are thanked for similar help with field work in Hawaii. T. Poulson and T. Hubbell verified identification of the Kentucky crickets. We also thank Harry Edwards and Joe Hudson for their assistance with the multiple regression analysis. Fieldwork in Hawaii was

supported in part by National Science Foundation Grant No. BSR-85-15183.

## REFERENCES


Ahearn, G.A., & Howarth, F.G., 1982, Physiology of cave arthropods in Hawaii: Journal of Experimental Zoology, v. 222, p. 227-238.

Allegracci, G., Caccone, A., Cesaroni, D., & Sbordoni, V., 1991, Evolutionary divergence in European cave crickets: A comparison of scDNA data with allozyme and morphometric distance: Journal of Evolutionary Biology, v. 5, p. 121-148.

Caccone, A., & Sbordoni, V., 1987, Molecular evolutionary divergence among North American cave crickets. I. Allozyme variation: Evolution, v. 41, p. 1198-1214.

Caccone, A., & Sbordoni, V., 2001, Molecular biogeography of cave life: A study using mitochondrial DNA from bathysciine beetles: Evolution, v. 55, p. 122-130.

Christiansen, K.A., 1995, Cave life in light of modern evolutionary theory, *in* Camacho, A., ed., The natural history of biospeleology: Madrid, Spain, Madrid Museo Nacional de Ciencias Naturales, p. 453-478.

Culver, D.C., 1982, Cave life-Evolution and ecology: Cambridge, Massachusetts, Harvard University Press, 189 p.

Culver, D.C., Kane, T.C., & Fong, D.W., 1995, Adaptation and natural selection in caves: The evolution of *Gammarus minus*: Cambridge, Massachusetts, Harvard University Press, 223 p.

Cyr, M., Studier, E.H., Lavoie, K.H., & McMillin, K.L., 1991, Biology of cave crickets, *Hadenoecus subterraneus*, and camel crickets, *Ceuthophilus stygius* (Insecta: Orthoptera)-Annual cycles of gonad maturation, characteristics of copulating pairs, and egg laying rates: American Midland Naturalist, v. 125, p. 231-239.

Holsinger, J.R., & Culver, D.C., 1970, Morphological variation in *Gammarus minus* Say (Amphipoda, Gammaridae) with emphasis on subterranean forms: Postilla, No. 146.

Howarth, F.G., 1979, Neogeoaeolian habitats on new lava flows on Hawaii Island: An ecosystem supported by windborne debris: Pacific Insects, v. 20, p. 133-144.

Howarth, F.G., 1982, Bioclimatic and geologic factors governing the evolution and distribution of Hawaiian cave insects: Entomology Gen, v. 8, p. 17-26.

Howarth, F.G., 1983, Ecology of cave arthropods: Annual Review of Entomology, v. 28, p. 365-389.

Howarth, F.G., 1987, Evolutionary ecology of aeolian and subterranean habitats in Hawaii: Trends in Ecology & Evolution, v. 2, p. 220-223.

Howarth, F.G., 1991, Hawaiian cave faunas: Macroevolution on young islands, *in* Dudley, E.C., ed., The unity of evolutionary biology: Portland, Oregon, Dioscorides Press, p. 285-295.

Hubbell, T.H., & Norton, R.M., 1978, The systematics and biology of the cave-crickets of the North American tribe Hadenoecini (Orthoptera Saltatoria: Ensifera: Rhaphidophoridae: Dolichopodinae): University of Michigan, Miscellaneous Publications of the Museum of Zoology, No. 156.

Northup, D.E., 1988, Community structure of the arthropods of Carlsbad Cavern emphasizing Rhaphidophoridae in the genus Ceuthophilus [MS thesis]: University of New Mexico, ix + 53 p.

Northup, D.E., Lavoie, K.H., & Studier, E.H., 1993, Bioenergetics of camel crickets (*Ceuthophilus carlsbadensis*, *C. longipes*, and *C. conicaudus*) from Carlsbad Caverns National Park, New Mexico: Comparative Biochemistry and Physiology, v. 106A, p. 525-529.

Otte, D., 1994, The crickets of Hawaii: Philadelphia, Pennsylvania, The Orthopterist Society, 396 p.

Poulson, T.L., & White, W.B., 1969, The cave environment: Science, v. 165, p. 971-981.

Poulson, T.L., Helf, K.H., & Lavoie, K.H., 1995, Long-term effects of weather on the cricket (*Hadenoecus subterraneus*, Orthoptera, Rhaphidophoridae) guano communities in Mammoth Cave National Park: American Midland Naturalist, v. 134, p. 226-236.

SPSS, 1993, SPSS base system users guide for SPSS 4.0: Englewood Cliffs, New Jersey, Prentice Hall, 113 p.

Studier, E.H., Lavoie, K.H., Wares, W.D., II, & Linn, J.A-M., 1986, Bioenergetics of the cave cricket, *Hadenoecus subterraneus*: Comparative Biochemistry and Physiology, v. 84A, p. 431-436.

Studier, E.H., Lavoie, K.H., Wares, W.D., II, & Linn, J.A-M., 1987a, Bioenergetics of the camel cricket, *Ceuthophilus stygius*: Comparative Biochemistry and Physiology, v. 86A, p. 289-293.

Studier, E.H., Wares, W.D., II, Lavoie, K.H., & Linn, J.A-M., 1987b, Water budgets of cave crickets, *Hadenoecus subterraneus*, and camel crickets, *Ceuthophilus stygius*: Comparative Biochemistry and Physiology, v. 86A, p. 295-300.

Studier, E.H., Lavoie, K.H., Nevin, D.R., & McMillin, K.L., 1988, Seasonal individual size distributions and mortality of populations of cave crickets, *Hadenoecus subterraneus*, 1987 Annual Report Cave Research Foundation: St. Louis, Missouri, Cave Books, p. 42-44.

Studier, E.H., & Lavoie, K.H., 1990, Biology of cave crickets, *Hadenoecus subterraneus*, and camel crickets, *Ceuthophilus stygius* (Insecta: Orthoptera): Metabolism and water economics related to size and temperature: Comparative Biochemistry and Physiology, v. 95A, p. 157-161.

Studier, E.H., Lavoie, K.H., & Chandler, C.M., 1991, Biology of cave crickets, *Hadenoecus subterraneus* and camel crickets, *Ceuthophilus stygius* (Insecta: Orthoptera): Parasitism by hairworms: Proceedings of the Helminthological Society of Washington, v. 58, p. 248-250.

Studier, E.H., 1996, Composition of bodies of cave crickets (*Hadenoecus subterraneus*), their eggs, and their egg predator, *Neaphenops tellkampfi*: American Midland Naturalist, v. 136, p. 101-109.

Vandel, A., 1965, Biospeleology-The biology of cavernicolous animals: London, England, Pergamon Press, 524 p.

Wilkinson, L., 1998, SYSTAT: The system for statistics: Evanston, Illinois, SYSTAT, INC., 822 p.

# MIDDLE PLEISTOCENE KARST EVOLUTION IN THE STATE OF QATAR, ARABIAN GULF

ABDULALI M. SADIQ AND SOBHI J. NASIR
*Department of Geology, The University of Qatar, P.O.Box 2713, Doha, QATAR sobhi@bigfoot.com*

*Karst is widespread on the peninsula of Qatar in the Arabian Gulf, including depressions, sinkholes, caves, and solution hollows. More than 9700 large and small depressions, and several exposed sinkholes and caves are known. Field and air-photo studies indicate that the depressions, sinkholes, and caves of Qatar are genetically related, sinkholes representing an early phase in the development of depressions. Karst is concentrated mainly within the limestone, dolomite, gypsum, and anhydrite horizons of the Eocene Rus and Dammam Formations. Most karst features in Qatar show NE-SW and NW-SE orientations, similar to the joint and fracture systems. This observation indicates that rock type and the presence of joints and fractures played a major role in the development of karst in Qatar. Cylindrical, bottle-shaped, compound, and bowl-shaped morphotype karst pits were identified. These forms represent a genetic sequence in which the bowl-shaped pits evolved through a series of cylindrical and bottle-shaped compound intermediate stages. Most karst of central Qatar was formed due to extensive subsurface dissolution of carbonate and sulfate deposits under Middle Pleistocene wet climatic conditions and consequent subsidence. Joint-flow drainage may account for differential dissolution resulting in the formation of a pitted karst terrain in the northern part of Qatar.*

Karst is a distinctive environment characterized by landforms that are the product of dissolution of surface and subsurface rock by natural water to a greater extent than in other landscapes. It occurs both as surface and underground features (White 1988; Ford & Williams 1989). The highly varied interactions among chemical, physical, and biological processes have a broad range of geologic effects, including dissolution, precipitation, sedimentation, and ground subsidence (White 1984; Trudgill 1985; Ford & Williams 1989; Smart & Whitaker 1991). Diagnostic features such as sinkholes (dolines), sinking streams, caves, and large springs are the result of the dissolving action of circulating groundwater (Ford & Williams 1989; Smart & Whitaker 1991).

Karst includes features such as large caves, called as *duhul* in Arabic. It is an important feature of Eocene exposure surfaces in Qatar as well as some large parts of the Arabian Peninsula (Abul-Haggag 1965; Edgell 1990; Mukhopadhyay *et al.* 1996). Several substantial caves are known in Qatar, but many have probably been filled with blown sand, or have collapsed to produce some of the thousands of depressions or dolines. The most pronounced topographic features of Qatar are created by the large number (9736) of shallow depressions (Embabi & Ali 1990). Many of these depressions are the surface expression of subsurface collapse structures. Most of them are circular with diameters ranging from a few hundred meters up to ~3 km. Some reach depths of 25 m while others are only a few centimeters deep. Embabi and Ali (1990) related most sinkholes to these depressions. Analysis of the morphometric and spatial distribution parameters of karst depressions reveals that the Qatari karst is represented by broad, shallow depressions with an average density of 1 depression per km² (Embabi & Ali 1990).

The purpose of this paper is to report the geologic evolution of exposed sinkholes in Qatar through an air photo study, field investigations, and petrology.


**Figure 1. Geologic map of Qatar (modified after Cavelier 1970) showing location of investigated sinkholes; (1): Alghosheimah, (2): Umkareibah, (3): Alsuberiat, (4): Hamam, (5): Duhail, (6) Mudhlem, (7): Musfer.**

## GEOLOGIC SETTING

Qatar forms an exposed part of the Arabian shelf between the Arabian Shield and the mobile belt of Iran. It is centered at about 25°N., 51°E. Topographically, Qatar has a low-relief


Copyright © 2002 by The National Speleological Society

landscape with a maximum elevation of ~110 m msl. Structurally, Qatar is an elliptical anticlinal arch with a N-S main axis (Fig. 1). The exposed geologic succession is made up of Tertiary limestone and dolomite with interbedded clay, shale, gypsum, and marl, covered in places by Quaternary deposits (Cavelier 1970). Major faulting is not observed. Tertiary sedimentation started in Qatar with a marine transgression in the Paleocene. Shallow-marine to sabkha conditions prevailed until the end of the Eocene; a carbonate-evaporite sequence (Rus and Dammam Formations) was deposited during this time. The sea regressed at the end of the Eocene, marked by a widespread unconformity, causing the absence of Oligocene deposits over most of the area. Depressions and sinkholes are mainly distributed south of latitude 25° 20', which coincides with the northerly limit of the deep gypsum and anhydrite horizons of Eocene age. Although a dry arid climate characterizes Qatar at present, moist and dry climatic conditions alternated during the Miocene and Pleistocene (Butzer 1961; Al-Saad *et al*. 2002). Karstification of the Upper Dammam Unit limestone, providing easier pathways for groundwater, took place during this period. Today, Tertiary sedimentary rocks constitute the main aquifers containing usable groundwater in Qatar, originating from recharge by occasional rainstorms on outcrops of the same rocks in Saudi Arabia. The water flows north and east in the direction of the regional dip and discharges along the present-day coast of the Gulf. The aquifers are presently being exploited at a comparatively high rate.

## STRATIGRAPHY

The exposed rocks in Qatar consist of the following formations (Fig. 2):

### LOWER EOCENE RUS FORMATION

The Rus Formation is composed of soft limestone, dolomitic limestone, chalky limestone, gypsum, anhydrite, and shale. The thickness ranges between 42-112 m. Most depressions are related to dissolution of the gypsum and anhydrite within this formation, resulting in the development of numerous surface-collapse depressions (Embabi & Ali 1990).

### LOWER-MIDDLE EOCENE DAMMAM FORMATION

The Dammam Formation conformably overlies the Rus Formation and covers most of Qatar (Cavelier 1970). It ranges in thickness between 30-50 m, and is divided into the Lower Dammam Unit and Upper Dammam Unit. The former consists of the Fhiheil limestone member, the Midra shale member, and the Dukhan limestone member. The Upper Dammam consists of the Simsima limestone and dolomite member and the Abarug dolomite and marl member. All sinkholes of Qatar occur within the Upper Dammam Unit.

### LOWER-MIDDLE MIOCENE DAM FORMATION

The Miocene was characterized by regression of the sea and continental erosion. The Dam Formation consists of shallow marine and lacustrine deposits, and reaches a thickness of 80 m.

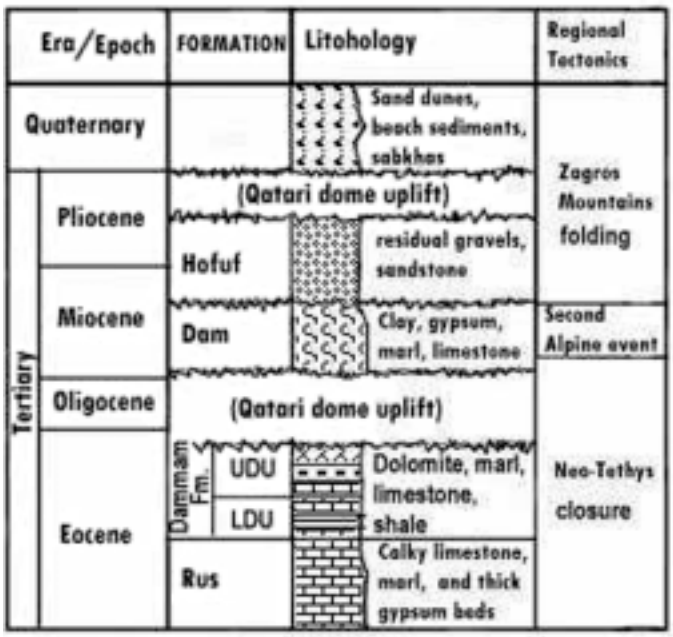


**Figure 2. Simplified lithostratigraphy of surface rocks in Qatar in relation to regional tectonics. UDU: Upper Dammam Unit; LDU: Lower Dammam Unit. (Modified after Cavelier 1970).**

### UPPER MIOCENE TO PLIOCENE HOFUF FORMATION.

The Hofuf Formation consists of fluvial sediments and is ~18 m thick. The deposits consist of coarse sand and sandstone with pebbles of various rocks, mostly derived from the Arabian shield and the Arabian shelf, and transported by large river systems (Al-Saad *et al.* 2002).

### QUATERNARY

Quaternary shallow-marine and continental sediments consists of sabkha deposits, sand dunes, and calcareous sand.

## SINKHOLES IN QATAR

Air photos show that karst in Qatar occurs as three types: sinkholes, simple depressions, and compound depressions. Simple depressions are those with a single center. Compound depressions have more than one center, and are large and rectangular or irregular in shape. These depressions seem to have formed through the amalgamation of several simple depressions. Field investigations indicate that the areas between the depressions are extensively stylolitized and likely were originally characterized by small-scale, fretted and sculpted karren forms typical of subaerial karstification. Sinkholes are concentrated in the central and northern parts of Qatar (Fig. 1). Analysis of sinkholes and the major axis orientations of depressions shows a structural control on the karst develop-

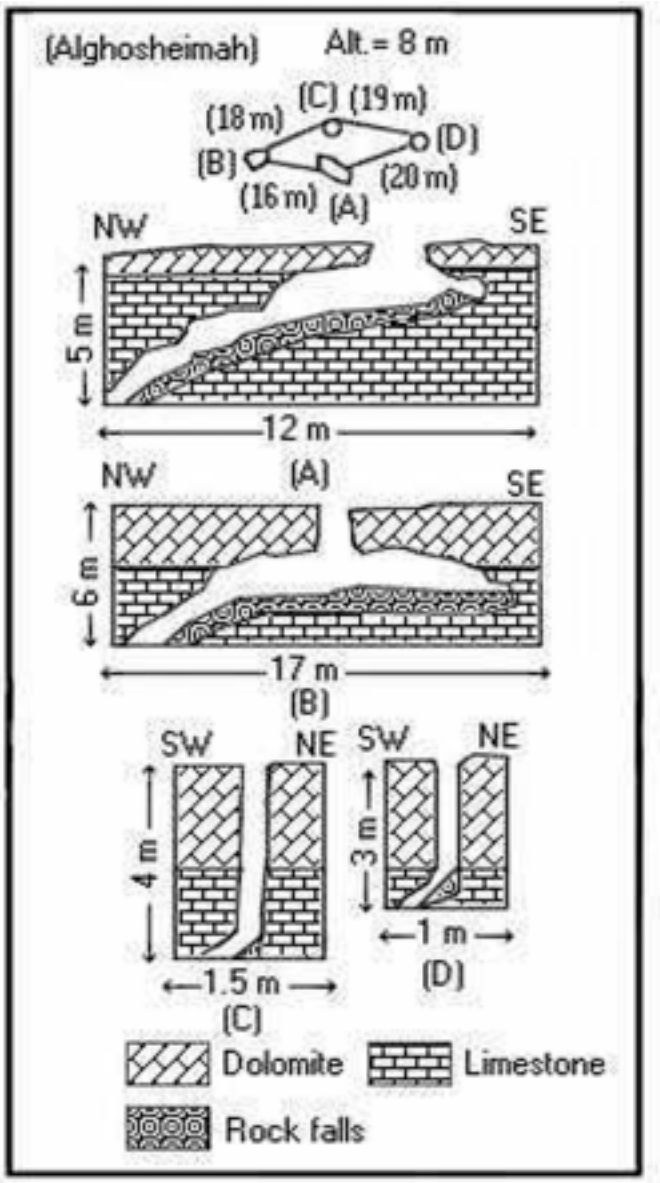


**Figure 3. Idealized lithologic profiles of the Algosheimah sinkholes. Alt.; Absolute altitude above sea level.**

ment. The long-axis orientations of sinkholes have pronounced NW-SE and NE-SW orientations, which correspond with the joint and fracture orientations in the study area. A 0.1-1 m thick calcrete surface is characteristic of karst areas in central Qatar. The wall rocks of sinkholes are highly jointed and fractured, with many stylolites, voids, and selective dissolution cavities. Thin-section studies of wall rocks from different sinkholes in northern Qatar show that the upper 1-2 m of the walls are dolomitic in composition, whereas the lower portion of the walls is biomicritic to biosparitic limestone with a significant proportion of dissolutional pores that are mostly filled with gypsum. The rocks belong to the Upper Dammam Unit. In central Qatar, marl underlies the upper calcrete whereas thick gypsum beds underlie the limestone. The rocks composing the

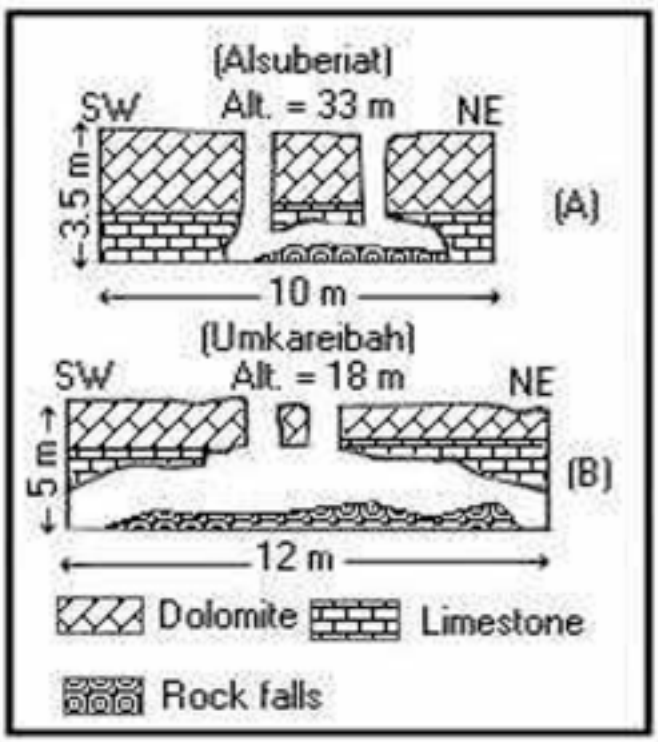


**Figure 4. Idealized lithologic profiles through the Alsuberiat (A) and Umkareibah sinkholes (B). Alt.; Absolute altitude above sea level.**

sinkholes of central Qatar belong to the Upper and Lower Dammam units. Speleothems, such as stalactites, stalagmites, columns, flowstone, and rimstone pools were not observed in any sinkholes or caves in the investigated areas. The lower part of most caves is either very dark or very steep and were not explored.

## SINKHOLES IN NORTHERN QATAR

Most sinkhole entrances in northern Qatar are vertical (Figs. 3, 4) and formed by dissolution along planes of structural weakness that extend to the surface. Sinkholes are found in the following areas:

### ALGHOSHEIMAH SINKHOLES (Fig. 3)

These are four vertical sinkholes formed in the Upper Dammam Unit. The holes are 15-20 m apart, occurring as an ellipse with a long axis of 40 m. Hole A is the largest (2 x 1 m); it is 1 m vertical then increases in size to 11 m in diameter with depth. Hole B has a smaller entrance (1.5 m in diameter), but is wider inside (12.5 m) than Hole A. Hole C has a small opening of 0.5 m and reaches a depth of 3.5 m. Hole D has an even smaller opening (0.4 m) and a depth of 2.5 m. Calcrete deposits (10 cm thick) cover the surface of all these holes. Holes C and D dip towards holes A and B. All holes may be interconnected.

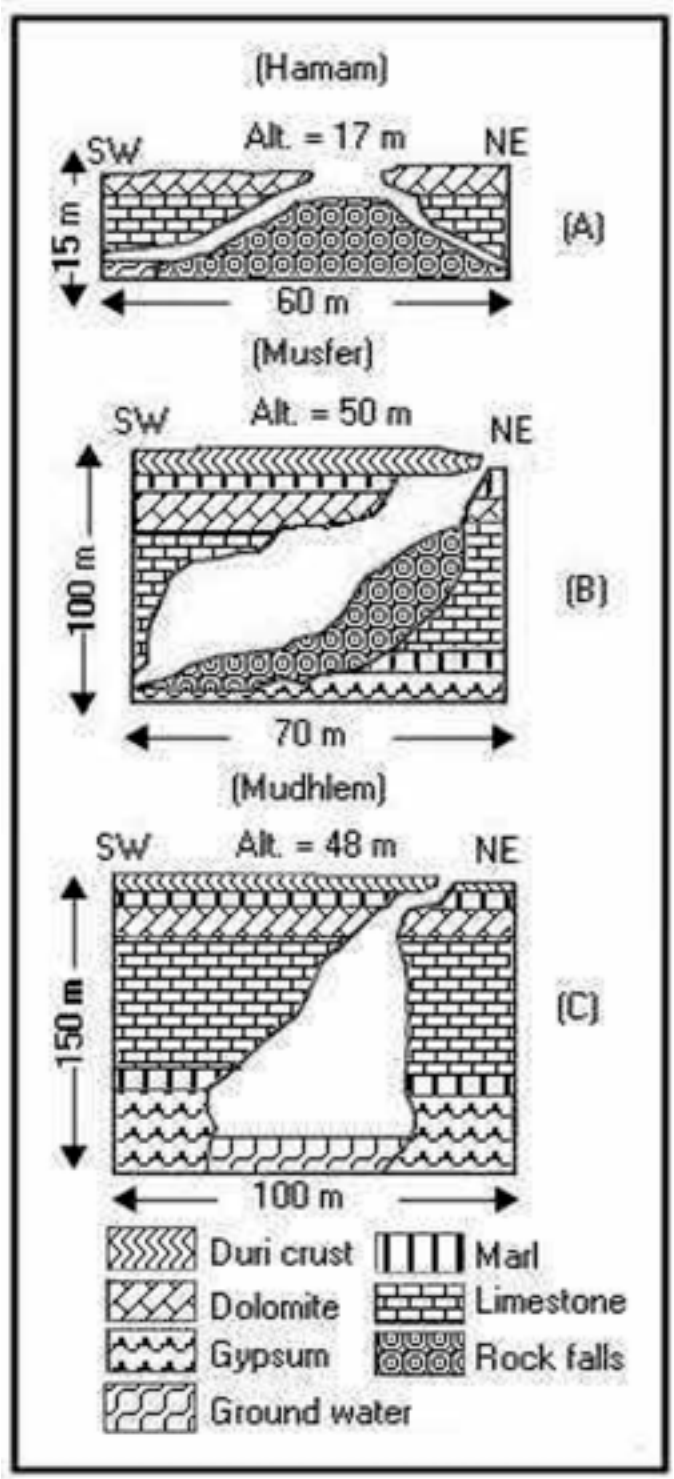


**Figure 5. Idealized lithologic profiles through the Hamam (A); Musfer (B) and Mudhlem (C) sinkholes. Alt.; Absolute altitude above sea level.**

ALSUBERIAT SINKHOLES (Fig. 4A)

The Alsuberiat area shows two separated sinkholes. Each has its own opening (0.8 m diameter), but they are connected at ~2-3 m depth. Both sinkholes are vertical and reach a depth of 3.1-3.3 m.

UMKAREIBAH SINKHOLES (Fig. 4B)

The Umkareibah sinkholes are similar to those of the Alsuberiat area and consist of two holes. The first has two openings, each 1.65 m in diameter and separated by ~1 m of dolomitic rock. The first sinkhole reaches a depth of 3 m and a size of 1.5-2 m in diameter. The second sinkhole (not shown) is of the vertical type, has an opening of 2 m in diameter, and reaches a depth of 2.3 m and a size of 13 m in diameter. All sinkholes dip in a NW-SE direction to unknown depth.

## SINKHOLES IN CENTRAL QATAR

Sinkholes in central Qatar are generally larger in size and depth than those of northern Qatar. They occur as vertical shafts connected to steeply inclined passages (Fig. 5). Most sinkholes reach the gypsum layers of the Lower Dammam Unit and the Rus Formation. The investigated sinkholes include the following:

HAMAM SINKHOLE (Fig. 5A)

This sinkhole has an oval opening (14.1 x 9.1 m), oriented in a NE-SW direction. It is the only sinkhole containing saline water at a depth of 15 m. The hole is connected to the Arabian Gulf, which is 4 km east of the sinkhole. Several types of small fish live in the water, and the tidal fluctuation of the water table is ~30 cm.

MUSFER SINKHOLE (Fig. 5B)

Musfer sinkhole has an opening of 12 x 4.5 m and is at least 100 m deep, though filled with sloping loose sand at the bottom. Gypsum layers of the Lower Dammam Unit and the Rus Formation occur at the bottom of this sinkhole. We suspect that this sinkhole is part of a much larger cave system.

MUDHLEM SINKHOLE (Figs. 5C, 6)

This particular sinkhole, whose Arabic name means “the Dark Cave” is ~150 m deep, filled with sloping loose sand and brackish water at the bottom. The hole has an opening of 15 m in diameter. Gypsum of the Rus Formation is in the lower parts of the sinkhole.

DUHAIL SINKHOLE (Fig. 7)

Duhail sinkhole has a circular opening 40 m in diameter and a depth of 5 m. This hole is transitional to becoming a depression, as indicated by the presence of a collapsed roof in its center. The Municipality of Doha City uses this sinkhole as a dumping area.

## MORPHOLOGY OF THE KARST PITS

Several types of karst-pit morphology/ies exist. Such variations in karst pit shape are illustrated by reference to distinct morphotypes, and shown on Figure 8:

**Cylindrical karst pits** have a narrow tubular form with verti-

**Figure 6. The main passage of Musfer sinkhole (Photo was taken in 2002).**

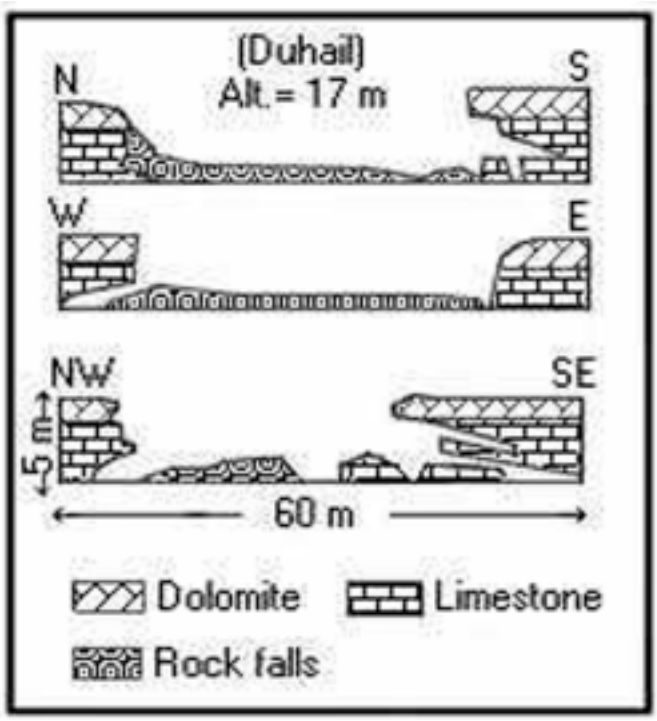


**Figure 7. Idealized lithologic profiles through the Duhail sinkhole. Alt.; Absolute altitude above sea level.**

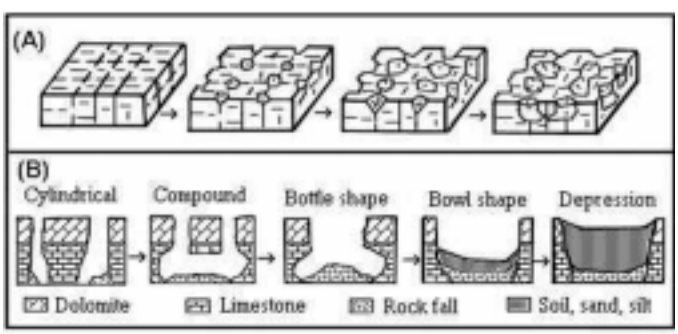


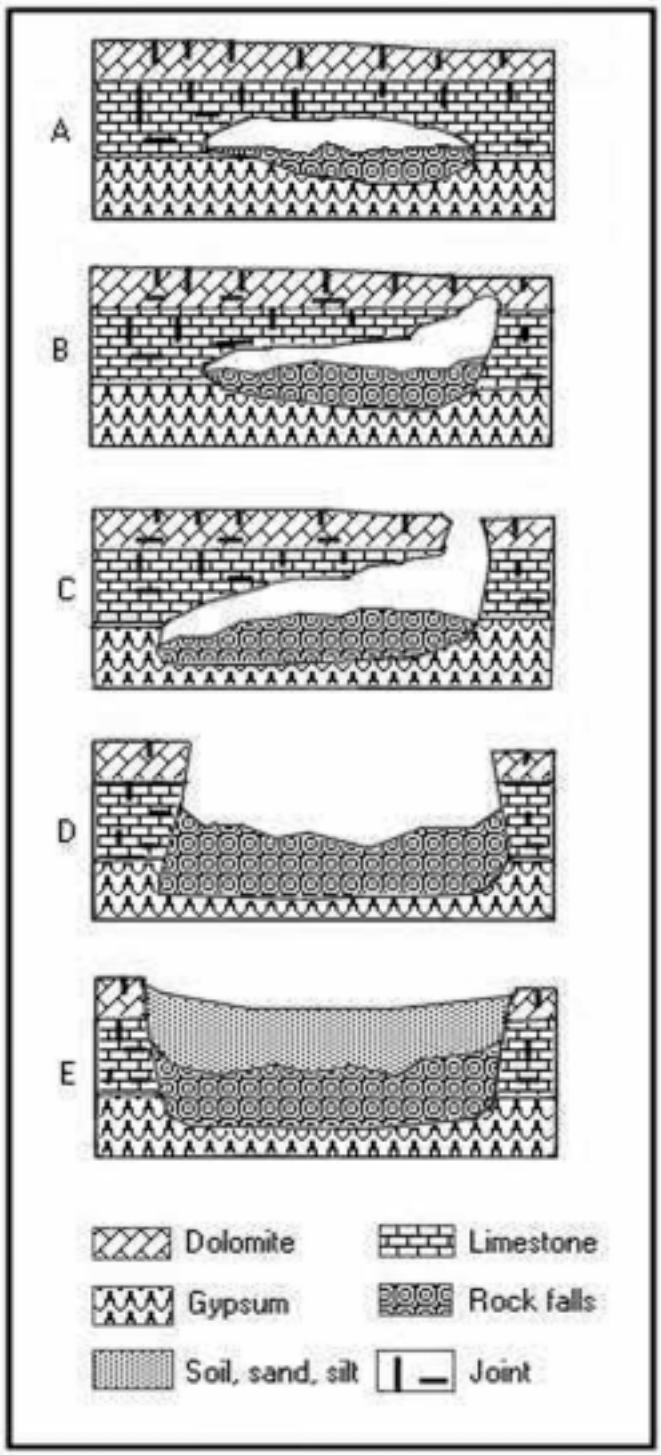


**Figure 8 (left). Model for the origin of sinkholes in northern Qatar.**
**Figure 9 (above). Model for the origin of sinkholes in central Qatar.**

**Table 1. A provisional chronology of Quaternary climate and lithostratigraphy in the southwestern part of the Rub' al Khali and Qatar. (Modified after Edgell 1990).**

| Epoch | Date in years | Climate | Lithology and topography |
|---|---|---|---|
| Holocene | 0-700 | Hyperarid | Dunes, eolian sand |
| | 700-5,500 | Slightly moist | Hofuf river, dunes, lakes |
| | 5,500-6,000 | Hyperarid | Dunes, eolian sand |
| | 6,000-10,000 | Wet (pluvial) | Lakes, lacustrine sediments |
| Late Pleistocene | 10,000-17,000 | Hyperarid | Dune, eolian sand |
| | 17,000-36,000 | Wet (pluvial) | Lakes, lacustrine sediments |
| | 36,000-70,000 | Arid | Dunes, eolian sand |
| | 70,000-270,000 | Moist | Glacial and interglacial |
| | 270,000-325,000 | Arid | Plateau caves, dunes |
| Middle Pleistocene | 325,000-560,000 | Wet | **Active karstification and cave formation** |
| | 560,000-700,000 | Arid | Dunes, eolian sand |
| Early Pleistocene | 700,000-2,500,000 | Wet humid (pluvial) | Large alluvial fans, early drainage systems |

cal or steeply inward inclined pit walls.

**Bottle-shaped karst pits** comprise cylindrical pits in which the lower portion of the pit wall has been removed to produce a beveled wall that slopes outwards.

**Compound karst pits** comprise two or more adjacent cylindrical or bottle pits with a common interpit area.

**Bowl-shaped karst pits** have steep sides with a gently concave, irregular, or flat base.

**Depressions** can be former sinkholes that are partly or completely filled with autochthonous material.

## DISCUSSION

Karstification in Qatar, as well as in other parts of the Arabian Gulf area (Abul-Haggag 1965; Al-Sayaro & Zötl 1978; Jado & Zötl 1984; Mukhopadhyay *et al.* 1996), is associated with the calcareous, dolomitic, and gypsiferous Dammam Formation of Eocene age. Local stratigraphy and petrography suggest that the primary karst-forming process affecting the Dammam Formation is a selective dissolution of rock driven by rainwater as well as groundwater. Such karstification takes place along the subsurface contact between the upper dolomite layers and the lower gypsum-bearing limestone of the Dammam Formation. This indicates that most sinkholes were formed because of preferential dissolution associated with the difference in composition between dolomitic, calcitic, and gypsum rocks. Karstification in the Arabian Gulf area mainly formed in the Middle Pleistocene, between 325,000 BP and 560,000 BP (Rauert *et al.* 1988; Edgell 1990). During this time, a wet climate predominated in the Arabian Gulf region (Edgell 1990: Table 1). In addition, the large volumes of Neogene sediment deposited indicate a pluvial and humid climate during the Miocene and Pliocene (Whybrow & McClure 1981). Similar indications are also apparent from the large alluvial fans of Early Quaternary age (Al-Saad *et al*. 2002).

The rate at which limestone and gypsum dissolution proceeds within the surficial meteoric environment is dependent upon several factors, including rainfall regime, temperature, distribution of soil-cover and biological activity, and structural weakness and lithology of the carbonate substrate (Trudgill 1985; White 1984; Ford & Williams 1989; Smart & Whitaker 1991; Reeder *et al.* 1996; Hose 1996; Miller 1996; Frank *et al.* 1998; Hill 2000). Of these, dissolution is directly impacted by the amount of rainfall (White 1984); an increase in precipitation always results in an increase in the rate of limestone dissolution. Temperature primarily influences limestone dissolution through its effect on the level of biological activity. Lithology of the carbonate substrate also has a profound effect on karstification, calcite dissolving more readily than dolomite due to its higher solubility (Martinez & White 1999). Karstification can take place where dolomite and gypsum are in contact with the same aquifer (Bischoff *et al.* 1994). Gypsum dissolution drives the precipitation of calcite, thus consuming carbonate ions released by dolomite. Gypsum-driven dedolomitization may be responsible for the karstic system (Bischoff *et al.* 1994), but dedolomitization was not observed in thin sections.

Karst pits making up the sinkholes and depressions in Qatar are structurally controlled and seem to be initiated through fractures and joint-flow drainage (Fig. 8A). The profiles of all types of sinkholes in northern Qatar indicate strong vertical control, which is attributed to the numerous fractures and joints in the bedrock. Based upon sinkhole long-axis data, it appears that such lines of structural weakness in the bedrock influence sinkhole orientation. Sinkholes commonly form along high-permeability pathways through the vadose zone, which are sites of fracture concentrations and intersections (White 1988).

Sinkholes may also become elongated along lines of major weakness by a combination of dissolution and collapse (Reeder *et al.* 1996). Collapse can originate at some depth in

the bedrock if it is assisted by fracture zones (Fig. 9). Rainwater, intercepted by joints and fractures, concentrates at specific sites on the emergent surface and causes dissolution along joint intersections, which produces cylindrical pits that propagate vertically downward with time (Fig. 8A). Gravity-driven drainage further explains the initial perpendicular attitude of the pits. In addition, joint-flow drainage accounts for the comparable width of shallow and deep cylindrical pits. Variations in depth may reflect differences in the length of time that drainage was focused at a particular site. Downward propagation of some pits was limited to the uppermost 1-2 m and enlargement primarily occurred through lateral amalgamation of adjacent pits. Once initiated, the continued development of the sinkholes would have been self-perpetuating. The smooth, rounded appearance of the investigated karst pits is comparable to that of modern karst terrains (Sweeting 1973; James & Choquette 1984).

A complete spectrum of karst-pit forms exists in Qatar. Cylindrical pits evolve into bowl-shaped ones and depressions through several bottle- and compound intermediates (Fig. 8B). This indicates that these forms represent a genetic sequence and that each started around a cylindrical pit. Figure 8B shows how sinkholes may represent the early phase in depression development. Dissolution and collapse caused the preferential removal of limestone and gypsum from the lower portion of the pit wall. Enlargement of the upper portion of the pit to form a bowl-shaped depression likely resulted from collapse (Fig. 7). The pathway along which further pit enlargement occurred was dependent upon the initial density of the cylindrical pits. Where pits were more densely packed, adjacent pits amalgamated through a gradual reduction in height of the interpit area, to form bowl-shaped pits (Fig. 8B). Once complete denudation of the interpit area had occurred, further dissolution at this site appears to have been minimal, pit enlargement occurring primarily through lateral dissolution and amalgamation.

As speculated by Walkden (1974), several features of the karst are consistent with the presence of a shallow water table during development. In particular, enlargement of the karst pits by lateral amalgamation rather than vertical deepening (Fig. 8B) and the occurrence of flat-based pits suggest that a water-saturated or carbonate-cemented zone existed a few meters beneath the sediment surface. Figures 8 and 9 synthesize the progressive formation of sinkholes in northern and central Qatar, respectively, as discussed above. The investigated sinkholes/depressions appear to have developed exclusively from collapse. However, other explanations are possible.

## CONCLUSIONS

Analysis of lithologic and geomorphic features within northern and central Qatar revealed that the karst landscape is generally influenced by the lithology and structure of the bedrock. The upper 1-2 m of the rock consists of dolomite and dolomitic limestone underlain by gypsum and gypsum-bearing biomicritic to biosparitic limestone. Joints and fractures, formed during periods of uplift in Qatar, govern the orientation of karst landforms, including the long axes of depressions and sinkhole passages. Uplift and fracturing increased the secondary permeability of the rocks, and rainwater during Pleistocene humid periods began to dissolve the carbonate and gypsum along these planes of structural weakness. In northern Qatar, each depression started around a cluster of vertical cylindrical solution pits, with each pit interpreted to have formed through joint-flow drainage. Fracture and joint-flow drainage focused dissolution at particular sites in the carbonate substrate, with the locus of dissolution extending vertically downward through time. In many cases, growth of the cylindrical pits was limited to the uppermost 1-2 m of the carbonate top, with subsequent development occurring through the lateral amalgamation of adjacent pits.

In central Qatar, most sinkholes formed due to subsurface dissolution of gypsum and subsequent collapse of the overlying beds making up the roofs.

## ACKNOWLEDGMENTS

The authors express their thanks to Darweish Al-Imadi for reading an early version of the manuscript. The comments and suggestions of H.M. Kluyver, BRGM Group, France, two anonymous reviewers, and the editors are acknowledged.

## REFERENCES

Abul-Haggag, A., 1965, A Recent karstic phenomenon in the limestone country of north central Najd, Saudi Arabia: Bulletin de la Société de Géographie d'Egypte, v. 38, p. 73-80.

Al-Saad, H., Nasir, S., Sadooni, F., & Al-Sharhan, A., 2002, Stratigraphy and sedimentology of the Hofuf Formation in the State of Qatar, in relation to the tectonic evolution of the Eastern Arabian Block: Neues Jahrbuch fuer Geologie und Palaeontologie Abhandlung.

Al-Sayari, S.S., & Zötl, J.G., 1978, Quaternary Period of Saudi Arabia: Wien-New York, Springer, 334 p.

Bischoff, J.L., Julia, R., Shank, W.C III, & Rosenbauer, R.J., 1994, Karstification without carbonic acid: Bedrock dissolution by gypsum-derived dedolomitization: Geology, v. 22, p. 995-999.

Butzer, K.W., 1961, Climatic changes in arid regions since the Pliocene, A history of land use in arid regions: Proceedings Arid Zone Research: Paris, UNESCO, p. 31-56.

Cavelier, C., 1970, Geologic description of the Qatar Peninsula (Arabian Gulf), Publication of the Government of Qatar, Department of Petroleum Affairs, 39 p.

Edgell, H.S., 1990, Evolution of the Rub'al Khali desert: Journal of King Abdel Aziz University: Earth Science, Special Issue: First Saudi Symposium on Earth Science, Jeddah, 1989, v. 3, p. 109-126.

Embabi, N.S., & Ali, A.A., 1990, Geomorphology of depressions in the Qatar Peninsula (in Arabic): Qatar University, Al-Ahleia Press, 357 p.

Ford, D.C., & Williams, P.W., 1989, Karst geomorphology and hydrology: London, Unwin Hyman, 320 p.

Frank, E., Mylroie, J., Troester, J., Calvin Alexander, E., & Carew, J., 1998, Karst development and speleogenesis, Isla de Mona, Puerto Rico: Journal of Cave and Karst Studies, v. 60, p. 73-83.

Hill, C., 2000, Overview of the geologic history of cave development in the Guadalupe Mountains, New Mexico: Journal of Cave and Karst Studies, v. 62, p. 60-71.

Hose, L., 1966, Geology of a large, high-relief, sub-tropical cave system: Sistema Purification, Tamaulipas, Mexico: Journal of Cave and Karst Studies, v. 58, p. 6-21.

Jado, A.R., & Zötl, J.G., 1984, Quaternary Period of Saudi Arabia: Wien-New York, Springer, 360 p.

James, N.P., & Choquette, P.W., 1984, Diagenesis 9. Limestones - The meteoric diagenetic environment: Geoscience Canada, v. 11, p. 161-194.

Martinez, M.I., & White, W., 1999, A laboratory investigation of the relative dissolution rates of the Lirio limestone and the Isla de Mona dolomite, and implications for cave and karst development on Isla de Mona: Journal of Cave and Karst Studies, v. 61, p. 7-12.

Miller, T., 1996, Geologic and hydrologic controls on karst and cave development in Belize: Journal of Cave and Karst Studies, v. 58, p. 100-120.

Mukhopadhyay, A., Al-Sulaimi, J., Al-Awadi, E., & Al-Ruwaih, F., 1996, An overview of the Tertiary geology and hydrogeology of the northern part of the Arabian Gulf region with special reference to Kuwait: Earth Science Reviews, v. 40, p. 259-296.

Rauert, W., Geyh, M.A., & Henning, G.J., 1988, Results of $^{14}C$ and U/Th dating of sinter samples from caves of the As Summan Plateau: Hannover, Institute of Hydrology, GSF Munich and Niedersachsisches Landesamt fuer Bodenforschung, 62 p.

Reeder, P., Brinkmann, R., & Alt, E., 1996, Karstification on the northern Vaca Plateau, Belize: Journal of Cave and Karst Studies, v. 58, p. 121-130.

Smart, P.L., & Whitaker, F.F., 1991, Karst processes, hydrology and porosity evolution, *in* Wright, V.P., ed., Palaeokarsts and palaeokarstic reservoirs, PRIS Occasional Publication Series No. 2. University of Reading, p. 1-55.

Sweeting, M.M., 1973, Karst landforms: Newport, Columbia University Press, 362 p.

Trudgill, S.T., 1985, Limestone geomorphology: London, Longman, 196 p.

Walkden, G.M., 1974, Palaeokarstic surfaces in Upper Viséan (Carboniferous) limestones of the Derbyshire Block, England: Journal of Sedimentary Petrology, v. 44, p. 1232-1247.

White, W.B., 1984, Rate processes: Chemical kinetics and karst landform development, *in* LaFleur, R.G., ed., Groundwater as a Geomorphic Agent: London, Allen and Unwin, p. 227-248.

White, W.B., 1988, Geomorphology and hydrology of karst terrains: New York, Oxford University Press, 464 p.

Whybrow P.J., & McClure, H.A., 1981, Fossil mangrove roots and paleoenvironments of the Miocene of eastern Arabia: Palaeogeography, Palaeoclimatology, Palaeoecology, v. 32, p. 213-225.

Jay A. Yoder, Horton H. Hobbs III, and Matthew C. Hazelton - Aggregate protection against dehydration in adult females of the cave cricket, *Hadenoecus cumberlandicus* (Orthoptera, Rhaphidophoridae). *Journal of Cave and Karst Studies 64*(2): 140-144.

# AGGREGATE PROTECTION AGAINST DEHYDRATION IN ADULT FEMALES OF THE CAVE CRICKET, *HADENOECUS CUMBERLANDICUS* (ORTHOPTERA, RHAPHIDOPHORIDAE)

JAY A. YODER, HORTON H. HOBBS III, AND MATTHEW C. HAZELTON
*Department of Biology, Wittenberg University, Springfield, OH 45501 USA, jyoder@wittenberg.edu*

*The role of aggregation in water conservation in adult female cave crickets,* Hadenoecus cumberlandicus, *in Laurel Cave (Carter Co., KY) was investigated. Grouped crickets retained water more effectively (water loss rates were lower) as densities increased from 1, 5, 10, and 20 crickets per cluster. Dry air currents (flow rate 43 mL/min) that passed over an aggregation of 20 eliminated the group effect with regard to water loss, suggesting that the mechanism operates by raising the relative humidity inside the cluster. Rapid water loss rate characterizes the water balance profile and is reflected by high activation energies for water loss and low quantities of cuticular lipid. There was no evidence for water vapor uptake. Natural gains and losses are high in* H. cumberlandicus, *and this agrees with their preference for the deep cave environment. Conversely, water turnover is lower for another trogloxenic cricket,* Ceuthophilus stygius, *that is less cave-adapted.*

Roosting aggregations of >200 cave crickets, *Hadenoecus cumberlandicus* Hubbell and Norton, are abundant year-round in the interior of Laurel Cave, a small, cold cave in eastern (Carter Co.) Kentucky (KY), USA (Pfeffer *et al*. 1981). The upper level of this cave, where these crickets reside, is unusual in that it is cold and relatively dry, with little, if any, free water in the cave (excluding ceiling condensation dampness) throughout most of the year, even after heavy rains. Greatest abundance and size of aggregations of *H. cumberlandicus* occur during the driest times of year, mainly in winter. Presumably, the aggregations begin as clusters of nymphs hatched from eggs laid on the cave floor. Nymphs move from the ground to more moisture-rich microhabitats associated with the ceiling and walls, roosting at those sites between above-ground foraging bouts during development into adults (Peck 1976). Positioning high above the cave floor puts them in the more moist, slower moving air of the cave ceiling, and, in certain parts of their geographical range, helps to prevent attack by ground-dwelling predatory beetles (Peck 1976). Cave crickets are trogloxenic (complete life history in caves but must feed in surface habitats; [Hobbs 1992]) and cave-adapted (elongated antennae and legs, reduced eyes and pigmentation, with a thin, translucent cuticle) (Peck 1976). They are active mostly at night, emerging from the cave to forage and then returning to roost, digest food, and defecate (Poulson *et al*. 1995). During winter, outside foraging activity of *H. cumberlandicus* is not as great, they move further into the dark zone of the cave, seeking moisture on the ceiling and recessed wall and ceiling depressions, and remain together for many months (H. Hobbs & M. Hazelton, unpub. observations).

Formation of aggregations has a profound impact on many insects by enhancing water conservation. As group size increases, loss component of water budget decreases. The typical mechanism operates by generating a higher relative humidity inside the cluster (Yoder & Smith 1997). Such behavioral regulation of water loss by forming groups is especially important for arthropods because their surface area is great relative to their volume, creating an extreme potential water loss problem (Hadley 1994). We hypothesized that grouped cave crickets may retain water more effectively than isolated individuals. This was examined by comparing water loss rates for female adult cave crickets, *H. cumberlandicus*, in groups of different sizes. In addition, water content, dehydration tolerance, critical transition temperature, activation energies for water loss, and quantities of cuticular lipid were determined. The possibility for water gain by atmospheric water vapor absorption also was examined.

To understand better the influence of cave-adaptation on water balance characteristics, a water balance profile was constructed for another Laurel Cave trogloxene, the camel cricket, *Ceuthophilus stygius* (Scudder). This cricket also occurs in fairly dense aggregations on the ceiling and in small hibernating groups in the dark zone in winter (Studier & Lavoie 1990). Unlike *H. cumberlandicus*, *C. stygius* favors entrance areas in Laurel Cave rather than the deep cave. Every few days during the warmer months *C. stygius* forages outside the cave. *H. cumberlandicus*, with its significantly larger, distensible crop for storing food (Peck 1976), may avoid the risk of dehydration and predation during surface foraging for up to several weeks.

## MATERIALS AND METHODS

### COLLECTION AND MAINTENANCE

Cave crickets, *H. cumberlandicus*, and camel crickets, *C. stygius*, were collected from the upper level of Laurel Cave, Carter Co., KY, USA, in late November. Crickets were held in large plastic coolers and supplied with moist leaf litter and paper towels until return to the laboratory. Since only a parthenogenetic population of *H. cumberlandicus* resides in Laurel Cave (Hubbell & Norton 1978) only female adult crickets, distinguished by a sclerotized ovipositor, were used in the experiment within 24 h of collection. An aspirator and forceps were used to transfer crickets.

BASIC OBSERVATIONS

Temperature was held at 20 ±1°C to permit comparison with other water balance literature (Hadley 1994); other temperatures were controlled by environment cabinets (± 0.5°C). Specimens were weighed using an electrobalance (CAHN 25, Ventron Co.; Cerritos, CA; precision of 0.2µg SD and accuracy of ±6µg at 1 mg). Crickets were weighed and returned to test conditions < 1 min. Relative humidities (% RH) were generated in hermetically sealed glass desiccators (8000 cc, L X W X H) with glycerol-distilled water mixtures (Johnson 1940) or saturated salt solutions containing an excess of solid salt (Winston & Bates 1960). Crickets were kept separated from mixtures by a perforated porcelain plate and could roost upside down in the chambers. Calcium sulfate (Drierite) provided 0% RH (Toolson 1978). Test atmospheres were measured with a hygrometer (±3.0% RH; Thomas Scientific, Philadelphia, PA).

Wharton's (1985) standard methods were used to determine water balance characteristics, and profile analysis follows interpretations by Hadley (1994). Thus, % RH was expressed as a water vapor activity ($a_v$, $a_v$ = % RH/100) and activity of the insect's body water ($a_w$) = 0.99 (Wharton 1985). Pretreatment consisted of 6 h starvation at 0.93 $a_v$ and then 0.33 $a_v$ until 4-6% body mass had been lost, so that mass changes reflect changes in water levels of the insects. Specimens were weighed individually within 1 min, without enclosure and without anesthesia, and were permitted to walk directly onto the weighing pan of the balance.

WATER LOSS RATES

To determine the body water loss that could be tolerated, crickets were weighed, placed at 0.0 $a_v$ and reweighed at 15 min intervals. Mass measurement when crickets were unable to right themselves and crawl one body length was defined as the critical mass (= dehydration tolerance limit). Amount of water loss, from initial to critical mass, was expressed as a percentage of initial mass (Yoder & Barcelona 1995).

Under 0.0 $a_v$ conditions, water loss is a function of exponential decay (Equation 1; Wharton 1985),

$$(1) \quad m_t = m_0 e^{-k_t}$$

or $\ln m_t / m_0 = -k_t$, where $m_0$ is the initial water mass, $m_t$ is the water mass at any time, t, and $k$ is the percentage of water lost in time, t, elapsed between $m_0$ and $m_t$ (Wharton 1985). The slope of a regression on a semi-logarithmic plot, thus, ln ($m_t$ / $m_0$) *vs*. time, is the rate of water loss (integumental plus respiratory water loss) and is expressed as %/h. Water mass ($m$) is the difference between initial and dry mass, and is expressed as a percentage of initial mass (= % body water content). The weighing interval for rate determinations was 1 h. Dry mass was determined according to Hadley (1994). Briefly, insects were killed by freezing and placed at 0.0 $a_v$ and 90°C until mass remained constant plus an extra full day of drying (total 3-4 days).

GROUP EFFECTS

To explore whether there is a group effect with regard to water loss, water loss rates (0.0 $a_v$; eqn. 1) were determined for individuals in groups of different sizes (1, 5, 10 and 20). Groups of crickets were housed directly within relative humidity chambers. Individuals for monitoring were designated with a small spot of white paint (Pactra, Van Nuys, CA) placed on the dorsum (Yoder & Grojean 1997). Removal of the cricket for mass determinations caused no observable disturbance to the cricket grouping. Paint had no effect on mass changes (data not shown). Mechanistic determination of the group effect was tested by passing dry air currents (flow rate 43mL/min; Wharton & Knülle 1966) over the cluster (Yoder & Smith 1997).

ACTIVATION ENERGIES

Passive water loss rates ($k$) were derived similarly, except specimens were first killed and temperature was varied. Freshly killed insects are required for this experiment (Wharton 1985; Hadley 1994); one group was killed by freezing and another group was killed by HCN vapor (<10 h). Thus, loss is attributed solely to that through the cuticle without a respiratory component (Wharton 1985). Activation energies, $E_a$, reflecting cuticular permeability (Yoder & Denlinger 1991), were derived from the slope of a regression on an Arrhenius plot (rate *vs*. reciprocal absolute temperature, T) in accordance with standard equations and methodology (Toolson 1978) (Eq. 2 & 3):

$$(2) \quad \ln k = - E_a \boldsymbol{R}^{-1} T^{-1} + \ln A$$

$$(3) \quad E_a = -\{(t_i \ln k_i - t_i n^{-1}) \text{ X } [t^2_i - (t_i)^2 n^{-1}]^{-1}\}\mathbf{R}$$

where $\boldsymbol{R}$ is the gas constant, $A$ is the frequency factor, and $t$ is the temperature over range $i$ with respect to the loss rate ($k$) of the amount ($n$) of water. Activation energies were expressed as J/mol. A change in $E_a$ denotes a new temperature range ($i$), indicated when R >0.95 (Yoder & Spielman 1992), and a critical transition temperature is found at the point of intersection describing the two $E_a$ s. The critical transition temperature is the temperature where a phase change occurs in epicuticular lipids resulting in a particularly rapid water loss.

WATER VAPOR ABSORPTION

To determine whether cave crickets can use water vapor as a primary source of water, pre-weighed crickets were placed at different relative humidities (85%, 93%, and 98% RHs = 0.85, 0.93, and 0.98 $a_v$s) and reweighed every 2 h. Ability to maintain a relatively constant water mass ($m$) in unsaturated air (that is, < 0.99 $a_w$ = body water) indicates that loss is balanced by gains from the air. Lowest $a_v$ where water gain from the air occurs is designated as the critical equilibrium activity (Wharton 1985) and shows where water balance (gain = loss) under these conditions is achieved.

### CUTICULAR LIPIDS

Cuticular lipid (nonpolar and polar lipids) was extracted by two, 2 min, washes in chloroform:methanol (2:1) and quantified as described for insects by Yoder *et al*. (1992). Prior to extraction, crickets were first killed by freezing and then thawed to room temperature. Extracts (N=15 crickets per extract) were passed through a silica gel column (Waters Assoc.) and eluted with 3 column volumes (2 mL) of solvent. The extract was concentrated to dryness with a stream of $N_2$ gas, reconstituted with 10µL of solvent, and dried onto preweighed aluminum pans at 0.0 $a_v$ under $N_2$. Pans were weighed and returned to these storage conditions (0.0 $a_v$ under $N_2$) until mass remained constant. Amount of lipid is expressed as µg/individual.

### DATA ANALYSIS

An analysis of variance (ANOVA) was used to compare data (Wharton 1985; Hadley 1994). For individual cricket tests, data are the mean ± SE of three replicates of 15 individuals each. In the group effect experiment, there were 45 groups tested with one designated, paint-marked, individual per group. Percentage data were arcsin transformed prior to analysis, and characteristics derived from regression lines were analyzed by a test for the equality of slopes of several regressions (Sokal & Rohlf 1981). Statistical analysis was set at P=0.05.

## RESULTS

### WATER BALANCE PROFILE OF *H. CUMBERLANDICUS*

A group effect with regard to water loss was observed for cave crickets in aggregations (Fig. 1). Compared to isolated specimens (water loss rate = 2.74 ±0.21%/h), rates for group-caged specimens of 20 individuals (1.63 ±0.29%/h) were reduced by approximately 1/2 (F=3.549; df=89; P<0.05). Water loss rates for crickets in test group sizes of 5 (1.84 ±0.33%/h) and 10 (2.08 ±0.17%/h) were between both extremes. In moving air, the water loss rate for an individual in a group size of 20 was 3.09 ±0.27%/h and was not different from a single, isolated individual (water loss rate = 2.74 ±0.21%/h); thus, moving air eliminated the group effect with regard to water loss rates. Initial, individual dry and water mass values were 0.389 ±0.09g, 0.111 ±0.04g and 0.278 ±0.05g, respectively, and the percentage body water content was 71.47 ±0.44% for all cave crickets in the experiment. In all cases, the water mass was a positive correlate of the dry mass (R≥0.98; P<0.001). Crickets were similar in size, shape, and water content in the experiment. We concluded that the nearly two-fold difference in water retention that we note is most likely group-related.

Cave crickets became irreversibly dehydrated once 24.59 ±0.76% body mass (= critical activity point) had been lost. This dehydration tolerance limit is reflected by survivability estimates of <12 h for isolated individuals and >12 h for group-housed individuals in dry air. Passive water loss rates for killed crickets were nearly tripled (6.12 ±0.52%/h) compared to living specimens. These passive water loss rates displayed direct Boltzmann dependence on temperature (R≥0.99; P>0.001; Fig. 2), yielding an $E_a$ for water loss of 9.28 J/mol. A temperature threshold for a particularly rapid water loss was not detected; *i.e.*, no critical transition temperature is present. No abrupt change in water loss occurred due to a temperature-induced phase change in epicuticular lipids; that is, the observed slope is continuous (a single component curve) over a broad (4-60°C) temperature range.

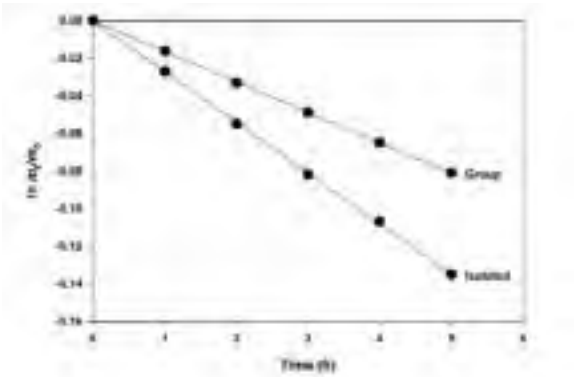


**Figure 1. Water retention of aggregated (group size of 20) and isolated (group size of 1) cave crickets, *Hadenoecus cumberlandicus* at 0.0 $a_v$ ($a_v$ = water vapor activity = percentage relative humidity/100) and 20°C. The slope of the line through the plot is the rate of water loss; $m_t$, water mass at any time t and $m_0$, initial water mass.**

Cave crickets did not absorb water vapor from the air. Water mass declined in all experimental $a_v$ s tested (Fig. 3). More water was retained as $a_v$ increased, implying passive gains by physical adsorption and passive chemisorption of water vapor. No active vapor uptake component appeared to be operating. Body water losses were not countered by gains from the air; *i.e.*, no equilibrium mass (gain = loss) was achieved. In absence of an active mechanism, the activity gradient between the cricket's $a_w$ (= 0.99; Wharton 1985) and that of ambient air (0.99 $a_w$ > 0.98 $a_v$ and below) produces a water loss by simple diffusion. Thus, in this cricket species, the critical equilibrium activity is >1.00 $a_v$, indicating that water must be imbibed as a liquid.

### COMPARATIVE OBSERVATIONS WITH *C. STYGIUS*

Water loss rate for the non-cave-adapted species, *C. stygius*, was 1.59 ±0.32%/h, nearly two times less than *H. cumberlandicus*, with a corresponding lower $E_a$ value of 3.77 ±0.44 J/mol (F=4.427; df=89; P<0.05). This cricket is much larger (initial mass = 1.245 ±0.15 g; dry mass = 0.391 ±0.08 g; and water mass = 0.854 ±0.12 g) than *H. cumberlandicus*, but both have a similar percentage body water content (68.59 ±0.51%; ANOVA; P>0.05). Like *H. cumberlandicus*, dry mass and water mass correlated positively (R≥0.96; P<0.001), the dehydration tolerance limit was 26.07 ±0.83%, no critical transition temperature was detected and the critical equilibrium activity is >1.00 $a_v$.

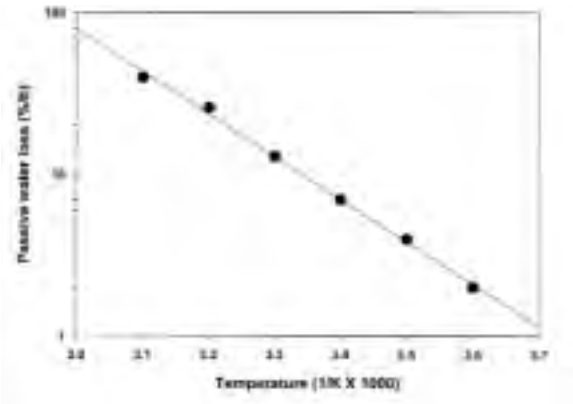


**Figure 2 (right - top). Possible presence of a critical transition temperature in freezer-killed adult females of the cave cricket, *Hadenoecus cumberlandicus*, examined by Arrhenius analysis. The continuous slope ($E_a$) indicates that no critical transition temperature is present.**

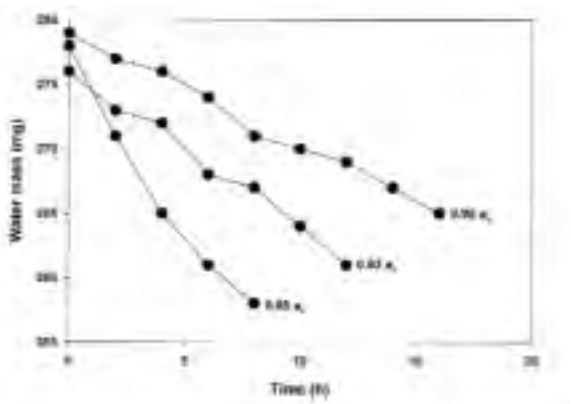


**Figure 3 (right - bottom). Water mass loss by cave crickets, *Hadenoecus cumberlandicus*, in unsaturated air at 20°C indicates failure to maintain equilibrium (gain is not equal to loss) by absorbing water vapor from the air. '$a_v$', water vapor activity = percentage relative humidity/100.**

### CUTICULAR LIPID

Quantity of cuticular lipid extracted from the surface of *C. stygius* was 386.41 ±0.64 µg/individual compared to significantly lower amounts of 202.33 ±0.67 µg/individual for *H. cumberlandicus* (F=3.457; df=89; P<0.05). The decreased water turnover associated with *C. stygius* correlated with their ability to survive longer in dry air than *H. cumberlandicus*. The only species-specific differences observed in this study between *C. stygius* and *H. cumberlandicus* were body size, water loss rate, and amount of cuticular lipid. We did not investigate the group effect in *C. stygius*.

## DISCUSSION

A group effect is a feature of the water balance profile of the cave cricket, *H. cumberlandicus*. Other water balance characteristics, such as 71% water content, 24% dehydration tolerance limit, and lack of critical transition temperature agree with most insects (Hadley 1994). An especially fast water loss rate is an additional feature of the cave cricket. Compared to *H. cumberlandicus*, the less cave-adapted camel cricket, *C. stygius*, retains water more effectively, in part, because of a greater amount of cuticular wax (decreased integumental water loss), and larger size (smaller surface area to volume ratio). Female adults of *H. cumberlandicus* regulate water loss behaviorally by forming aggregations. The importance of a group effect with regard to enhancing survival is apparent in many arthropod species (*e.g.*, Glass *et al*. 1998; Yoder & Knapp 1999; Yoder & Smith 1997; Yoder & Grojean 1997; Grassé & Chauvin 1944), but is not always linked to water conservation (Yoder *et al*. 1994; Yoder & Hoy 1998). Whether water conservation is facilitated through group formation by the camel cricket, *C. stygius*, is not known. It also remains unclear whether the group effect is restricted to female adults, *H. cumberlandicus*, or to Laurel Cave, and we are presently investigating these questions.

Examination of activation energies ($E_a$s) provides an explanation for the fast water loss rate of *H. cumberlandicus*. $E_a$s for water loss, describing passive water loss over a broad temperature range, have not been previously determined in crickets, nor have $E_a$s been used to examine cave adaptation. Though fluctuations in deep cave temperature rarely occur, the importance of $E_a$ pertains to properties of the cricket cuticle. Lower $E_a$ values are associated with extra cuticular lipid (Yoder & Denlinger 1991; Yoder *et al*. 1992), a barrier that restricts integumental water loss, because fewer molecules of water (*n*; eqn. 3) escape through a less permeable cuticle (Wharton 1985). Conforming to this reasoning, lower $E_a$s of the more waxy camel cricket, *C. stygius*, reveal a cuticular modification compared to the less waxy *H. cumberlandicus*. Indeed, our results indicate that *C. stygius* has nearly double the amount of cuticular lipid as *H. cumberlandicus*. This quantitative difference in cuticular lipid is sufficient to explain the lower $E_a$ of *C. stygius* because more energy is required to move water from the exchangeable water pool (*m*; eqn. 1) through a thicker wax layer. Lower $E_a$ for *C. stygius* suggests that they are more water-tight than *H. cumberlandicus*. Thus, more rapid water loss rate of *H. cumberlandicus* is attributed, in part, to a lower amount of cuticular wax. A less waxy cuticle has been touted to contribute to the extreme sensitivity to drying for cavernicoles (Peck 1976), but this is the first direct evidence that this is the case.

The high relative humidity (usually above 95 $a_v$ in deep cave; H. Hobbs, unpublished observations for Laurel Cave) of the deep cave habitat would appear to be ideal for active water vapor absorption. Use of atmospheric water has not been previously examined in cave crickets. However, cave crickets failed to maintain an equilibrium water content (*i.e.*, gain is not equal to loss) in unsaturated air in the experiment. Arthropods capable of such a feat pump water actively against the 0.99 $a_w$ of their body water and show no losses of water in unsaturated air, sustaining a constant water mass (*m*; eqn. 1) for many days (Wharton 1985). In the absence of an active mechanism, water loss by *H. cumberlandicus* occurs in unsaturated air because

the ambient test $a_v < 0.99\ a_w$ of the cricket, and the water mass depletes by simple diffusion. No gain was detected that could not be explained by wholly passive processes; water was not added to the exchangeable water pool (*m*; eqn. 1), and the amount gained correlated closely with increasing $a_v$ (Wharton 1985). Water must be imbibed as a liquid, because the critical equilibrium activity >1.00 $a_v$. Thus, the most likely source of water is free water from droplets or by ingesting moist food like most insects (Hadley 1994).

### GENERAL INTERPRETATIONS

One benefit of cricket aggregation is enhanced water conservation for survival throughout the year, particularly in Laurel Cave where somewhat dry conditions prevail year-round, and especially during harsh winters or unusually hot and dry summer conditions. Another possible benefit obtained by aggregation formation is a higher rate of completing development by nymphs, because the 'group' operates by generating a higher relative humidity within the aggregation (Yoder & Smith 1997), satisfying an absolute moisture requirement for development (Peck 1976). From a water balance perspective, *H. cumberlandicus* is hydrophilic because of its fast water loss rate according to Hadley (1994). This matches their preference for caves with atmospheres that are generally close to saturation, and, especially, the stable, more humid conditions of the cave ceiling. Laurel Cave is ideal because it is cold, lowering water loss rates of these otherwise 'leaky' crickets by suppressing integumental and respiratory water loss components (this study; Studier *et al*. 1987).

Frequent outside surface foraging trips are detrimental to survival, because cave crickets are extremely sensitive to dehydration and vulnerable to predation. Enhanced water conservation by low temperature and group effects, plus a distensible crop for food and water storage, enable *H. cumberlandicus* to remain inside the protected, cold arena of Laurel Cave for longer periods of time, and, thereby, avoid the high-risk surface environment. In contrast to *H. cumberlandicus*, the less cave adapted water balance profile of the camel cricket, *C. stygius*, correlates with their greater abundance near cave entrances rather than in the less variable deep cave, and their greater outside surface foraging activity (every few days compared to every few weeks for *H. cumberlandicus*; H. Hobbs, unpublished observations), and suggests that low temperature is less crucial for maintaining water balance.

## ACKNOWLEDGMENTS

We thank M. A. Goodman (Wittenberg University) and the anonymous reviewers for their helpful comments.

## REFERENCES

Glass, E.V., Yoder J.A., & Needham, G.R., 1998, Clustering reduces water loss by adult American house dust mites, *Dermatophagoides farinae* (Acari: Pryoglyphidae): Experimental and Applied Acarology, v. 22, p. 31-37.

Grassé, P.P., & Chauvin, R., 1944, L'effet de groupe et la survie des neutres dans les sociétés d'insects: Revue Science, v. 82, p. 461-464.

Hadley, N.F., 1994, Water relations of terrestrial arthropods: New York, Academic Press, 356 p.

Hobbs, H.H. III., 1992, Caves and springs, *in* Hackney C.T., Adams, S.M., & Martin, W.M., ed., Biodiversity of the Southeastern United States: Aquatic communities: London, Wiley, p. 59-131.

Hubbell, T.H., & Norton, R. M., 1978, The systematics and biology of the cave-crickets of the North American Tribe Hadenoecini (Orthoptera Saltatoria: Ensifera: Rhaphidophoridae: Dolichlpodinae): Miscellaneous Publications of the Museum of Zoology, v. 156, p. 1-124.

Johnson, C.G., 1940, The maintenance of high atmospheric humidities for entomological work with glycerol-water mixtures: Annals of Applied Biology, v. 27, p. 295-299.

Peck, S.B., 1976, The effect of cave entrances on the distribution of cave-inhabiting terrestrial arthropods: International Journal of Speleology, v. 8, p. 309-321.

Pfeffer, N., Madigan, T.J., & Hobbs, H.H. III., 1981, Laurel Cave: Pholeos, v. 2, p. 10-13.

Poulson, T.L., Lavoie, K., & Helf, K.L., 1995, Long-term effects of weather on the cricket (*Hadenoecus subterraneus*, Orthoptera, Rhaphidophoridae) guano community in Mammoth Cave National Park: American Middle Naturalists, v. 134, p. 226-236.

Sokal, R.R., & Rohlf, F.J., 1981, Biometry: New York, W.H. Freeman and Company, 714 p.

Studier, E.H., Wares II, W.D., Lavoie, K H., & Linn, J.A.M., 1987, Water budgets of cave crickets, *Hadenoecus subterraneus* and camel crickets, *Ceuthophilus stygius*: Comparative Biochemistry and Physiology, v. 86A, p. 295-300.

Studier, E.H., & Lavoie, K.H., 1990, Biology of cave crickets, *Hadenoecus subterraneus*, and camel crickets, *Ceuthophilus stygius* (Insecta: Orthoptera): Metabolism and water economies related to size and temperature: Comparative Biochemistry and Physiology, v. 95A, p. 157-161.

Toolson, E.C., 1978, Diffusion of water through the arthropod cuticle: Thermodynamic consideration of the transition phenomenon: Journal of Thermal Biology, v. 3, p. 69-73.

Wharton, G.W., & Knülle, W., 1966, A device for controlling temperature and relative humidity in small chambers: Annals of the Entomological Society of America, v. 59, p. 627-630.

Wharton, G.W., 1985, Water balance of insects, *in* Kerkut, G.A., & Gilbert, L.I., eds., Comprehensive insect physiology, biochemistry and pharmacology: Oxford, Pergamon Press, p. 565-601.

Winston, P.W., & Bates, D.S., 1960, Saturated solutions for the control of humidity in biological research: Ecology, v. 41, p. 232-237.

Yoder, J.A., & Denlinger, D.L., 1991, Water balance in flesh fly pupae and water vapor absorption associated with diapause: Journal of Experimental Biology, v. 157, p. 273-286.

Yoder, J.A., & Spielman, A., 1992, Differential capacity of larval deer ticks (*Ixodes dammini*) to imbibe water from subsaturated air: Journal of Insect Physiology, v. 38, p. 863-869.

Yoder, J.A., Denlinger, D.L., Dennis, M.W., & Kolattukudy, P.E., 1992, Enhancement of diapausing flesh fly puparia with additional hydrocarbons and evidence for alkane biosynthesis by a decarbonylation mechanism: Insect Biochemistry and Molecular Biology, v. 22, p. 237-243.

Yoder, J.A., Rivers, D.B., & Denlinger, D.L., 1994, Water relationships in the ectoparasitoid, *Nasonia vitripennis*, during larval diapause: Physiological Entomology, v. 19, p. 373-378.

Yoder, J.A., & Barcelona, J C., 1995, Food and water resources used by the Madagascar hissing-cockroach mite, *Gromphadorholaelaps schaeferi*: Experimental and Applied Acarology, v. 19, p. 259-273.

Yoder, J.A., & Smith, B.E., 1997, Enhanced water conservation in clusters of convergent lady beetles, *Hippodamia convergens*: Entomologia Experimentalis et Applicata, v. 85, p. 87-89.

Yoder, J.A., & Grojean, N.C., 1997, Group influence on water conservation in the giant Madagascar hissing-cockroach, *Gromphadorhina portentosa*: Physiological Entomology, v. 22, p. 79-82.

Yoder, J.A., & Hoy, M.A., 1998, Differences in water relations among the citrus leafminer and two different populations of its parasitoid inhabiting the same apparent microhabitat: Entomologia Experimentalis et Applicata, v. 89, p. 169-173.

Yoder, J.A., & Knapp, D.C., 1999, Cluster-promoted water conservation by larvae of the American dog tick, *Dermacentor variabilis* (Acari: Ixodidae): International Journal of Acarology, v. 25, p. 55-57.

Jasinto Robles, Joaquin Arroyo-Cabrales, Eileen Johnson, B.L. Allen, and Georgina Izquierdo - Blue bone analyses as a contribution to the study of bone taphonomy in San Josecito Cave, Nuevo Leon, Mexico. *Journal of Cave and Karst Studies 64*(2): 145-149.

# BLUE BONE ANALYSES AS A CONTRIBUTION TO THE STUDY OF BONE TAPHONOMY IN SAN JOSECITO CAVE, NUEVO LEON, MEXICO

JASINTO ROBLES
*Laboratorio de Rayos X, Subdirección de Laboratorios y Apoyo Académico, Instituto Nacional de Antropología e Historia*
*Moneda # 16, Col. Centro, 06060 México, D.F., MEXICO*
JOAQUIN ARROYO-CABRALES
*Laboratorio de Arqueozoología "M. en C. Ticul Alvarez Solórzano", Subdirección de Laboratorios y Apoyo Académico*
*Instituto Nacional de Antropología e Historia, Moneda # 16, Col. Centro, 06060 México, D.F., MEXICO*
EILEEN JOHNSON
*Museum of Texas Tech University, Box 43191, Lubbock, Texas 79409-3191 USA*
B.L. ALLEN
*Plant and Soil Science Department, Texas Tech University, Lubbock, Texas 79409-2122 USA*
GEORGINA IZQUIERDO
*Instituto de Investigaciones Eléctricas, Cuernavaca, Morelos, MEXICO*

*Blue-stained bones, collected along a single stratigraphic level in San Josecito Cave, Nuevo León, México, were analyzed in order to better understand the diagenetic processes that pertained to their formation, and in order to ascertain if those processes could be used in inferring past environmental conditions. Using XRD, two minerals were identified as composing the fossil bone, hydroxylapatite and calcite. INAA, ICPS, XRFS, and colorimetric methods were used to quantify trace elements, including Cu, Sr, Zn, F, and Cl (in descending order). The findings point to the presence of a physical phenomenon produced by transition metal ions impurities, that in turn seems to be associated with physical and chemical processes occurring inside the cave, rather than with outside paleoenvironmental conditions.*

Cave deposits often occupy much of the space eroded out of bedrock. They affect processes enlarging the space, supplement erosional records of cave history, provide means of absolute chronology, and provide evidence of regional environmental change (Jennings 1985). Caves constitute highly efficient sediment traps; their stability within the changing landscape facilitates geologic concentration and attracts diverse organisms in search of shelter (Collcutt 1979).

Caves frequently contain rich fossil deposits because they serve as refuge for wild animals, and are converted into focal points for bone accumulation at death. Bone deposits in caves usually are not the result of long-distance transport, but reflect local environments (Harris 1977). The catchment size, or area sampled, for cave faunas is partially dependent upon the size of the internal drainage system (small compared to open fluvial systems), the home range and prey selection of predators or scavengers serving as vectors for bone accumulation (particularly microvertebrates preyed on by owls), and pit fall entrapment of individuals living near the cave entrance. Therefore, cave paleocommunities do not represent a complete spectrum of the past biota, but instead a regional thanatocoenose (death assemblage; Shipman 1981) produced by several types of sampling (Graham 1986; Guilday 1962). In this respect, it is essential to consider in detail how collections of fossil organisms have been accumulated. A comprehensive taphonomic analysis is critical to address the least-known aspect of paleoecology, i.e., the role of fossil samples as components of ecosystems (Gifford 1981).

San Josecito Cave (Fig. 1) is one of a few localities in México containing a detailed fossil record for the late Pleistocene (Kurtén & Anderson 1980). This cave and its paleontological materials have been the focus of several studies in the past 12 years (Arroyo-Cabrales 1994; Arroyo-Cabrales & Johnson 1997, 1998; Arroyo-Cabrales *et al.* 1989, 1993, 1995). A major goal of these studies has been to understand the taphonomic history of the bone fossils and to reconstruct a sound paleoecological interpretation. In order to address the taphonomic history, studies of sediments (Rolong *et al.* 1994) and specific features on bones (Arroyo-Cabrales and Johnson 1997) have been undertaken.

The current research focuses on the authigenic evolution of secondary minerals on the bat and rodent bones in the cave. This study is important for three major reasons. Mineralogically, from the fossilized bones, it is possible to infer chemical and physical conditions from both the actual molecular structure and the diagenetic processes produced by sedimentary environments. These effects are shown by the inclusion of organic and inorganic materials into the buried bones. Taphonomically, from the recognition of the diagenetic processes that the bone underwent, it is possible to propose what has happened since the animal died, and to infer local environmental conditions around the cave at different geolog-

Copyright © 2002 by The National Speleological Society

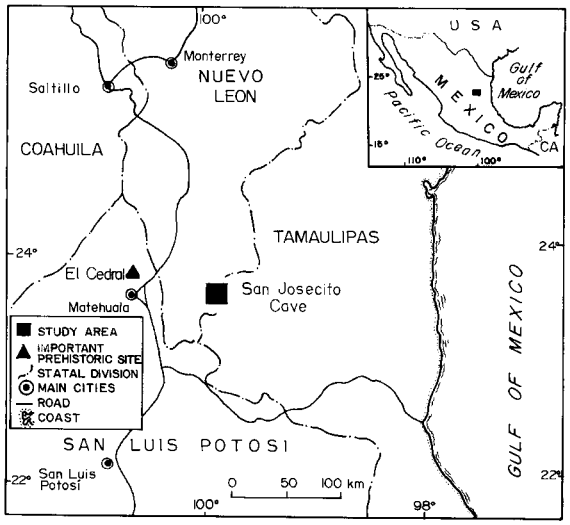


**Figure 1. Location of San Josecito Cave, Nuevo León.**

ic times. Archaeologically, results of the study may allow the environmental reconstruction for a region and period in which the earliest purported human evidence in México (approximately 33,000 years BP) has been found at El Cedral, San Luis Potosí, located less than 100 km to the west of the cave (Lorenzo & Mirambell 1986; Fig. 1).

## STUDY SITE

San Josecito Cave is located on the western flank of Sierra Madre Oriental, at the edge of the Mexican Plateau, in the southern part of the Mexican state of Nuevo León (Fig. 1). Paleontological quarrying of the cave deposits by personnel from the California Institute of Technology (1935-1941) yielded a large vertebrate fossil assemblage (Stock 1943; Kurtén & Anderson 1980; Arroyo-Cabrales 1994). More recently, controlled excavations by a collaborative endeavor between the Museum of Texas Tech University and the Instituto Nacional de Antropología e Historia, México (INAH) has added to the fossil record, geochronology, and microstratigraphy of the cave (Arroyo-Cabrales 1994; Arroyo-Cabrales *et al.* 1995; Mead *et al*. 1999; Rolong *et al*. 1994). This material has been the basis for important taxonomic and systematic studies of several animal groups, including shrews, bats, birds, carnivores, and ungulates (see Arroyo-Cabrales & Johnson 1998 for a comprehensive listing). Radiocarbon dates from the different strata have provided evidence of an age range between 45,000 and 11,000 years BP (Arroyo-Cabrales *et al.* 1995). Several cave faunal assemblages are from the Wisconsinan Pre-Pleniglacial (Arroyo-Cabrales 1994).

In 1990, Mexican-US renewed excavations were undertaken with a strict stratigraphic control. Two test units were opened, excavated stratigraphically, and all sediments were water-screened. Samples from most strata were collected for various studies in laboratories in México and the United States (Arroyo-Cabrales & Johnson 1998).

Materials from one of the strata (770) showed a very characteristic blue-greenish stain. An early report pointed to the presence of copper (Arroyo-Cabrales & Johnson 1997) as the cause for the coloration. However, the small amount of copper present in the bone warranted further chemical and mineralogical analyses to explain the staining. Furthermore the original copper source has not been identified. A more comprehensive understanding of the "blue bone" from San Josecito Cave is now documented.

## PREVIOUS STUDIES ON FOSSILIZED BONE FROM STRATUM 770

Previous assays of the "blue bone" included X-ray diffraction and energy-dispersive X-ray (EDAX) techniques (Arroyo-Cabrales & Johnson 1997). The diffraction patterns pointed to the presence of two mineral fractions, a principal one that has the same interplanar spacing values of the hydroxylapatite [$Ca_5(PO_4)_3OH$]. In the same sample, another mineral related to the carbonate group (calcite, $CaCO_3$) was identified; this mineral formed after the bone underwent an internal mineralization process.

From the energy-dispersive X-ray (EDAX) fluorescence test, qualitatively the main constituents were phosphorus (P) and calcium (Ca). Trace elements were copper (Cu), zinc (Zn), bromide (Br), and strontium (Sr). This analysis pointed to the presence of copper as the staining mineral, while zinc was only providing the metallic shine, and bromide was intrusive.

## EXPERIMENTAL ASSAYS

The stratum 770 sample is composed of small vertebrate bones including lizards (*Barisia imbricata*; Mead *et al*. 1999), bats (*Desmodus rotundus*, *Leptonycteris* sp.), and rodents (*Neotoma* sp., *Peromyscus* sp.) (Arroyo-Cabrales 1994). Some bones were compressed strongly, probably due to sediment load (Arroyo-Cabrales & Johnson, 1997). Most bones are stained completely, including the overall shaft, and a subsample from blue bone fragments was chosen for analysis (~10 g).

The initial sample analyses were conducted at the Geology and X-Ray laboratories of the Subdirección de Laboratorios y Apoyo Académico, Instituto Nacional de Antropología e Historia. Observations were done using both a stereoscope and a petrographic binocular microscope.

Two mineral components were observed with the stereoscope. One had a fine and homogeneous texture with blue-green tones, and some lighter concretions of different composition. This same observation was enhanced using a scanning electron microscope (Fig. 2). Such concretions were tested with hydrochloric acid, and the reaction supported its identification as carbonate, and characterization as calcite ($CaCO_3$) by DRX and SEM probes.

The blue-greenish bone component was sorted carefully and ground to obtain fractions with a diameter range between 20-30 µm. The powder was put in a polished glass to get an even distribution of material. The sample was assayed with

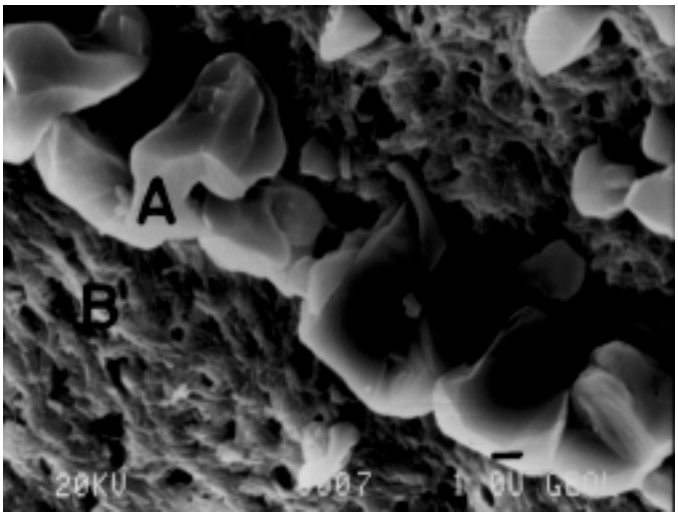


**Figure 2. SEM image of blue-greenish bone showing calcite crystals (A) over phosphasized bone (B). Scale bar on lower right side equals 1 µ.**

copper X-rays (Cuλ = 1.54 Å), and scanning conditions of 20 Kv - 20 mA, signal counting each second, scintillation detector (Sc), 1° collimator, and Ni filter. The diffraction pattern was compared to the Diffraction Standard Manual for powder samples (Berry *et al*. 1974). From a diffractogram, two minerals were identified: hydroxylapatite, $Ca_5(PO_4)_3OH$; and calcite, $CaCO_3$ (Fig. 3a).

Comparative analyses were assayed with yellowish bone from level 740-750 (Fig. 3b). The results indicated that the main constituent in both samples is hydroxylapatite, but their megascopic color is not the same. Microscopically, crystalline arrangements in blue-green bone showed alternate anomalous reddish-yellowish-bluish interference colors of second order, not common for hydroxylapatite (Fig. 4).

To address these anomalies, sample analysis using X-ray fluorescence spectrometry (XRFS) was undertaken with model JEOL-JSDX-60P3A spectrometer, Cr anode, TAP analyzer crystal and flux detector. The search for fluorine used the comparative fluorite ($CaF_2$) standard. This element was not quantifiable in the problem sample due to the small sample size and low level of F concentration. However, Energy Dispersive Analyses by X ray fluorescence (EDAX) in scanning electron microscope JEOL-JSM-35C, with detector crystal Si-Li, berilium windows and Tracor Northern analyzer system, and colorimetric method revealed the level of chlorine (500 ppm), and fluorine at less than 1 ppm.

Complementary chemical analysis by instrumental neutron activation (INAA) in light-blue bones was performed in a reactor with Am-Be source and 6.1 x 106 n/cm². Concentrations of Cu were <4 ppm in a pallid blue-greenish sub-sample. However, inductively coupled plasma spectrometry (ICPS), in a Thermo Jarrell Ash Atom Scan 16 spectrometer, showed Cu concentrations between 21.08-38.8 ppm for a dark blue-greenish sub-sample, strontium at 4.94 ppm, and Zn less than 5 ppm; a yellowish bone subsample from above stratum 800 resulted

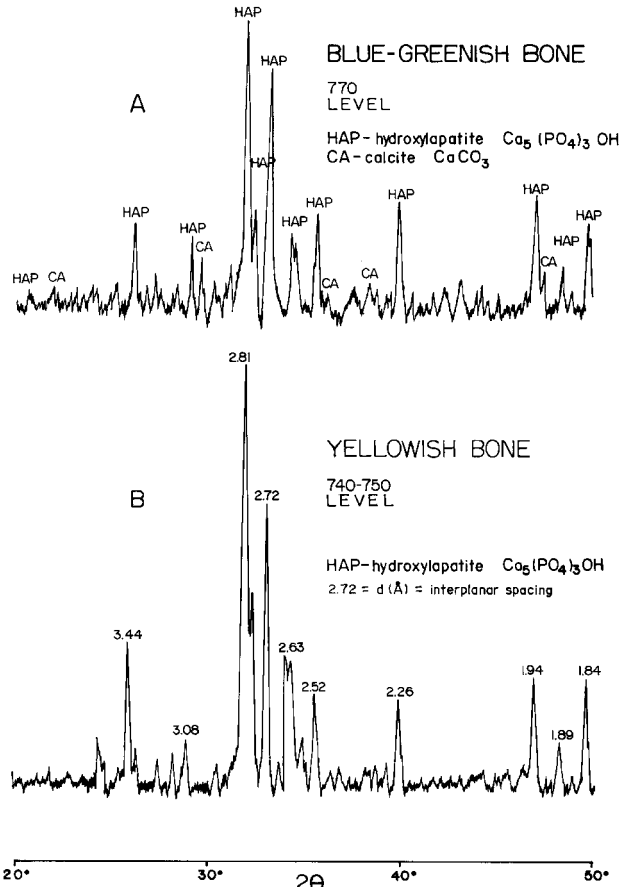


**Figure 3. X-Ray diffraction patterns of fossilized bones collected from different stratigraphic levels in San Josecito Cave; although the bones produce the same diffraction response for hydroxylapatite (HAP), they do not show the same color effects.**

in Cu concentrations of 54.95 ppm, Sr at 247.4 ppm, and Zn at 5.94 ppm (Table 1).

## PROBABLE CAUSES OF THE COLORATION IN THE BONES

The phenomenon of blue coloration in the bones was analyzed based on diagenetic processes, due to the fact that the studied samples present an almost total degree of replacement. The minerals are colored upon absorbing certain wavelengths of light. Therefore, the observed color is the result of the combination of wavelengths that arrive to the eye (Hurlbut and Klein 1985; White 1997). Within the factors that could cause the coloration of the analyzed bones, the presence of the mineral vivianite and forms of odontolite, fossil turquoise, or fluorapatite may be suspected, but other phenomena also could be causing the blue-green coloration. The first cases were discarded based on the results of X-ray diffraction, while the second was rejected by the lack of concentrations of Cu greater than 7% total weight (Palache *et al.* 1951). The third case was rejected due to the low fluorine concentration (<1 ppm); several authors have shown that fluorine concentrations on the

**Table 1. Synthesis of chemical analyses in fossilized bones from Stratum 770 (blue), and from above stratum 800 (yellowish) in San Josecito Cave, Nuevo León, México.**

| Technique | Trace elements | Total bulk | |
|---|---|---|---|
| | | Blue | Yellowish |
| X-ray fluorescence spectrometry (XRFS) | F | Not detected | |
| Instrumental neutron activation analysis (INAA) | Cu | 4 ppm[1] | |
| Scanning microscopy with X-ray analysis (EDAX) | Cl | 500 ppm | |
| Inductively coupled plasma spectrometry (ICPS) | Cu | 21.08-38.8 ppm[2] | 54.95 ppm |
| | Sr | 4.94 ppm | 237.4 ppm |
| | Zn | < 5 ppm | 5.94 ppm |
| Colorimetric method | F | < 1 ppm | |

[1] Pallid blue-greenish sub-sample [2] Dark blue-greenish sub-sample

order from 2% and 3.73% were required for fluorapatite (Chang *et al.* 1996; Fleet & Pan 1997; Hurlbut & Klein 1985; Palache *et al.* 1951).

Results of the different analyses assayed during this study provided the basis for another explanation of the blue-green color, indicating that the color is due to the presence of transition trace metal ions. It is suggested that a chemical element in sufficient concentrations to form molecules is not the unique cause of color in minerals. Chemical impurities in small quantities can be incorporated into defective structures named transition metal ions, and intensely absorb the light to give the mineral an intensive color sensation (Nassau 1978; White 1997). Among the elements that can provide intensive colorations to the minerals are Cr, Mn, Fe, Co, Ni, and Cu. Which element is providing the intense coloration cannot be predicted as the same element in different structural environments presents different transitional energy and causes different coloration (Blackburn & Dennen 1988; Hurlbut & Klein 1985).

The fossilized bones from stratum 770 are blue-green stained due to impurities within the transition metal ions. Particularly, copper in concentrations between 21 and 38.8 ppm is the main cause for this phenomenon. Similar cases, where Cu promotes blue-green color are turquoise, azurite, malachite (Nassau 1980) or allophane and other amorphous aluminum silicates (White 1997).

## DISCUSSION

The minerals identified in the rodent bones from stratum 770 of the San Josecito Cave are hydroxylapatite and calcite. The first occurs as a product of the local authigenic mineralogical progression, while the second is a response of carbonate precipitation from saturated solutions and/or by Ca exsolution from the bone.

The authigenic mineralogy of the bat bones, which constitutes the focus of the present study, was accomplished in three stages. First, during mineral nucleation, apatite was developed in the bones. This development was due to contact with $Ca^{2+}$ and $Mg^{2+}$ rich solutions with the bones. Those solutions previously had to cross bat guano. With these characteristics, the environment was modified, and reducting conditions formed in the humid space. Second, the authigenic mineralogy evolved to a most stable phase (hydroxylapatite) by enrichment of the environment with $OH^-$ ions. And third, the final phase was identified with the taphonomic study, and corresponds to a demurrage where the hydroxylapatite has incorporated chemical element ions as Cu, Zn, Br, Sr, Cl, F into its crystalline structure, producing optical property distortions.

The first stage of mineralization, considered as nucleation, is deduced from observations made on buried bones, in caves all over the world (Courty *et al.* 1989). The bone, in the current phase, presents a blue-green coloration, associated with the influence of impurities of transition metal ions, produced by the absorptive capacity of the light elements mainly as copper. The source of origin of the ions incorporated into the bones probably is the calcareous rocks that constitute the cavernous structure (Table 1), but only in stratum 770 were blue-greenish bones are present. This was possibly also caused by lithostatic change in a focused humid environment (as shown by the compressed blue bones).

## CONCLUSION

This study has addressed one question regarding the presence of stained bluish bone of small vertebrates in cave sediments. The small vertebrate bones exclusively come from a very thin stratigraphic unit. It seems reasonable to constrain the explanation of the color presence to a single sedimentary period, between ca. 28,000 and 11,500 years BP (Arroyo-Cabrales *et al.* 1995).

The results of the analyses point to a color phenomenon due to the influence of transition metal ions. Furthermore, the abundance of small vertebrates, mainly lizards and bats, accounting for the presence of large amounts of guano, could contribute to the chemical processes accounting for the blue staining of bone. Finally, it is shown that research on paleontological and archaeological bones would gain from an in-depth analysis of the different diagenetic taphonomic features

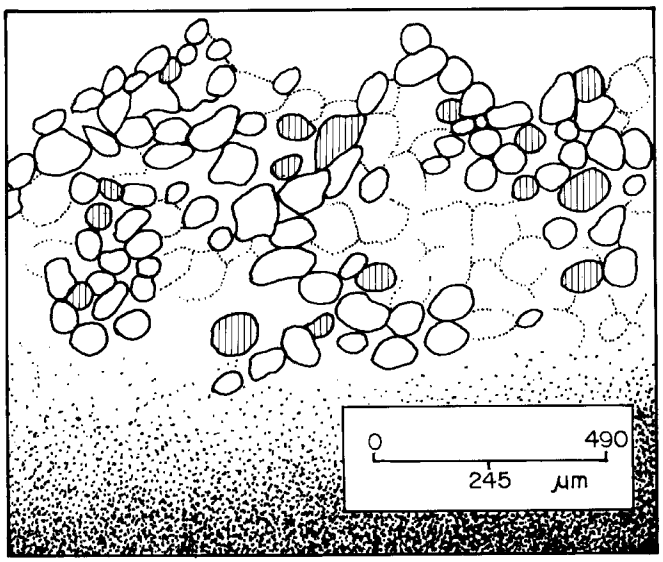


**Figure 4. Schematic view of the thin section of fossilized bone from stratum 770 at San Josecito Cave; under petrographic microscope, vertical shadowed bars represent hydroxylapatite minerals with second order interference colors.**

present in them.

## ACKNOWLEDGMENTS

The authors thank the collaboration of Margarita Reyes, from the Instituto de Geología, and Faustino Juárez, Instituto de Geofísica, both from the Universidad Nacional Autónoma de México. Also, several institutions supported parts of the research: National Geographic Society (Grant # 3102-89 to EJ); National Speleological Society Research Grants (1989 & 1993 to EJ); The Graduate School and Museum of Texas Tech University; and the Subdirección de Laboratorios y Apoyo Académico, Instituto Nacional de Antropología e Historia, México. This manuscript represents part of the ongoing regional research of the Lubbock Lake Landmark into Quaternary cultural and ecological changes on the Southern Great Plains under the auspices of the Museum of Texas Tech University.

## REFERENCES

Arroyo-Cabrales, J., Johnson, E, & Ralph, R.W., 1989, An initial reappraisal of San Josecito Cave and its Late Pleistocene fauna: Current Research in the Pleistocene, v. 6, p. 63-65.

Arroyo-Cabrales, J., Johnson, E., & Ralph, R.W., 1993, New excavations at San Josecito Cave, Nuevo León, México: Current Research in the Pleistocene, v. 10, p. 91-94.

Arroyo-Cabrales, J., 1994, Taphonomy and paleoecology of San Josecito Cave, Nuevo León, México [PhD thesis]: Texas Tech University.

Arroyo-Cabrales, J., Johnson, E., Haas, H., de los Ríos Paredes, M., Ralph, R.W., & Hartwell, W.T., 1995, First radiocarbon dates for San Josecito Cave, Nuevo León, México: Quarternary Research, v. 43, p. 255-258.

Arroyo-Cabrales, J., & Johnson, E., 1997, Preliminary analyses of bone from San Josecito Cave, Nuevo León, México, *in* Hannus, L.A., Rossum, L., & Winham, R.P., eds., Proceedings of the 1993 Bone Modification Conference, Hot Springs, South Dakota, Archeology Lab Augustana College, Occasional Papers 1, p. 50-64.

Arroyo-Cabrales, J., & Johnson, E., 1998, La Cueva de San Josecito, Nuevo León, México: Una primera interpretación paleoambiental, *in* Carranza, C.O., & Córdoba, M.D.A., eds., Avances en investigación. paleontología de vertebrados: Universidad Autónoma del Estado de Hidalgo, Instituto de Investigaciones en Ciencias de la Tierra, Publicaciones Especiales 1, p. 120-126.

Berry, L.G., Post, B., Weissmann, S., McMurdie, H.F., & McClune, W.F., 1974, Joint Committee on Powder Diffraction Standards: Philadelphia, Pennsylvania, p. 55, File 5-586; p. 177, File 9-432.

Blackburn, W.H., & Dennen, W.H., 1988, Principles of mineralogy: Dubuque, Iowa, Brown Publishers.

Chang, L.L.Y., Howie, R.A., & Zussman, J., 1996, Rock forming minerals. Non-silicates: sulphates, carbonates, phosphates, halides. v. 5B, 2nd ed: London, Longman Group Limited.

Collcutt, S.N., 1979, The analysis of Quaternary cave sediments: World Archaeology, v. 10, p. 290-301.

Courty, M.A., Goldberg, P., & Macphail, R., 1989, Soils and micromorphology in archaeology: Cambridge, Cambridge University Press.

Fleet, M.E., & Pan, Y., 1997, Site preference of rare earth elements in fluorapatite: Binary (LREE+HREE)-substituted crystals: American Mineralogist, v. 82, p. 870-877.

Gifford, D.P., 1981, Taphonomy and paleoecology: A critical review of archaeology sister disciplines, *in* Schiffer, M.B., ed., Advances in archaeological method and theory, v. 4: New York, Academic Press, p. 365-438.

Graham, R.W., 1986, Response of mammalian communities to environmental changes during the late Quaternary, *in* Diamond, J., & Case, T.J., eds., Community ecology: New York, Harper & Row, p. 300-313.

Guilday, J.E., 1962, The Pleistocene local fauna of the Natural Chimneys, Augusta County, Virginia: Annals of the Carnegie Museum, v. 36, p. 87-122.

Harris, A.A., 1977, Wisconsin age environments in the northern Chihuahuan Desert: Evidence from the higher vertebrates: Transactions of the Symposium on the Biological Resources of the Chihuahuan Desert Region - US and Mexico: US Department of the Interior, National Park Service Transactions and Proceedings Series 3, p. 23-52.

Hurlbut, C.S., & Klein, C., 1985, Manual of mineralogy (after James D. Dana): New York, John Wiley & Sons.

Jennings, J.N., 1985, Karst geomorphology: Oxford, England, Basil Blackwell.

Kurtén, B., & Anderson, E., 1980, Pleistocene mammals of North America: New York, Columbia University Press.

Lorenzo, J.L., & Mirambell, L., 1986, Preliminary report on archaeological and paleoenvironmental studies in the area of El Cedral, San Luis Potosí, México, 1977-1980, *in* Bryan, A.L., ed., New evidence for the Pleistocene peopling of the Americas: Center for Study of the Early Man, University of Maine, Orono, Peopling of The Americas Series, p. 107-113.

Mead, J.I., Arroyo-Cabrales, J., & Johnson, E., 1999, Pleistocene lizards (Reptilia: Squamata) from San Josecito Cave, Nuevo León: México: Copeia 1999, p. 163-173.

Nassau, K., 1978, The origins of color in minerals: American Mineralogist, v. 63, p. 219-229.

Nassau, K., 1980, The causes of color: Scientific American, v. 243, p. 106-123.

Palache, C., Berman, H., & Frondel, C., 1951, Dana´s system of mineralogy: New York, John Wiley and Sons.

Rolong, N., Arroyo-Cabrales, J., Allen, B.L., & Johnson, E., 1994, Sediment properties from San Josecito Cave, Nuevo León, México, Transactions of the 15th World Congress of Soil Science, v. 6a, Commission V: Simposia, p. 129-141.

Shipman, P., 1981, Life history of a fossil. An introduction to taphonomy and paleoecology: Cambridge, Mass., Harvard University Press.

Stock, C., 1943, The cave of San Josecito, Mexico: New discoveries of the vertebrate life of the ice age: Balch Graduate School of the Geological Sciences, California Institute of Technology Contribution 36, v. 1-5.

White, W.B., 1997, Color of speleothems, *in* Hill, C., & Forti, P., eds., Cave minerals of the world, National Speleological Society, p. 239-244.

## JCKS SEEKS PALEONTOLOGY AND HISTORY EDITORS

The *Journal of Cave and Karst Studies* seeks 2 new Associate Editors. The *Journal* is establishing a new Associate Editor position covering **Paleontology**. In addition, the current **History** Associate Editor, Marion Smith, has indicated an interest in stepping down from that position when a new person is identified.

The responsibilities of the Associate Editors include soliciting articles, arranging for appropriate reviews of papers in their fields of expertise, working with authors to prepare their manuscripts for publication, making recommendations concerning acceptance and rejection of submitted papers, and assisting the Editor in gathering material for the non-refereed section of the *Journal*. Advice from the Associate Editors, along with the *Journal*'s Advisory Board, is commonly solicited on editorial policy decisions.

The *Journal* desires pro-active scholars with contacts in the respective communities of Quaternary Paleontology and History as related to caves and karst, and experience in scholarly publishing. Interested candidates for the Paleontology position are asked to send a letter of interest with a C.V. by October 15th to the editor at: Hose@chapman.edu. Similar information will be accepted from potential History candidates until the position is filled.

National Speleological Society
2813 Cave Avenue
Huntsville, Alabama 35810-4431